

ELECTROMECHANICAL AND THERMAL EFFECTS OF FAULTS UPON

SUPERCONDUCTING GENERATORS

by

David Lee Luck

LIBRARY
NAVAL POSTGRADUATE SCHOOL
MONTEREY, CALIF. 93940

ELECTROMECHANICAL AND THERMAL EFFECTS OF FAULTS UPON
SUPERCONDUCTING GENERATORS

BY

David Lee Luck

B.S., Ohio University
(1963)

S.M.E.E. Massachusetts Institute of Technology
(1969)

Nav. E. Massachusetts Institute of Technology
(1969)

Submitted in Partial Fulfillment of the Requirements

for the Degree of
Doctor of Philosophy

at the

Massachusetts Institute of Technology

June, 1971

ELECTROMECHANICAL AND THERMAL EFFECTS OF FAULTS UPON
SUPERCONDUCTING GENERATORS

by

David Lee Luck

Submitted to the Department of Electrical Engineering
on May 7, 1971, in partial fulfillment of
the requirements for the degree of Doctor of Philosophy

ABSTRACT

The effects of power system faults upon a generator with a superconducting field winding are presented and discussed. Induced current, heating, and electromechanical stress effects upon the superconducting field winding and rotor structure are investigated. Design criteria are developed which insure that a superconducting generator can survive a power system fault.

Two classes of faults are considered and design criteria relating to each are developed. Survival of a short-term fault which is cleared by a system circuit breaker requires maintenance of super conductivity; survival of a sustained fault which cannot be cleared requires maintenance of machine structural integrity without permanent damage.

An example design for a 1000 MVA superconducting generator is developed. The design illustrates that it is possible to satisfy the criteria for fault survival, while maintaining the advantages of lower weight, lower synchronous reactance, improved efficiency, better damping characteristics, larger $I_2^2 t$, and higher rotor natural frequencies than for a comparable conventional generator.

THESIS SUPERVISOR: Herbert H. Woodson

TITLE: Philip Sporn Professor of Energy Processing

ACKNOWLEDGEMENT

Completion of this work brings to mind many people whose attitudes and efforts have contributed to my educational pursuits: my parents, who very early convinced me of the value of education; my wife, who patiently endured my many hours of study.

More immediate to this work, I appreciate the guidance and enthusiasm of Professor Herbert H. Woodson, who served as Thesis Supervisor. Professor James R. Melcher, both during my Master's work and the present work, has provided valuable advice. Professors Joseph Smith and Philip Thullen gave willingly of their time to provide many useful ideas and help me learn some mechanical engineering. The efforts of this committee have made this exercise a meaningful learning experience. I also appreciate having had the opportunity to work with Professor Charles Kingsley. I hope that a little of his understanding and feel for electric machinery has rubbed off onto me.

I also wish to thank my typist, Mrs. Evelyn Holmes, for her patience in typing all those equations, and in changing the word 'electrothermal' to 'electrical'. Finally, a word of appreciation to my fellow graduate students who have helped to create an environment which was both enjoyable and broadening.

The work was supported by a grant from the Edison Electric Institute.

TABLE OF CONTENTSPage NO.

Chapter I	- Introduction and Statement of the Problem	12
Chapter II	- Results and Example Design	20
II-1	<u>Keeping the Superconductor Superconducting</u>	24
	Induced Current in the Field Winding	27
	Heating in the 4.2°K Region During Faults	31
II-2	<u>Maintaining Structural Integrity of the Rotor</u>	
	<u>During Faults</u>	35
	Rotor Fault Torques	35
	Field Winding Fault Torques	35
	Fault Torques on the Electrical Shield	37
	Normal Stresses on the Electrical Shield	40
	Thermal Capacity of the Electrical Shield	42
II-3	<u>Steady-State Performance of the Electrical Shield</u>	
	<u>for Unbalanced Loads</u>	48
II-4	<u>1000 MVA Superconducting Generator; an Example</u>	50
Chapter III	- Steady-State Effects upon the Electrical and Thermal Shields	62
III-1	<u>Heating of the Rotor</u>	62
	a) Sources of Heating	62
	1) Radiation	62
	2) Stator Phase Unbalance	63
	3) Stator Harmonics	64
	b) Distribution of the Rotor Heat Load	66
	1) Electrical Shield Heat Load	66
	2) Stainless Steel Containment Vessel	
	Heat Load	67
III-2	<u>Alternating Currents in the Field Winding Due to Negative Sequence</u>	69
III-3	<u>Steady-State Mechanical Excitation of the Electrical Shield</u>	70

Chapter IV - Electromechanical and Thermal Effects of Faults	73
IV-1 <u>The Effects of Fault Torques</u>	74
a) Torque upon the Field Winding	75
b) Torque upon the Electrical Shield	78
IV-2 <u>The Effect of Normal Electromechanical Stresses</u>	82
IV-3 <u>Rotor Heating During Faults</u>	85
IV-4 <u>The Field Current During Faults</u>	89
Chapter V - Experiments	95
V-1 <u>Armature-Produced Magnetic Field</u>	95
V-2 <u>Shield Time Constant</u>	98
V-3 <u>Attenuation Factor of Thick and Thin Shields</u>	100
V-4 <u>Power Dissipation in a Shield</u>	101
V-5 <u>Sudden Short Circuits of the MIT Experimental Generator</u>	102
V-6 <u>Induction Motor Loss Experiment</u>	104
V-7 <u>Slotted Electrical Shields</u>	107
Chapter VI - Conclusions and Suggestions for Further Study	109
VI-1 <u>Conclusions</u>	110
VI-2 <u>Suggestions for Further Study</u>	111
Appendix I	113
A-1 <u>Lumped-Parameter Machine Model</u>	113
A-1-a <u>Lumped-Parameter Model Including Resistances</u>	114
Definitions of reactances x , x' , x''	125
Definitions of time constants T'_{do} , T'_d , T''_{do} , T''_d (3 ϕ fault)	126
Definitions of time constants $T''_{d\ell}$, etc. (line-line faults)	126
Definitions of time constants $T'_{d\ell}$, etc. (arbitrary closure)	127

Alternating Field Current	127
A-1-b <u>Lumped-Parameter Model Neglecting Resistances</u>	129
Fault Currents and Torques as Functions of Trapped Fluxes	135
Definitions of Trapped Fluxes (ψ_{d1} , ψ_{q1} etc.)	136
Torque During Subtransient Period	140
Rotor Torques - Field Winding Torques	142
Definitions of i_2 , i_o , Δi_1 for Various Faults	144
A-2 <u>Quasistatic Magnetic Field Model</u>	146
A-2-2 Thin-Shield Steady-State Magnetic Field Model	147
A-2-b Thick Shield Steady-State Model	151
A-2-c Transient Magnetic Field Model	156
Thin-Shield Time Constant	156
Thick Shield Time Constant	157
A-2-d Transient Forces on a Conducting Shield	160
A-3 <u>The Thin Shell Mechanical Model</u>	163
Shell Deflection	165
Natural Ring Frequencies	165
Bibliography	168
Biographical Note	170

LIST OF FIGURES

<u>Fig. No.</u>		<u>Page No.</u>
I-1	Superconducting Generator Configuration	14
II-1	Damping and Field Current Surge vs Shield Time Constant	30
II-2	Temperature Rise in 4° K Region vs Shield Atten- uation Factor	33
II-3	Shield and Field Winding Support Thickness vs. Outer Support Radius	39
II-4	Max. Radial Shield Deflection and Natural Ring Fre- quency vs Shield Support Thickness	41
II-5	Slotted Shield Cross Section	46
II-6	1000 MVA Design Schematic	54
II-7	1000 MVA Design Rotor Cross Section	55
V -1	Flux Density vs Axial Position for 80 KVA Machine	97
V- 2	Shield Time Constant Experimental Setup	99
V -2a	Shield Attenuation Factor Experimental Setup	101
V -3	Oscillograms of Sudden Short Circuit Tests on 80 KVA Machine	103
V -4	V Curve for 80 KVA Machine	106

LIST OF TABLES

	<u>Page No.</u>
II-1 Fault Torques	36
II-2 Cooling Power for Shield vs Shield Temperature	49
II-3 1000 MVA Superconducting Generator Characteristics	56
IV-1 Increase in Positive Sequence Direct-Axis Armature Current Following a Fault	90
IV-2 Magnitude of Direct-Axis Alternating Current Following a Fault	93
V - 1 Experimental Shield Time Constant	99
V - 2 Experimental Shield Attenuation Factors	100
V - 3 Experimental Reactances of 80 KVA Machine	102

GLOSSARY OF SYMBOLS

B	- flux density
E	- Young's Modulus
e_f	- per-unit field voltage
F_o	- outer field winding support radius
f_t	- torsional natural frequency
H	- magnetic field intensity
I_2	- per-unit steady-state negative sequence armature current
I_a	- rated armature current
i_o	- per-unit zero sequence current
i_2	- per-unit negative sequence current
i_x	- current (subscript indicates circuit)
$I_2^2 t$	- rotor thermal capacity (units-seconds)
J_A	- rated armature current density
j	- $\sqrt{-1}$
K_D	- damping coefficient
$K_{D \text{ opt}}$	- optimum damping coefficient
K_{att}	- shield attenuation factor
l_m	- machine active length
l_t	- end-turn length
L_x	- self-inductance (subscript indicates particular circuit)
M_{xx}	- mutual inductance (subscripts indicate particular circuit)
p	- d/dt
R	- shield geometric mean radius
R_i	- shield inner radius
R_o	- shield outer radius
r_x	- resistance (subscript indicates particular circuit)
S_i	- stator inner radius
S_o	- stator outer radius
T_{s1}	- shield time constant
T_{sn}	- shield higher order diffusion time constants
T	- inner radius of iron shield (or conducting stator shield)

Glossary of Symbols (continued)

$T'_{do}, T''_{do} \dots$ etc. - transient and subtransient time constants
defined in Appendix I

T_f - field time constant

V_a - machine rated terminal voltage

$v_\alpha, v_{s\alpha}, v_d, v_q \dots$ etc. - voltages used in Appendix I

x, x_d - per-unit synchronous reactance

x - if used in expression for flux density, $x = S_1/S_0$

x', x'_d - per-unit transient reactance

x'', x''_d - per-unit subtransient reactance

x_e, x_s - per-unit system or external reactance

x_{max} - maximum radial deflection of shield for 3ϕ fault

Greek Symbols

Δi_f - per-unit increase in field current following fault

ΔT - temperature rise

Δ - shield thickness

Δ_f - field support thickness

Δi_{d1} - per unit increase in positive sequence, direct-axis
current following a fault

δ - magnetic skin depth

λ_x - flux (subscript indicates particular circuit linking flux)

μ_0 - permeability of free space

ν - Poisson's Ratio

ρ - electrical resistivity

ρ_m - mass density

σ - electrical conductivity

σ_y - yield strength in tension

σ_s - yield strength in shear

σ_T - tensile stress due to rotation

σ_r - radial mechanical stress

τ - torque (total on rotor)

τ_x - torque (subscript indicates structure to which torque is
applied)

Glossary of Symbols (continued)

- ψ_x - flux (subscript indicates circuit linking flux)
- ω_s - angular swing frequency of machine
- ω_o - line angular frequency
- ω_c - ring frequency of cylindrical shell

CHAPTER I

Introduction and Statement of the Problem

The increasing demand for electric power has made practical the use of higher and higher rated generating units. Economic advantages are realized in the capital and operational costs of both the prime mover and the generator as the unit rating increases [1]. A point of diminishing returns in economic advantage is reached for the generator above ratings of about 1000 MVA for the reasons given below. Generators with superconducting field windings can extend this limit; thus, the economies of scale can be realized in even higher rated units. [2]

The economy realized in conventional generators from increased rating is the result of better armature cooling and thus more effective use of the armature copper. However, as the rated current for a given machine is increased, the per-unit reactances of the machine are increased and the inertia constant is decreased, both of which degrade the transient stability margin. To decrease synchronous reactance, air gap lengths must be increased, resulting in the requirement for more excitation power and greater power loss in the field winding. Hence, the larger rated machine with the better utilized armature becomes less efficient and less economical in an operational sense. The crossover occurs at a rating of about 1000 MVA.

The capital cost advantage associated with higher rated units is offset above 1000 MVA for conventional generators by construction and shipping considerations. The stator iron makes the larger machines so heavy that they must be shipped in pieces and assembled at the site.

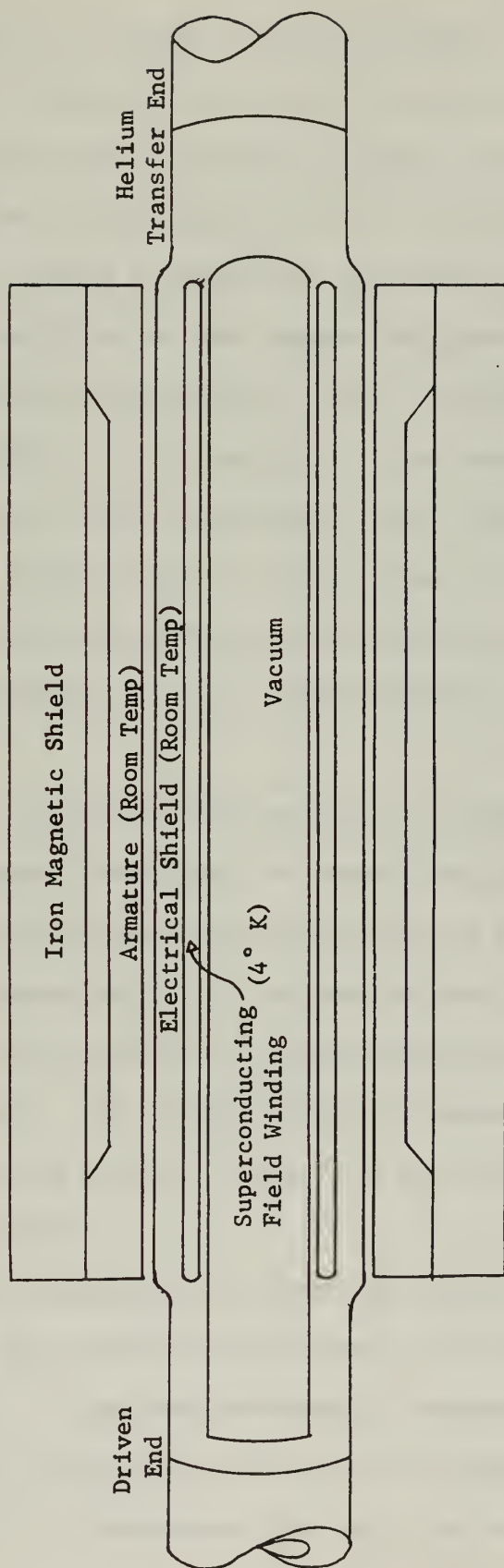
Rotor diameters are limited by mechanical stresses requiring length increases for increased power ratings. Therefore, weight increases proportional to length further complicate shipping and assembly. Lower rotor mechanical natural frequencies are another result of increased length.

Generators with superconducting field windings do not require iron in the rotor or stator to produce high magnetic flux density at the armature bars. With no resistance loss in the field winding, and no concern with iron saturation, the ampere turns of the field winding can be increased to produce up to about 50 kilogauss in the machine center and 20 to 30 kilogauss in the armature region.

Elimination of iron has several beneficial effects. First, machine weight is reduced; also, the elimination of iron within the armature provides space for more armature conductors. The machine volume for a given power rating is thus reduced. Insulation problems in the armature are also reduced because of the absence of iron at ground potential; machines can thus be designed for higher voltages. Second, machines without iron have lower reactances. Even though the inertia is reduced, transient stability margin has been shown to improve over conventional machines [5]. Third, the superconducting generator is slightly more efficient because of the elimination of field winding resistance losses.

The configuration for a superconducting generator is as shown in Fig. I-1. The armature is at room temperature; it is similar to a conventional armature except for the absence of iron interleaved with the conductor bars. A winding scheme developed by Kirtley and Smith [21] permits use of much less insulation, and provides better utilization of the armature space for carrying current. A laminated iron shield

FIGURE I-1
1000 MVA Superconducting Generator



surrounds the armature to provide a uniform boundary for the magnetic fields and eliminate unbalanced forces upon the field winding.

The superconducting field winding is located inside a liquid helium space in the rotor and is maintained at 4.2° K. Surrounding the field winding is a thermal shield maintained at approximately 20° K to intercept thermal radiation from the room temperature parts. The outer part of the rotor is a conducting electrical shield to intercept asynchronous magnetic fields produced in the armature. If the superconducting field winding were exposed to these asynchronous fluxes, losses would be produced and the field winding could be driven normal. The layer of stainless steel beneath the electrical shield provides structural support for the shield when it is subjected to large electromechanical stresses under fault conditions.

Superconducting generators have been shown to possess several operational and economic advantages over conventional machines. However, the effects of faults upon these generators have not been studied. The large oscillating torques and large armature currents producing rotor heating following a short circuit on a power system have been known and studied for many years. The internal effects produced by these fault conditions would seem to be more severe in a superconducting generator for the following reasons:

- 1) The thermal isolation of the rotor to minimize conduction heat leak into the cryogenic region makes it structurally more vulnerable to large electromechanical stresses.
- 2) Low thermal capacity of rotor parts at cryogenic temperatures can result in a temperature rise due to rotor heating during

faults. Small temperature rise in the superconductor can cause it to go normal.

- 3) Induced currents in the field winding may cause it to go normal if the critical current is reached, or if hysteresis losses raise its temperature sufficiently.

The first consideration in making superconducting generators able to withstand the effects of faults is the superconducting winding itself. If a short-term fault drives the superconductor normal, it might be necessary to remove the generator from the system, whereas maintenance of superconductivity would probably make continued operation possible after the fault is cleared. The superconductor can be driven normal if (a): the current rises above the critical value; (b): the temperature rises due to heat transfer from other rotor parts, or due to internal heat generation in the superconductor itself; (c): possibly, excess motion of the superconductor results during the fault.

The electrical shields, cylindrical conducting shells around the field winding, serve to mitigate all of these fault effects. A large portion of the induced currents, eddy current heating, and oscillating stresses associated with the period following a fault, are transferred from the superconducting winding to these shields. The problems of keeping the superconductor superconducting are, in part, traded off for problems of making the electrical shields able to withstand the fault effects.

The second consideration in making the superconducting generator able to survive faults concerns the structural integrity of the rotor.

The generator rotor is subjected to large electromechanical stresses following a fault. These stresses include not only the well known shear stresses associated with fault torques, but also normal stresses, because of the initial exclusion of demagnetizing armature flux from the rotor. The rotor torque-supporting structure at the rotor ends of a superconducting generator is minimized to reduce heat leak by conduction to the cryogenic region. In addition, much of the fault torque is taken by the electrical shield, which is of relatively thin material. Hence, both the rotor thermal distance pieces and the electrical shield are vulnerable to fault torques. The electrical shield is also subjected to the normal electromechanical stresses. Its only radial support is at the ends, to prevent thermal communication directly to the field winding region, making it particularly susceptible to deformation from these radial stresses.

The electrical shield has evolved from the standard thermal radiation shield used in helium dewars. The original function of the thermal shield was to intercept steady-state radiant energy from the room-temperature stator. Also, it intercepts electromagnetic energy in the form of asynchronous magnetic fields produced by armature phase imbalance, and serves as a damper winding to damp machine oscillations. This study shows that it can also provide protection for the superconducting winding during fault conditions. Providing protection from asynchronous magnetic fields is shown to imply that the shield intercepts the transient electromechanical stresses during faults.

To provide sufficient mechanical support for the electrical shield, it is more efficient to place the electrical shield at room temperature to minimize conduction heat leak into the cryogenic region. The function of thermal radiation shielding is then transferred to a radiation shield at cryogenic temperatures. The electrothermal shield proposed by Thullen [17] has thus become an electrical shield at room temperature to intercept asynchronous flux and take the electromechanical stresses, and a thermal shield at cryogenic temperature to intercept thermal radiation.

This study of fault effects in the superconducting generator reveals additional benefits of the electrical and thermal shields for fault protection, but at the same time yields requirements upon their design to insure the ability of the generator to survive faults. This study is an attempt to develop the analytical tools necessary to predict the environment to which the rotor is subjected following the fault. The electrical, thermal, and mechanical responses of the affected parts are investigated in an attempt to identify potential critical failures. The steady-state aspects of the shields' performances are also compiled. Sample calculations have been made for the existing 80 KVA machine, the 2 MVA machine now being built, and power system size generators of 1000MVA rating, which is included in Chapter II to indicate the relative importance of the fault effects and the measures necessary to protect against them.

The ultimate test of how a superconducting generator performs under fault conditions can be answered only with some experimental experience with a real generator subjected to a fault. This study is primarily analytical, but supporting experiments to check critical aspects of the analytical models were performed and are reported in Chapter V.

The existing 80 KVA generator was subjected to a three-phase fault at low level. More experiments are planned for this machine and for the 2 MVA machine being built.

CHAPTER II

Results and Example Design

The purpose of this study is to evaluate the performance of a power-system size superconducting generator under fault conditions normally encountered in operation. The design requirements necessary to insure that the generator can survive fault conditions are to be identified and established. Two classes of fault conditions will be considered. The first will be a short-term fault which is cleared by a system circuit breaker. The duration of a short-term fault will be five to 15 cycles, depending on the type of circuit breaker. The second class of fault will be a sustained fault which occurs on the machine side of the system circuit breaker, such as the machine terminals, and cannot be cleared by circuit breaker action.

The criteria for survival of these two classes of faults will be as follows. To survive the short-term fault, superconductivity of the field winding must be maintained. If the superconducting winding is driven normal during the period before the fault is cleared, the machine must be removed from the system. If superconductivity is maintained, the machine can continue to supply power to the system through the remaining unfaulted lines after the fault has been cleared. To survive a sustained fault, structural integrity of the generator must be maintained so that permanent damage does not result.

Maintenance of superconductivity through a short-term fault requires that heat dissipation be limited in the cryogenic region where the field winding is located, and that the level of current induced in the field winding be limited. Superconductors can be driven normal, if their

temperature rises more than a few degrees, or if their current level increases above a critical level. Maintenance of structural integrity during a sustained fault requires that the rotor parts subjected to the large electromechanical stresses be substantial enough not to yield. The yielding criterion also applies to the short-term fault, but it is more critical for the sustained fault because of the large amount of heating due to the dissipation from induced currents in the rotor structure.

To maintain superconductivity, a rotating, electrically conducting shield must be provided to intercept the asynchronous magnetic fields produced by trapped armature fluxes and unbalanced conditions of the armature phases. The damper windings or bars of conventional generators serve this purpose, and limit heating of the rotor iron. However, for the superconducting generator, the electrical shield must not have thermal communication with the field winding region. The induced currents and dissipation must be intercepted outside the cryogenic region. This study shows that a shield which intercepts the induced currents and dissipation also intercepts the large electromechanical stresses associated with faults. To support these stresses, considerable mechanical structure must be provided for the electrical shield. A room-temperature electrical shield appears to be the most economical design, because of the large conduction heat leak through the structure which would result for a cryogenic shield.

To intercept thermal radiation from the room-temperature electrical shield, a secondary thermal shield is provided at a temperature somewhat above that of the field winding (e.g., 20° K). The electrothermal shield proposed by Thullen [17] thus becomes a room-temperature electrical shield to intercept dissipation and electromechanical stresses and a cryogenic

thermal shield to intercept thermal radiation.

The transfer of transient electromechanical stresses from field winding to a room-temperature electrical shield is very desirable, since it permits the use of minimum structure to support the field winding, and thus limit heat conduction into the 4.2° K region. However, during fault conditions, the power dissipation rate in the electrical shield far exceeds the cooling rate; therefore the electrical shield's temperature will rise, depending on its thermal capacity. Since structural properties of metals are degraded as their temperatures rise above room temperature, the ability of the electrical shield to withstand the electromechanical stresses is related to its thermal capacity.

In addition to the fault survival criteria which affect the electrical shield design, certain steady-state requirements must be considered. First, the electrical shield will serve as a damper winding to damp machine oscillations following a transient. Second, a steady-state electrical dissipation will occur due to slight armature current phase unbalance. The rotor cooling system must be designed to remove this heat. To minimize steady-state losses in the electrical shield, a highly electrically conducting material is desirable. This also makes the shield effective in intercepting asynchronous magnetic fields during fault conditions. But a highly conducting shield with sufficient thickness to provide thermal capacity provides very little damping. Conflicting requirements therefore result from shielding, steady-state dissipating, and damping.

The requirement upon the electrical shield design can be summarized as follows:

- 1) Keep steady-state power dissipation to a level acceptable for a reasonable cooling system.
- 2) Provide as much damping of machine oscillations as possible.
- 3) Maintain sufficient shielding of asynchronous magnetic fields to protect the superconducting winding in the steady state, and during short-term faults.
- 4) Provide thermal capacity to absorb transient dissipation without excessive temperature rise for a sustained fault.
- 5) Provide sufficient structure to support the transient electro-mechanical stresses.
- 6) Insure that no rotor mechanical natural frequencies are near frequencies of electromechanical or rotational stresses.

This study provides a quantitative expression of the above effects in order to arrive at an acceptable design which compromises between the conflicting requirements. The following sections of this chapter discuss the tradeoffs of shielding, damping, structural integrity, thermal capacity, and steady-state performance. Section II-4 presents a design for a 1000 MVA machine which is based upon these requirements. Chapters III and IV present in more detail the analytical tools which have been developed to evaluate the fault effects and steady-state requirements on the superconducting generator. Chapter V is a summary of experiments which have been performed to lend credence to some of the analytical expressions. Chapter VI is a summary of results and conclusions with suggestions for further work.

II-1 Keeping the Superconductor Superconducting

During the period immediately following a fault, the most adverse conditions are developed, which can tend to drive the superconducting field winding normal. Alternating currents are induced in the field winding, as well as a rise in the dc current level due to the demagnetizing effect of the armature fault currents. A large heat load is imposed in the rotor, due to trapped flux in the armature, and resulting imbalance of shorted armature phases. Alternating stresses are exerted in the rotor which can produce motion of the winding, and possibly degrade its performance. Just how critical each of these effects is in producing a superconducting to normal conductivity transition in the winding will require experimental investigation, as can be done with the generator presently being built. This section is intended to illustrate the design requirements for a shield to mitigate the adverse effects upon the field winding.

The degree of protection which the electrical shield affords the superconducting field winding is related to the shield attenuation factor. This factor indicates the degree to which asynchronous magnetic flux, produced in the stator, is excluded from the rotor, and is numerically equal to the ratio of the asynchronous magnetic field inside the shield to the asynchronous field which would exist without the shield. The factor is involved in expressions for induced field current, rotor heating in the cryogenic region, and mechanical stresses excited upon the field winding.

The attenuation produced by an electrical shield is a steady-state phenomenon dependent on the frequency of the asynchronous magnetic flux. Associated with any conducting cylindrical shield there is an L/R time constant equivalent to the time constant of the damper winding circuit

used to model generators. Due to the process of magnetic diffusion in the continuum conducting shield, there are in fact an infinite number of such time constants, but the longest of these we will call the "electrical shield time constant", T_{s1} and it is given by

$$T_{s1} = C\Delta\sigma\mu_o R$$

Δ = shield thickness

R = shield radius

σ = shield electrical conductivity

where C is a constant depending upon geometry. The relationship between attenuation factor and the shield time constant is simple for a shield whose thickness is less than the magnetic skin depth for the frequency of the asynchronous magnetic fields. If the shield is thicker than a skin depth, the expression is less direct.

For $(\omega_x T_{s1})^2 > 1$, ω_x = angular frequency of asynchronous flux, relative to the rotor,

$$K_{att} = \begin{cases} \frac{1}{\omega_x T_{s1}} & \delta > \Delta \\ 2\sqrt{2} \frac{\delta}{\sqrt{R_1 R_0}} e^{-\frac{\Delta}{\delta}} & \delta < \Delta \end{cases} \quad (II-1)$$

$$\delta = \left(\frac{2}{\omega_x \sigma \mu_o} \right)^{1/2} \quad \text{skin depth at frequency } \omega_x$$

Δ = shield thickness

R_1, R_0 are the inner and outer shield radii.

The above expressions do not correspond for $\delta = \Delta$ because higher-order correction terms have been omitted from the second expression for $\delta < \Delta$. However, it should be clear that, as the shield thickness Δ or

the shield conductivity σ increases, T_{s1} increases, and the attenuation factor becomes a smaller number.

Since protection of the field winding against conditions tending to drive it normal is related to the attenuation factor, the first impression is that K_{att} should be made as small as possible. This implies a shield with a very long T_{s1} . However, the shield must also serve as a damper winding. A shield with a long time constant has a low resistance, and is not very effective in damping machine swings. Reference [5] has shown that the optimum value of shield time constant for damping is given by

$$\omega_s T_{s1} = \frac{x + x_e}{x'' + x_e} \quad (\text{II-2})$$

where ω_s is the angular frequency of machine swings, and x_e is the external reactance through which the machine is connected to an infinite electrical bus. Reference [5] shows that this optimum shield time constant is nearly independent of x_e because of the dependence of ω_s upon x_e . Therefore, given the synchronous and subtransient reactances, the shield time constant for optimum damping is fairly well determined. As T_{s1} is increased or decreased from this optimum value, the damping coefficient is decreased, as predicted by reference [5].

Shield time constant and attenuation factor are related, as was indicated previously. Therefore the shield time constant cannot be set arbitrarily at the optimum damping value without consideration of the requirements for attenuation. These will be set by the induced field current and thermal dissipation in the cryogenic region during faults which can drive the superconductor normal. To provide a basis for the tradeoff consideration between damping and attenuation, induced field

current and heating are covered in the following section.

Induced Current in the Field Winding

Type II superconductors carrying direct currents with no loss will exhibit a transition to normal conductivity if sufficient alternating current is superimposed on the direct current. Losses are known to be associated with the alternating currents, [11,12], but evidence does exist that the transition is not independent of the dc level; that is, the transition appears to occur if the peak current (ac and dc) attains a critical value [10].

Following any type of short circuit on a synchronous generator, there is a rise in the direct current level in the field winding, and a superimposed alternating current. These changes in field current are due to the demagnetizing effect of the armature fault currents and the magnetic flux trapped by the shorted armature phases.

A conducting shield surrounding the field winding will attenuate the level of alternating current induced, but can only limit the rate of rise of the direct current level. In section IV-4, expressions for the induced field currents, ac and dc, for three-phase and line-to-line short circuits on a generator are presented. Following a three-phase short circuit on a generator occurring at $t = 0$, the field current will have the following form, assuming that the field time constant is much longer than the shield time constant:

$$i_f = i_{fo} \left[1 + \frac{x - x'}{x'} (1 - e^{-\frac{t}{T_d''}}) \right] + i_{fac}$$

The field current is expressed in per-unit, where the base is the field current necessary to produce rated open-circuit voltage. The

value i_{fo} is the per-unit field current before the fault; x, x' are the synchronous and transient reactances in per unit; T_d'' is the short circuit subtransient time constant which is related to T_{s1} by Eq. (A-15); i_{fac} is the peak per-unit value of induced alternating current in the field winding after the fault.

The field current before the short circuit i_{fo} will increase by an amount $\Delta i_f = (x - x') \Delta i_d'$ due to the demagnetizing effect of the armature currents. (For the three-phase fault $\Delta i_d' = V_{oc}/x'$, but other cases can be evaluated using Table IV-1.) This rise occurs exponentially with the subtransient time constant (which is related to the field time constant). The maximum level reached by the field current will depend upon the time necessary for the circuit breaker to interrupt the fault, and upon the value of the field time constant. If we assume that the circuit breaker can operate in 5 cycles, the maximum per-unit increase in field current can be calculated as a function of the field time constant. For a subtransient time constant short compared to 5 cycles, the field current rise will be about 0.6 per unit for a three-phase short circuit upon the 1000 MVA machine of section II-4. Other cases can be slightly worse. For example, operation at zero power factor overexcited with a line-to-line short circuit produces a field current of .84 per unit. Other cases can be estimated, using Table IV-1. Unsymmetrical short circuits from load depend on initial conditions and system reactance.

The point of the last paragraph is that, for a representative fault condition, such as a three-phase short circuit, it is possible to relate field current rise to shield time constant. The longer the shield time constant, the less the rise. But in making the shield time constant longer, damping ability of the shield is degraded. From reference [5] it is possible to calculate the change in damping coefficient for an increase in shield time constant above the optimum value. In addition, the level of induced alternating field current can be calculated, using Eqs. (III-8), Table IV-2, and Eqs. (A-53-54).

The results are plotted in Fig. II-1. The ratio $K_D/K_{D \text{ opt}}$ relates damping coefficient to its optimum value and the ratio $T_{s1}/T_{s1 \text{ opt}}$ relate shield time constant to the value of T_{s1} producing optimum damping. The plot of $K_D/K_{D \text{ opt}}$ versus $T_{s1}/T_{s1 \text{ opt}}$ indicates the loss of damping versus increase (or decrease) of shield time constant from its value for optimum damping. Also plotted are the per-unit values of field current rise and peak alternating induced field current versus $T_{s1}/T_{s1 \text{ opt}}$ for a three-phase short circuit from load with breaker opening after 5 cycles. For example, if T_{s1} is increased to twice its optimum value, damping will be 80% of optimum, field current rise will be limited to .39 per unit, and peak induced alternating field current will be 0.25 per unit.

Figure II-1 is intended to give an indication of the loss of damping associated with limiting the field current rise during a fault. The requirements of machine damping will depend on the installation. The field current rise will determine how the operating point of the superconductor is set so that superconductivity will not be lost before the breaker opens. It is obvious from Fig. II-1 that, even for the best

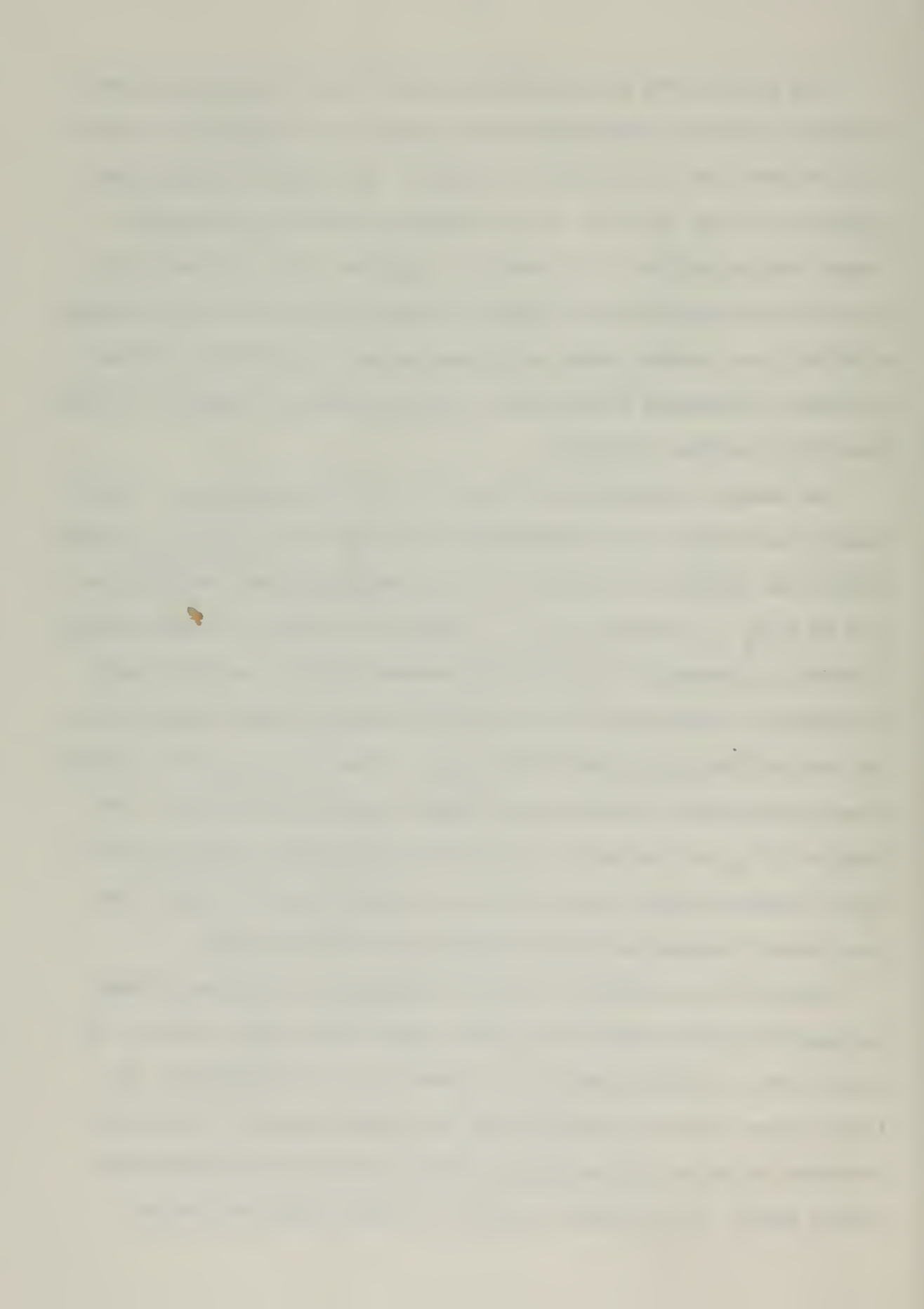
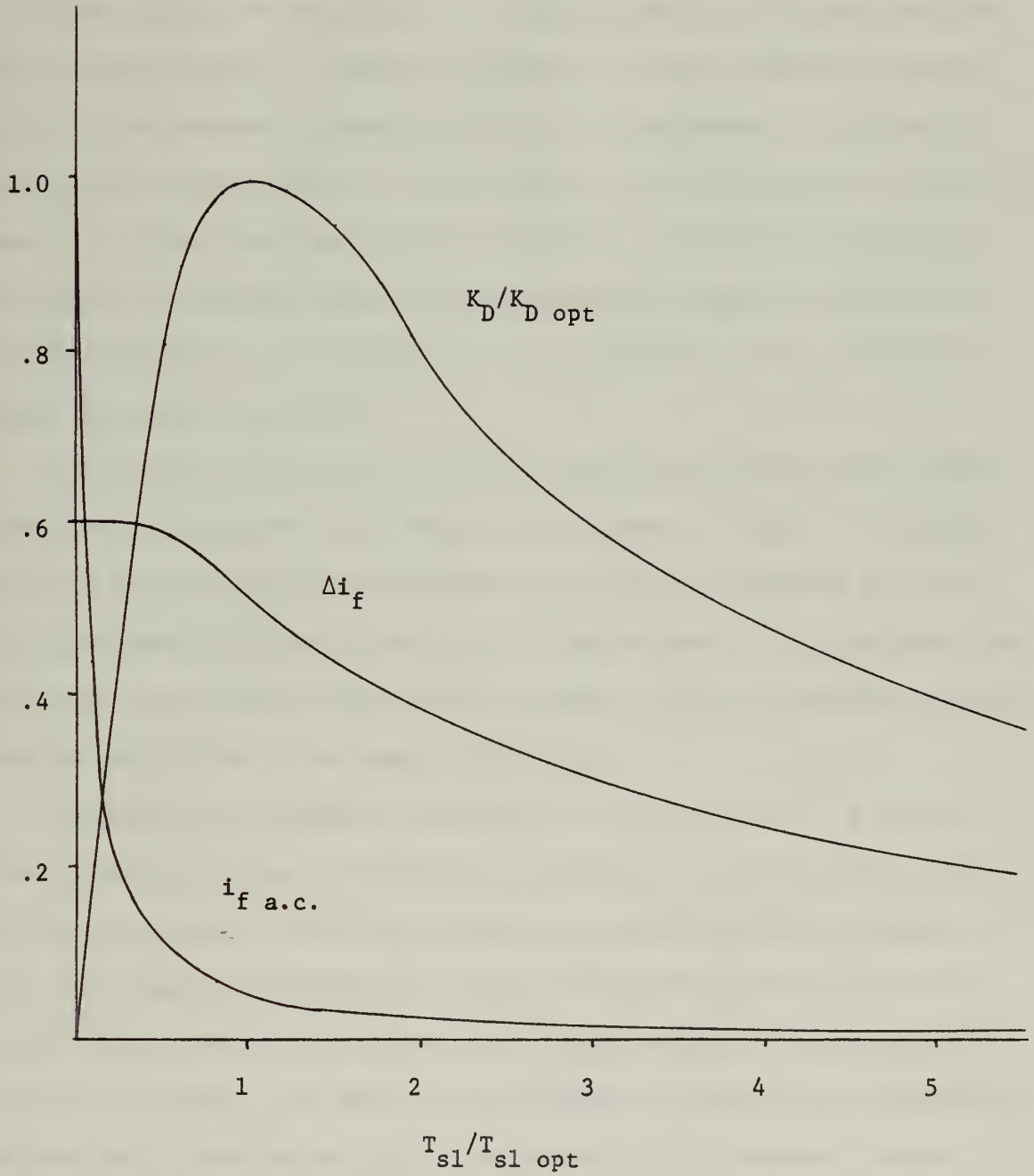


FIGURE II-1

Damping and Field Current Surge vs. Shield Time Constant



damping shield, the induced ac is small and the dissipation will probably have a smaller effect in causing a transition than the current level rise.

Heating in the 4.2° K Region During Faults

During the period immediately following a fault, considerable heating occurs within the rotor, due to trapped armature flux and imbalance of the shorted phases. The heating which is of most immediate interest, as far as maintenance of superconductivity is concerned, is the heating which occurs within the 4.2° K region where the field winding is located. There is a steady heat leak into this region, due to conduction through the mechanical supports from the room-temperature region radiation from the thermal shield, and dissipation from asynchronous flux which penetrates the electrical shield.

The cooling system must be sized to handle this steady-state energy input rate. During the fault period, an increase in this 4.2° K region heat load is experienced, the magnitude of which is dependent upon the electrical shield's attenuation factor. The sources of this increase are the larger asynchronous flux during the fault, and the increased radiation from the shield due to its temperature rise.

Two cases are of interest concerning heating in the 4° K region. First is the short-term fault which is cleared in 5 to 15 cycles. The total energy input to the 4° region must not raise the field winding above its critical temperature, so that superconductivity is not lost. Second is the case of a sustained fault which cannot be interrupted by the circuit breaker. In this case, the primary concern is not necessarily maintenance of superconductivity, but prevention of permanent damage to

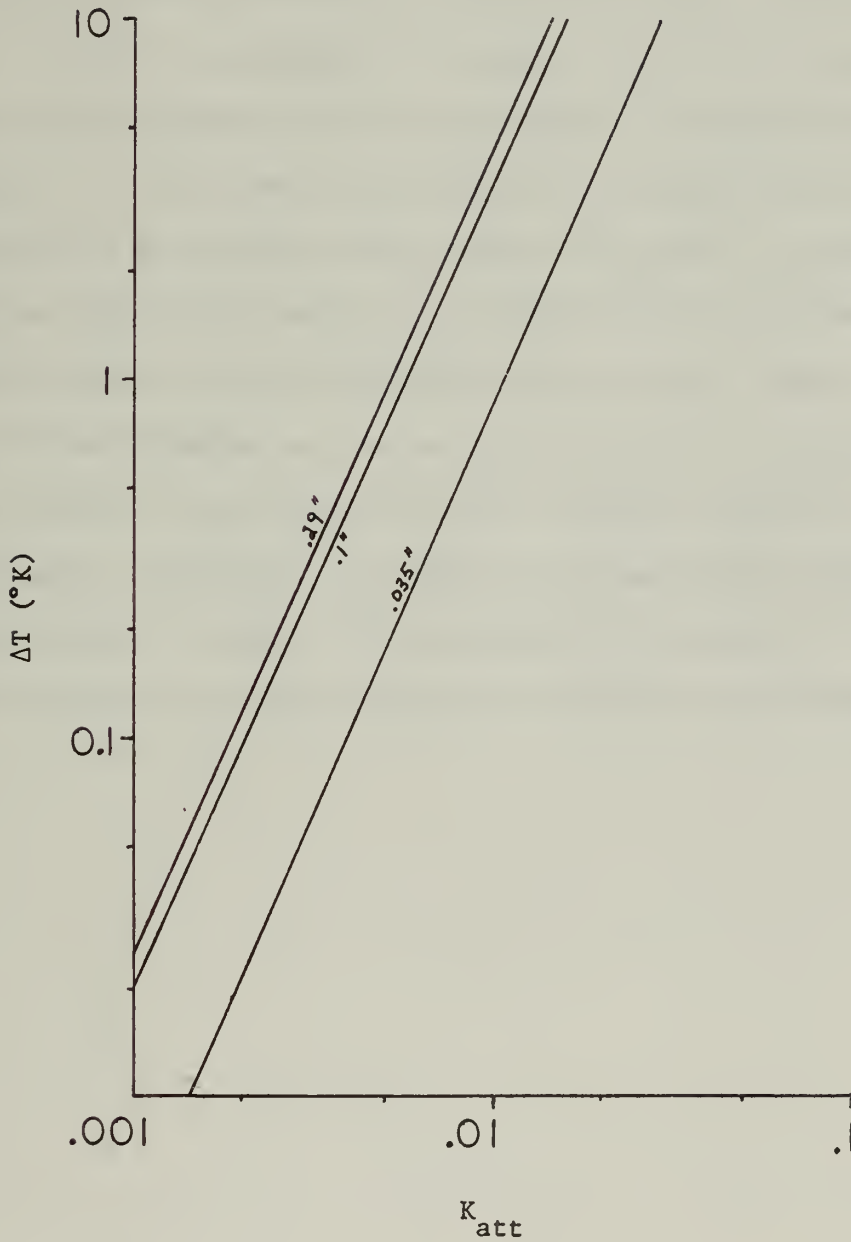
the machine. If the field winding is driven normal, a large dump of magnetic energy will occur within the cryogenic region. This must be anticipated in order that the rotor be designed to withstand such an occurrence.

The rate of energy dissipation in the containment vessel depends on the attenuation factor of the electrical shield, and on the thickness of the stainless steel vessel. For the 1000 MVA machine of section II-4a, stainless steel thickness of .29 inches gives maximum dissipation. A thinner shell is resistance-limited; a thicker one is reactance-limited until the shell is thicker than a skin depth, which is about 1.8 inches. The short term (5 cycles) temperature rise in the 4° region is shown in Fig. II-2 as a function of the electrical shield attenuation factor, and with containment vessel thickness as a parameter. This temperature rise depends upon the thermal capacity of the rotor. The liquid helium has by far the largest specific heat of any material in the 4.2° K region, and contributes almost all the total heat capacity. It has been assumed here that helium occupies 10% of the field winding volume. A larger percentage would give more heat capacity; however, if the field winding goes normal, all the liquid will be vaporized and must be vented. Therefore, for safety reasons, it is probably advisable to keep the percentage of helium as low as possible.

The results shown in Fig. II-2 indicate that maintenance of superconductivity for a short circuit cleared in five cycles will require that the attenuation factor for frequency ω_0 be kept below .01 in order to keep the temperature rise less than one degree. Optimum damping can still be realized for an attenuation factor less than .01 if the shield is thick compared to a skin depth, i.e., when the second part of Eq. (II-1)

FIGURE II-2

Temperature Rise in 4 Region vs. Shield Attenuation Factor



(Temperature rise for 3 phase fault cleared after 5 cycles
with containment vessel thickness as a parameter.)

applies. In section II-4 is presented an example in which optimum damping is obtained with an attenuation factor of .0016.

Another interpretation of Fig. II-2 is to say that the containment vessel should be made of a nonconducting material, or that some provision be made for breaking up the long eddy current paths in the containment vessel. However, stainless steel appears to be the best structural material for the containment vessel, and design of a laminated vessel would be difficult. It is probably more practical to assume that the proposed configuration of a stainless steel vessel will be used. In such case, an electrical shield with adequate attenuation will be required. Additional benefits result from an attenuation factor of .01 or less, as will be shown in the following section concerning structural integrity of the field winding. This attenuation can be realized consistent with reasonable damping. Therefore, it remains to be demonstrated that a shield can be designed to produce this attenuation and damping, and have sufficient structural and thermal capacity to survive fault condition itself.

II-2 Maintaining Structural Integrity of the Rotor During Faults

During the period following an armature short circuit, very large stresses are exerted on the rotor. The parts which are subjected to these stresses are at the same time being heated by induced currents, with the result that their structural properties are degraded. Maintenance of structural integrity involves consideration of the thermal capacity of the rotor parts subjected to the stresses and heating. The following sections discuss the magnitudes of the stresses exerted on the field winding and the electrical shield. The thermal capacity of the rotor for sustained faults is then investigated.

Rotor Fault Torques

The torque exerted upon the rotor following a short circuit has a large oscillating component and a much smaller unidirectional component. The maximum torque occurs during the subtransient period; if the rotor can survive the first few cycles, it will survive the fault, provided the mechanical natural frequencies of the turbine generator rotor are not excited by the oscillating stresses. A structurally sufficient model must therefore be substantial enough to resist the subtransient stresses and have its natural vibrational frequencies above the excitation frequencies.

Field Winding Fault Torques

One of the principal benefits of the electrical shield is the attenuation of oscillating torques applied to the field winding. Table II-1 shows the peak per unit total torque upon the rotor and the torque on the field winding for several types of faults from various conditions

of loading. The supporting calculations are from Appendix I with the analytical expressions from Chapter IV. For attenuation factors less than .01, as were seen to be required for maintenance of superconductivity during short term faults, the level of alternating field winding torque is less than 3 % of rated torque.

Table II-1 Fault Torques

Condition	Peak per unit Torque on Rotor	Peak Torque upon Field Winding for Various Attenuation Factors $K_{att} (\omega_o)$		
		.001	.01	.1
Three-phase short circuit at terminals from load at $p_f = .85$	6.7	.0025	.025	.25
Line-line short circuit at terminals from rated load at $p_f = .85$	10.5	.0017	.017	.17
Closure out of phase by 120° ($x_e = .26$)	6.35	.0014	.014	.14

The maximum torque which will be exerted upon the field winding is essentially the rated torque of the machine. The benefit of field winding fault torque limitation is that the structural supports for the field winding can be minimized. The conduction heat leak into the 4.2° K region can be reduced, thus reducing the capacity of the refrigeration system required.

Fault Torques Upon the Electrical Shield

The total reaction torque upon the rotor can be calculated independent of the details of damper shielding, as is done in many references (e.g. [14]). The total torque acting on the rotor is exerted primarily on the electrical shield, if the attenuation factor is low as is required to maintain superconductivity during the short-term fault. The peak alternating torques in per-unit acting on the shield are calculated from the expressions in section A-1-b and are listed in Table II-1 for various fault conditions.

If the electrical shield is to withstand the fault torques, the yield stress in shear of the shield material must not be exceeded at the maximum temperature reached by the shield under the fault condition. Torsional buckling of the shield is also possible, but for practical shield designs is a higher limit than yielding in shear. Torsional oscillation natural frequencies of practical shields are always considerably above the double line frequency of the fault torque for unbalanced faults. In section II-4 of this chapter, a shield design is proposed which is sufficient to resist these modes of failure.

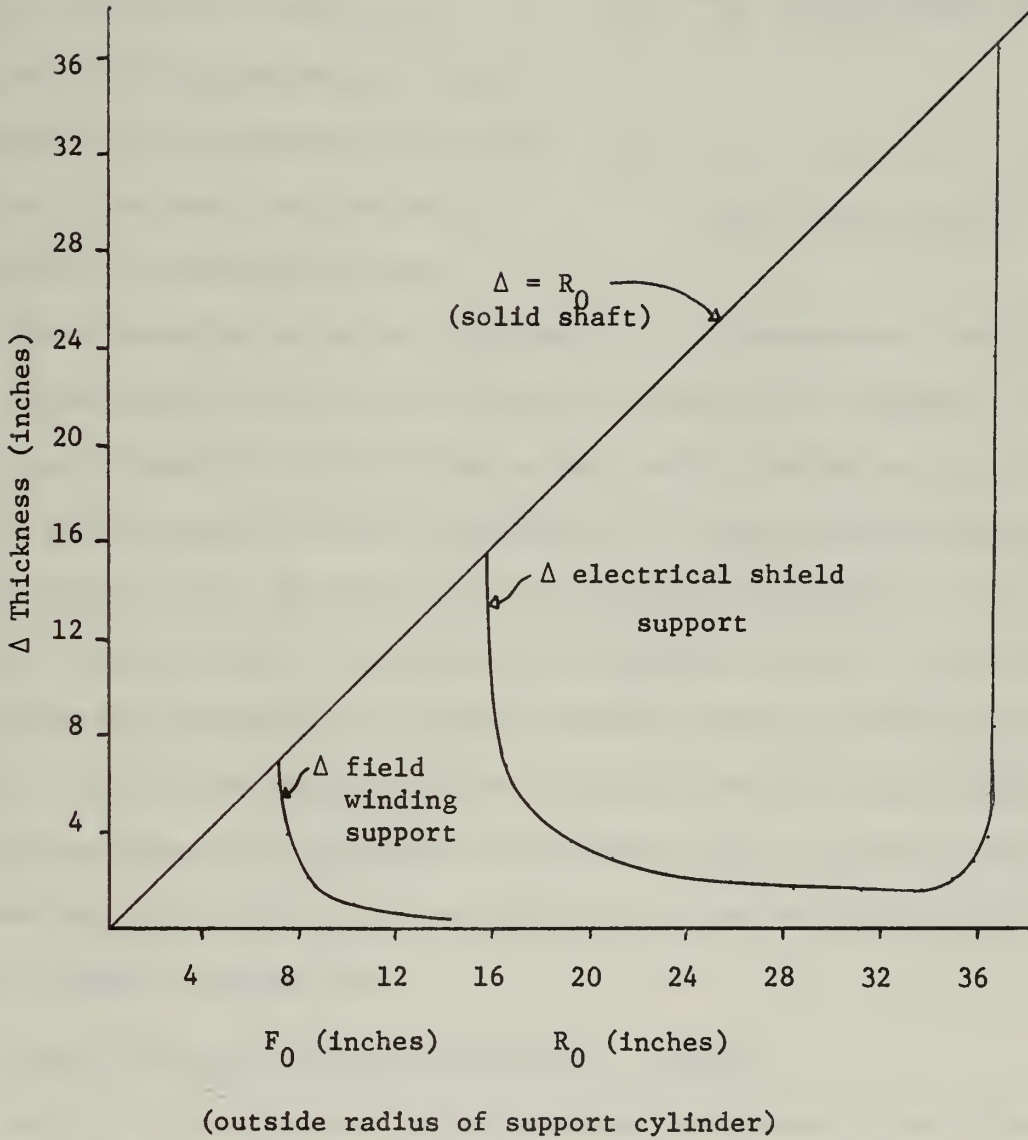
Since most of the fault torques are taken by the shield, its supports must have considerably more structural strength than the field winding supports. It is therefore more difficult to provide thermal isolation of the electrical shield consistent with adequate mechanical support. Although the MIT 2 MVA machine has a 20° K shield rotating in a vacuum relative-motion gap, it appears, based on structural support of the shield, that a room-temperature shield would be more practical for power-system-size generators. This assumes that adequate steady-state

cooling of the shield under slight imbalance is possible. This will be considered in the section on steady state performance. However, the most practical configuration for the 1000 MVA machine rotor appears to be a heavy, well supported, room-temperature electrical shield with the 4.2° K region containing the field winding, supported by thermal distance pieces which need to support only slightly above rated torque and can minimize the conduction heat leak. A secondary shield can be provided at approximately 20° K to intercept thermal radiation from the room-temperature shield. The conduction heat leak through the field winding supports can also be intercepted at 20° K, making the heat load in the 4.2° K region quite small.

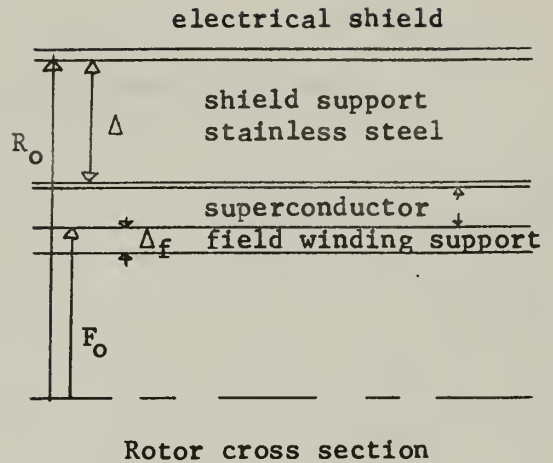
The amount of structure necessary to support the transient torques upon a 1000 MVA machine is considerable. Let us assume that the field winding is supported by a structure adequate to withstand rated torque, which is about the maximum it will feel as was shown in the last section. If the field winding is supported by a solid shaft of stainless steel with yield stress of 60,000 psi, it must be seven inches in radius. To allow for the helium plumbing and current leads, the support must, in fact, be hollow. Figure II-3 shows the required field support thickness Δ_f as a function of the outer field winding support radius F_o . As F_o increases, the required Δ_f decreases, lowering the heat leak to the 4.2° F region. For a value of $F_o = 9$ in., the rate of gain in thermal isolation is decreasing. If a 2-inch buildup of superconductor is assumed, the inner radius of the shield support is set. The right-hand portion of Fig. II-3 then indicates the required thickness of the shield support to withstand the maximum transient torque, which is approximately 10 per

FIGURE II-3

Shield and Field Winding Support Thickness vs.
Outer Support Radius



unit. The resulting shield support is roughly 5.4" in thickness. If the shield were to be run at cryogenic temperature, the heat leak through the supports would be at least 5 KW. Coupled with the steady-state shield dissipation (as discussed in the next section), this would require nearly a megawatt of refrigerator power.

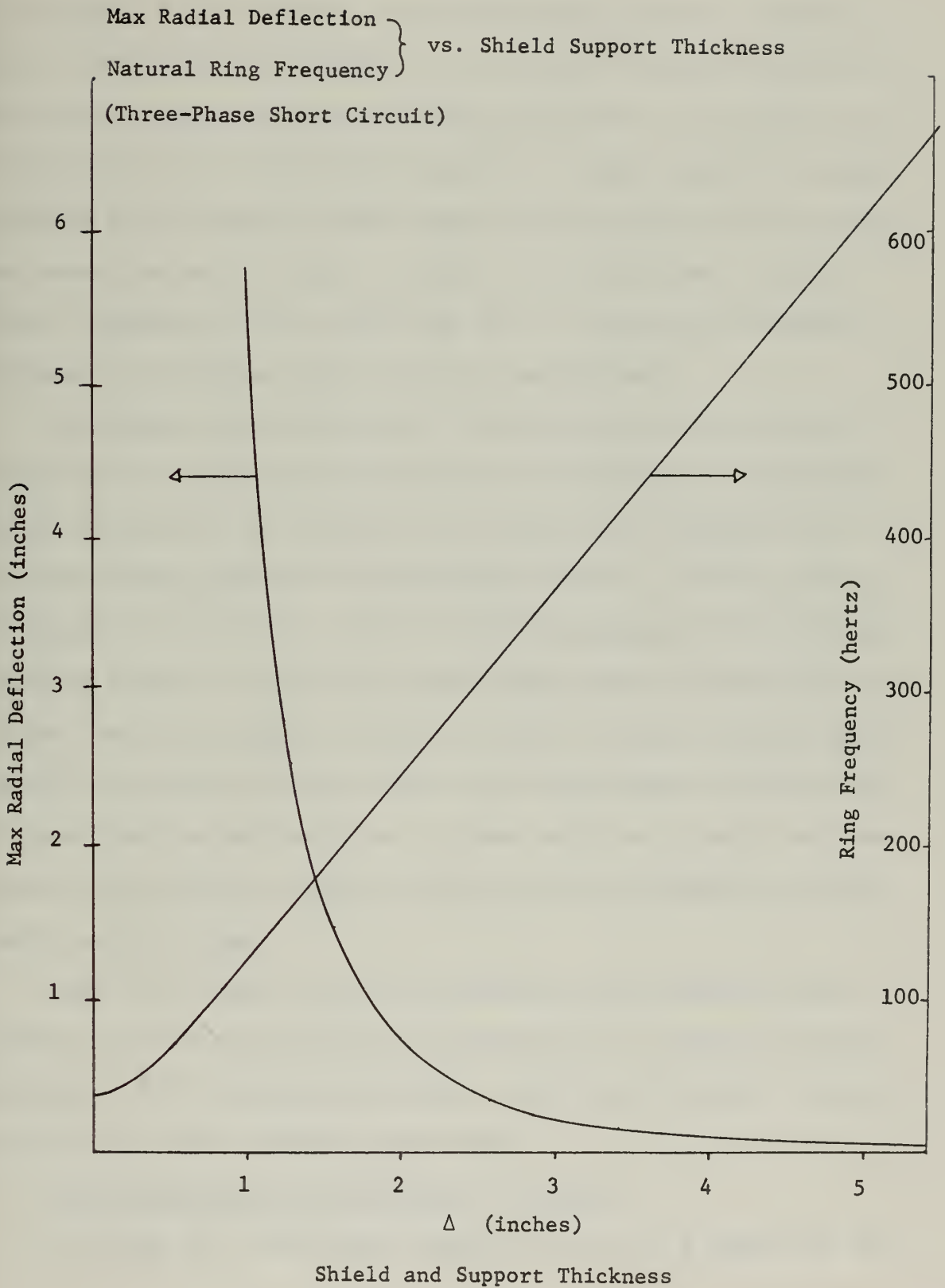


The alternative is to run the shield at room temperature, cooling it in a manner similar to the rotor cooling of conventional machines. The heat leak through the field winding support can be limited to about 523 watts, and no negative sequence dissipation is experienced under steady-state because of the shielding of the room-temperature shield. A second cryogenic shield at a temperature slightly above the field winding can be used to intercept the thermal radiation from the room-temperature shield. This second shield can also be used to provide a lower effective attenuation factor to asynchronous flux during faults, and thus limit the temperature rise during short-term faults. The over-all configuration will be given in section II-4.

Normal Stresses Upon the Electrical Shield

During the subtransient period following an armature short circuit, the demagnetizing flux produced by the armature fault currents is excluded from the electrothermal shield. A normal stress is produced which is nonuniform around the shield, and which tends to flatten it into an elliptical shape. In addition, the asynchronous fluxes as seen on the

FIGURE II-4



rotor produced by trapped armature fluxes and armature imbalance are also excluded from the shield. These fluxes also produce a traveling wave of deflection on the shield, so it must have sufficient rigidity to this type of stress to limit the maximum deflection to a tolerable level. If the shield is not sufficiently resistant to radial deflection itself, provision must be made for radial stops upon the surface of the containment vessel inside, to limit the extent of the deflection. The ring natural frequencies of the shield must also be kept above the highest frequency of excitation, which is twice line frequency.

The maximum radial deflection of the shield and its ring natural frequencies are primarily functions only of its thickness. Additional radial stiffness can be obtained by the addition of a stainless steel cylindrical shell inside the electrothermal shield. As will be seen in the design in section II-4, this is probably necessary to withstand the transient torques. In addition, radial stops located on the helium containment vessel and supported radially through the field winding support can also be provided. Contact would not be made between the shield and the stops under normal conditions, so there would be no radial heat conduction. Only during a transient deflection would the shield come into contact with the stops.

Figure III-4 shows a plot of the maximum radial deflection under transient and the lowest natural ring frequency as a function of shield thickness. For a self-supported shield, considerable material thickness is required to limit resulting deflections.

Thermal Capacity of the Electrical Shield

In section II-1, the thermal capacity of the 4.2° K region was con-

sidered to determine the temperature rise for a short-term fault in order to maintain superconductivity in the field winding. For a sustained fault upon a machine which cannot be interrupted, such as a three-phase short circuit at the machine terminals, the primary concern is the ability of the electrical shield to absorb the resultant heating without suffering permanent damage. The measure of a machine's ability to absorb transient heating which greatly exceeds the cooling rated is expressed by the quantity $I_2^2 t$, where I_2 is the per-unit negative sequence armature current, and t is the time for which I_2 is applied. For example, a machine with $I_2^2 t = 8$ seconds would withstand $I_2 = 1$ for a period of 8 seconds without permanent damage. The industry standard for turbine generators is $I_2^2 t \geq 8$ seconds. The standard is presently under discussion. Turbine generator manufacturers are trying to have the standard lowered, because of the difficulty of obtaining thermal capacity in conventional generator designs. To satisfy this requirement, the electrical shield must have sufficient heat capacity to absorb energy equivalent to $I_2^2 t \geq 8$ seconds without damage. A value of $I_2^2 t$ greater than 8 seconds would be very desirable.

If the material and thickness of an electrical shield is selected, a value for $I_2^2 t$ can be determined by assuming an initial operating temperature for the shield and performing a step-by-step calculation of the temperature as a function of time for $I_2 = 1$, taking into account the dependence of conductivity and specific heat upon temperature. The maximum temperature is determined by the loss of yield strength with increased temperature. At cryogenic temperature, specific heat and electrical resistivity of materials are both low; as temperature is increased,

both increase, but specific heat levels off near room temperature, while resistivity continues to increase. The result is that the $I_2^2 t$ associated with a temperature rise from 20° K to 300° K is about the same as that for a rise from 300° K to 650° K .

The nature of an $I_2^2 t$ number like 10 seconds is misleading. It implies that a machine can withstand a fault condition for 10 seconds, in which case thermal diffusion would permit heat to be distributed to all structure in contact with the electrical shield, and additional thermal capacity would be available from the stainless steel reinforcement backing the shield. In fact, what we are trying to provide is sufficient thermal capacity such that a terminal three-phase short circuit will not heat the shield to a point where structural damage can result. For a three-phase fault, the value of I_2 is of the order of $(x'')^{-1}$ which is 6.25 per unit, and the duration of the heating is approximately the armature time constant, which is about 0.3 second. In a period of .3 seconds, almost no heat is conducted into the underlying stainless steel because of its lower thermal conductivity. The value of $I_2^2 t$ required to absorb the dissipation of a three-phase terminal short circuit is

$$(I_2^2 t)_{3 \phi \text{ short circuit}} = \frac{V_{oc}}{x''} (T_a + T_d'')$$

This number is $I_2^2 t = 12.7$ seconds for the 1000 MVA machine of section II-4. In order to provide this thermal capacity, only the heat capacity of the conducting material of the shield can be relied upon. The implication is then that the conducting material must be made thick enough to provide the thermal capacity. However, from Eq. (A-56), it is seen that the shield time constant increases as the thickness. Calculation shows that a shield with sufficient thermal capacity at room temperature

initially, and of high-conductivity copper to reduce steady-state loss, would have a time constant three times the value for optimum damping, thus reducing the damping to 60% of optimum. For a copper shield at 20° K if sufficient thickness for heat capacity is provided, the electrothermal shield time constant will be nearly 150 times the optimum value, and produce almost no damping.

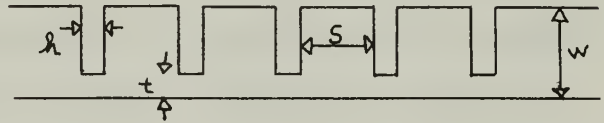
In order to overcome this problem, there are two possible alternatives. We can use a material of lower conductivity, permitting a thicker shield without an excessively long time constant. In order that the shield attenuate the asynchronous fields sufficiently to limit dissipation in the stainless steel support structure below it, the shield material should be thicker than the magnetic skin depth at the asynchronous frequency. The steady-state power dissipation is proportional to the square root of the shield resistivity. Hence, the higher-resistance material will result in larger steady-state shield dissipation.

A second alternative for providing thermal capacity of the shield, and limiting the shield time constant, is the use of a circumferentially slotted shield. This technique permits the designer to use a high-conductivity material for the shield, like electrolytic copper, and reduce the steady-state losses. The disadvantage is that the copper has low yield strength and must be held down upon its supporting tube with steel banding. The technique of slotting does permit independent selection of thermal capacity and time constant with the use of high-conductivity, low-loss material. The slotting technique is explained in the following paragraphs.

If narrow circumferential slots are machined into the shield, the

time constant of the shield is reduced because the resistance of the shield to axial current flow has been increased. In chapter V are presented expressions for the resistance increase associated with such an operation, along with experimental verification. The result is that, by proper selection of depth and spacing of slots, it is possible to adjust the time constant (and hence the attenuation factor) of a conducting shield without seriously affecting its thermal capacity.

Figure II-5 shows the cross-section of a shield taken by a plane containing the cylindrical axis. The shield's resistance to current flow and hence its time constant, are determined by the quantities S , t , and h , while the thermal capacity is determined primarily by the thickness, w .



Slotted shield cross section

Figure II-5

For example, a room-temperature copper shield 1.5 inches thick in the 1000 MVA machine would have an $I_2^2 t = 20$ seconds, but a time constant of $T_{s1} = .384$ seconds. Slots .1 inch wide and one inch deep, spaced one inch apart, will reduce the time constant to $T_{s1} = .189$ seconds, but maintain $I_2^2 t = 18.8$ seconds. The thermal diffusion time associated with conduction of heat through the one-inch-thick "fins" is .52 seconds, indicating that, for a .327 sec. armature time constant, approximately full advantage of the copper's thermal capacity will be realized. However, the thermal diffusion time for one inch of stainless steel is 14.5 sec., indicating that it will provide very little thermal capacity for transients.

Determination of the thermal capacity, or $I_2^2 t$, of a shield, depends on the maximum temperature to which the shield will be permitted to rise. For the example quoted in the last paragraph, the copper shield was permitted to rise to 650°K or 377°C . This is consistent with the temperature rise estimated for the amortissement of conventional generators for an $I_2^2 t$ of 8 seconds [20]. The rotor surface temperature for conventional generators for $I_2^2 t = 8$ seconds is estimated at 460°C and for $I_2^2 t = 12$ seconds, at 580°C from reference [20].

A temperature of 377°C is in the low annealing range for copper; hence, the maximum yield strength which can be counted upon is about 2000 psi for fully annealed copper. As shown in section II-4, this is insufficient to withstand the centrifugal stresses; sufficient strength to withstand the fault stresses can be provided by stainless steel backing. The big problem is in holding the copper on with steel banding.

Use of the slotted electrical shield proposed above can permit the machine designer to determine the thermal capacity, and hence the $I_2^2 t$, of the generator consistent with damping and attenuation requirements. It is possible to provide larger thermal capacity with the thick copper shield than with the iron rotor of a conventional machine, because of the larger thermal conductivity of copper. The iron rotor of the conventional machine is heated to extremely high temperatures before much heat has been conducted into the bulk of the rotor.

The first alternative, of a thick shield of higher resistance material, has been chosen for the design presented in section II-4. The material selected for the shield (Phosphor Bronze) has considerably higher yield strength than electrolytic copper; it can therefore withstand

the centrifugal stresses without external support rings, and can carry a significant portion of the shear stresses resulting from fault torques. The steady state dissipation for armature imbalance is higher than it would be for a slotted high-conductivity shield, but it is still small compared to the rotor heat load of a conventional machine of comparable size.

II-3 Steady-State Performance of the Electrical Shield for Unbalanced Load

The primary design consideration concerning steady-state operation of the electrical shield is the power dissipation due to armature current imbalance. To keep this dissipation as low as possible for a given material, the shield must be thicker than the skin depth of the induced currents due to imbalance, which is twice line frequency. The dissipation is then proportional to the square root of shield resistivity. This implies that advantage is gained from a cryogenic shield; however, the important factor is the amount of refrigerator power required to remove the heat dissipated in the shield. Added to this negative-sequence heating is the conduction heat leak for a refrigerated shield. Because of the heavy supports necessary to support transient torques, this heat leak is quite large.

Table II-2 gives a comparison between the heat loads due to negative sequence and conduction for shields at room temperature, 77° K, and 20° K. Also computed are the refrigerator power for the cryogenic shields and the cooling power for the room-temperature shield. The numbers concerning refrigerator power should be taken only as qualitative, but do indicate the very definite trend that higher shield temperature can be cooled

more economically.

Table II-2

Cooling Power Required for Shield as a Function of
Shield Temperature

Shield Temp- erature °K	Conduction Heat Load (KW)	Dissipation for I = .1 (KW)	Total Heat Load (KW)	$\frac{P_{\text{compressor}}}{P_{\text{refrig.}}}$	Total blower or compressor Power (KW)
20	5	10	15	50	750
77	4	35.4	39.4	9.4	370
300	0	150	150	(add 100KW for fan power)	250

The other steady-state considerations of the shield's performance are its mechanical natural frequencies, and the centrifugal stress level in the conducting layer. The critical natural frequencies include the torsional frequency of the shield, the ring natural frequency for radial vibration, and the lateral vibration frequency of the shield between its end supports. The formulae for these calculations are given in chapter III, and results for a 1000 MVA machines are in section II-4. None of these natural frequencies appears to be a problem because of the thick shield support required by transient torques.

The stress in an outer, high-conductivity copper layer due to centrifugal stress is a problem, because of the rotor diameter. The yield stress of the copper is low because of its purity and annealed condition. The critical radius for centrifugal stress at a yield stress of 10,000 psi is 13 inches. Since the rotor must be larger than this, it would be necessary to provide retaining rings of stainless steel upon the copper

shield. The dissipation in these rings is small because of their limited axial length. Another possibility is to use fiberglass or some other nonconductor to tie down the electrothermal shield copper layer. Use of a lower-conductivity, higher-strength material can eliminate this problem, as has been done in the design presented in section II-4.

II-4 1000 MVA Superconducting Generator; an Example

Designs for 1000 MVA superconducting generators by Thullen [17] and Kirtley [21] have not included consideration of the electromechanical stresses imposed on the rotor during faults. Least-weight designs have been developed, but calculations show that they are not structurally sufficient in the rotor to withstand the transient torques and forces. The design presented in this section has started with the least-weight configuration developed by Kirtley [21] and altered it in such a manner as was necessary to produce a machine which can survive fault conditions consistent with the results of this study.

Considerable weight has been added to the rotor; however, this is necessary to provide structural integrity. The least-weight machine on the basis of Kirtley's work, had been shown to be long and small in diameter, as opposed to the previous design developed by Thullen [17]. It has been necessary in the present design to increase rotor diameter somewhat; however, an effort was made to keep the rotor diameter as small as possible, in the belief that this is probably nearer the least-weight configuration that could be developed consistent with fault-survival ability. No weight optimization has been done for the present design, but it can be done using Kirtley's techniques with the requirement for fault survival included. The design used by Kirtley did not have an

iron shield over the end turns. The end turns are then assumed to contribute inductance, but generate no voltage. More recent designs have included iron shielded end turns which contribute more to effective length. Therefore, optimum designs may in fact be shorter and larger in diameter. Such a machine makes satisfaction of fault-survival criteria even easier, because of the increased effectiveness of rotor structure at a larger radius.

It was decided to develop a design which maintained a subtransient reactance of .15 per unit. Decreasing the subtransient reactance to a lower value results in a rapid increase in the maximum per-unit transient torque which must be tolerated. A 15% subtransient reactance results in a maximum subtransient torque of about 10 per unit; this is for a line-to-line short circuit at the terminals while operating at rated condition. The three-phase short circuit at the terminals results in a maximum torque of 6.7 per unit. The case of 10 per unit torque may seem rather drastic, but the object is to show that it is possible to develop a design consistent with such a requirement; the occurrence of such a fault is entirely conceivable.

The thermal capacity of the shield for this design will have a thermal capacity indicated by an $I_2^2 t$ of 20 seconds for a 361°C temperature rise of the shield. This is considerably more than the available $I_2^2 t$ for conventional generators of similar rating.

Maintenance of superconductivity through the short-term fault depends upon the shield attenuation factor and the thermal capacity of the liquid helium region. The attenuation resulting from the electrical shield for this design is .0016; the temperature rise in the helium region

for a short circuit cleared in five cycles less than $.1^{\circ}$ K, and for one cleared in 15 cycles is less than $.3^{\circ}$ K. The induced alternating field current is .0048 per unit, and the dc rise is .24 per unit. Proper placement of the superconducting winding operating point relative to short sample characteristics should guarantee maintenance of superconductivity through these conditions. The secondary, or thermal, shield can be designed to decrease the problem of field current surge. Since this shield is subjected to almost no electromechanical stresses, it can be designed with the proper time constant necessary to limit the field current surge consistent with the ability of the exciter to control the field current change.

The damping coefficient of the present design has been optimized for the estimated swing frequency of the turbine-generator system. The amount of damping will depend on the shield temperature during the period of machine swinging. However, the power dissipated in swinging will be distributed throughout both the shield and its stainless steel support tube. Considerable thermal capacity is therefore available, and the temperature rise should be rather small. Therefore the effective time constant and damping coefficient should not change radically throughout the period of machine oscillations.

Mechanical natural frequencies of the rotor relative to lateral vibrations, torsional oscillation, and ring vibrations are all high enough that they should cause no problems. The field winding supports have been minimized, making the lateral natural frequency of the field winding the lowest expected natural frequency. This calculation has neglected any stiffening due to the winding itself; the true lateral

natural frequency will therefore be somewhat higher. Steady-state dissipation due to 10% negative sequence is 141 KW. The windage will be comparable to a conventional machine. However, the shield dissipation is less than 5.2% of the field winding i^2R losses for a conventional generator of this size. Therefore, cooling of the shield by conventional techniques should not be difficult; the rotor could operate in a partial vacuum to eliminate windage, but shaft seals must then be provided.

The heat load in the 4.2° K region under steady-state conditions is primarily conduction through the supports and radiation from the secondary shield. These losses can be intercepted at a slightly higher temperature, such as 20° K, reducing the 4.2° K heat load to a few watts. The secondary shield will act primarily as a radiation shield, and will not be subjected to the subtransient mechanical stresses and heating during faults which is taken by the primary, room-temperature shield. The cryogenic secondary shield can be made quite thin, of high-conductivity material, and cooled by conduction from the ends.

Figure II-6 shows a drawing of the proposed design, and Fig. II-7 shows more detail of the rotor. Table II-3 lists machine parameters and characteristics.

Figure II-6

1000 MVA Superconducting Generator

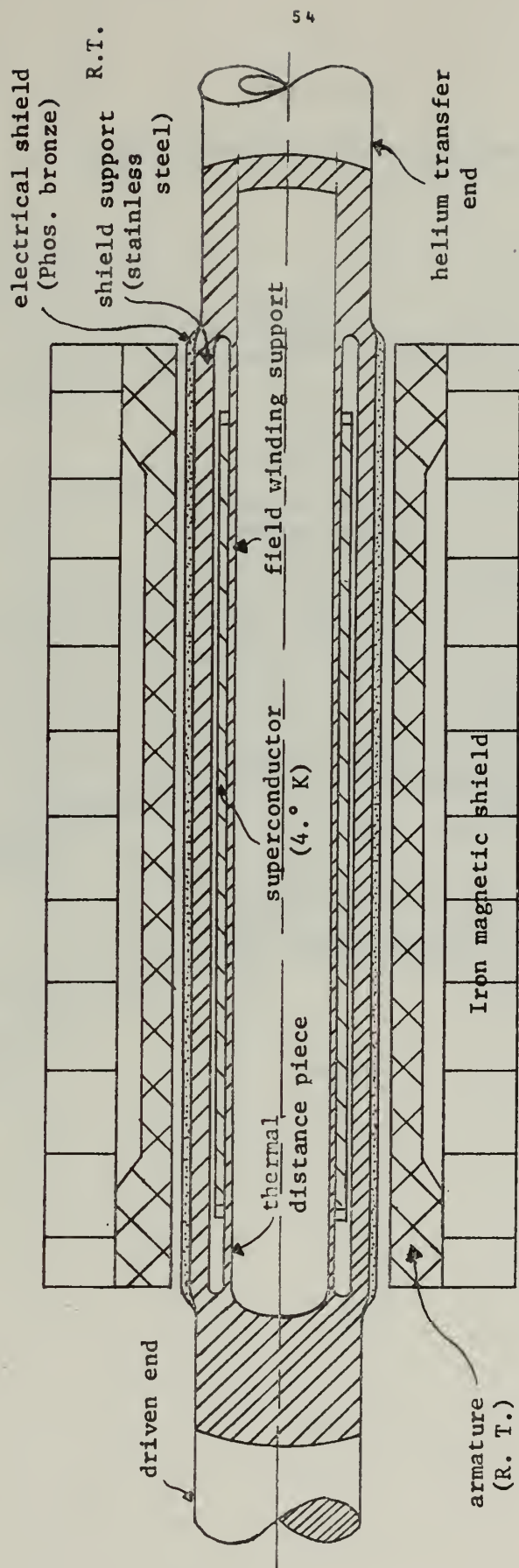
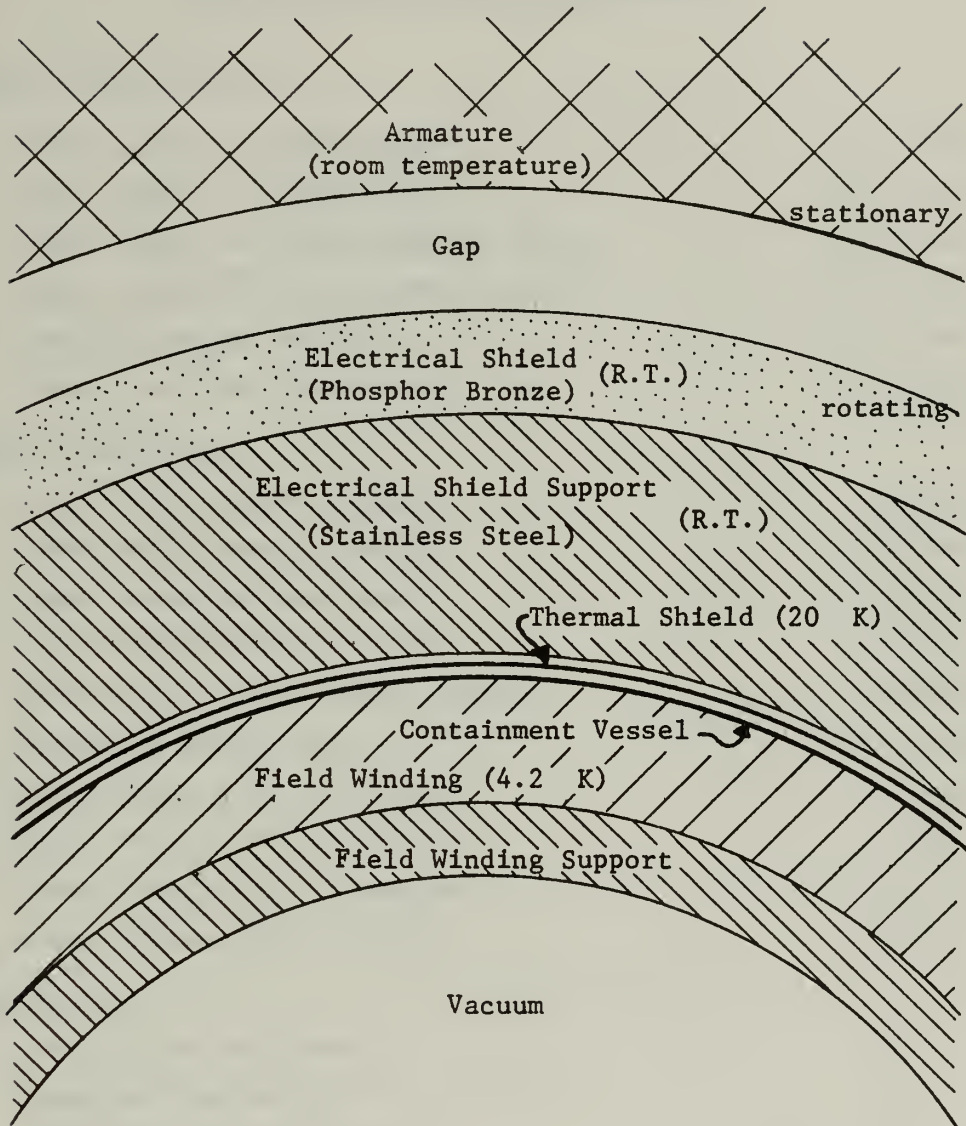


FIGURE II-7

1000 MVA Design Rotor Cross Section



Axis

+

Table II-31000 MVA Superconducting Generator

Stator Dimensions:

Inner Radius of Conductors	19.5 in.
Outer Radius of Conductors	25.0 in.
Inner Radius of Iron Magnetic Shield	29.0 in.
Outer Radius of Iron Magnetic Shield	41.7 in.
Length Straight Section	121.3 in.
Length Each End-turn Region	22.5 in.

Rotor Dimensions:

Inner Field Support Radius	8.95 in.
Outer Field Support Radius	10.0 in.
Inner Superconductor Radius	10.0 in.
Outer Superconductor Radius	12.0 in.
Helium Containment Vessel Radius	12.0 in.
Secondary Shield Radius	12.1 in.
Inner Primary Shield Support	12.2 in.
Outer Primary Shield Support	16.0 in.
Inner Primary Shield Radius	16.0 in.
Outer Primary Shield Radius	17.6 in.

Reactances:

Synchronous Reactance x	.59
Transient Reactance x'	.37
Subtransient Reactance x''	.15

Primary Shield and SupportShield Material:

Phosphor Bronze A

95% Cu, 5% Sn

Hardness: Rockwell B-91

 $\sigma_y \approx 80,000 \text{ psi}$; Fatigue Strength for 10^8 cycles = 33,000 psi $\rho(300^\circ \text{ K}) = .107$; $\delta(\omega_o) = .835''$, $\delta(2\omega_o) = .59''$ Shield Support Material:Stainless Steel $\sigma_y \approx 60,000 \text{ psi}$ $\rho(300^\circ \text{ K}) = .725$; $\delta(\omega_o) = 2.17''$, $\delta(2\omega_o) = 1.54''$

	<u>Thickness</u>	<u>Time Constant (ms)</u>
Shield Primary	1.6''	159
Support Material	3.8''	$\frac{55.5}{214.5} \text{ ms.}$

 T_{s1} optimum damping = 212 ms for $\omega_s = 10$;, i.e., $f_s = 1.6 \text{ hz.}$

Power Dissipation in Phosphor Bronze:

$$I_2 = .1$$

141 KW

$$K_{att}(\omega_o)_{\text{bronze}} = .0207 \quad K_{att}(\omega_o)_{ss} = .076$$

Stresses in Shield

$$\sigma_{\text{yield stainless steel}} = 60,000 \text{ psi}$$

$$\sigma_{\text{yield phosphor bronze}} = 80,000 \text{ psi}$$

$$\text{Max. Transient Torque} = 10 = 240 \times 10^6 \text{ in. lbf.}$$

$$\sigma_{\text{shear due to transient torque}} = \frac{2 T R_o}{\pi(R_o^4 - R_i^4)} = 36,440 \text{ psi}$$

$$\sigma_t \text{ (centrifugal hoop stress)} = 18,340 \text{ psi}$$

Max. shear from Mohr's circle

$$\sigma_{s \text{ max}} = 37,500 \text{ psi} = .47 \sigma_{\text{tensile yield}}$$

Overspeed centrifugal stress (5,400 rpm)

$$\sigma_t \text{ (5400 rpm)} = 41,100 \text{ psi}$$

$$\sigma_{\text{shear max}} = 20,600 \text{ psi}$$

Maximum Radial Deflection for 3 ϕ Short Circuit = .037 in.

Mechanical Natural Frequencies

$$\text{Lateral Vibration of Shield } f_1 = 176 \text{ hz.}$$

$$\text{Lateral vibration of Field Winding } f_1 = 50 \text{ hz.}$$

$$\text{Torsional Natural Frequency Shield } f_t = 442 \text{ hz.}$$

Torsional Natural Frequency Field

$$\text{Winding } f_t = 256 \text{ hz.}$$

$$\text{Ring Frequency at Standstill Shield} = 655 \text{ hz.}$$

Ring Frequency at Standstill Field

$$\text{Winding} = 177 \text{ hz.}$$

Thermal Capacity

Shield Initial Temperature = 27° C

$I_2^2 t$	T_{\max} Phosphor Bronze
10 sec.	193° C
20 sec.	361° C
25 sec.	446° C

Max Shield Temp. for three-phase short circuit

at terminals = 251° C

Max Shield Temp. for line-to-line short circuit at terminals

assuming field winding discharged in 5 sec. = 273° C

Heat Loads in Cryogenic Region

Secondary Shield at 20° K

Thermal distance piece length	= 16 in.
thickness	= 1.05 in.
Conduction	523 watts
Radiation	103 watts
Negative sequence (< 1 watt)	<u>0</u>
	626 watts @ 20° K

Field Winding Region 4.2° K

Thermal distance piece length	= 8 in.
thickness	= 1.05 in.
Conduction	2 watts
Radiation	neg.

Refrigerator Compressor Power 33.3 KW (< 10⁻⁴ of machine rating)

Estimated Weights

Rotor:

Field winding support	320
Field winding	5070
Shield Support	14680
Shield	9190
Shaft (20 inches each end)	<u>8060</u>
	37,320 lbs. rotor

Stator:

Armature	24970
Iron Shield	<u>136700</u>
	<u>161,670 lbs. stator</u>
	198,990 lbs. total

Rating 985 MVA

.202 lbs/KVA

The proposed design has a synchronous reactance of .59 compared to nearly 2.0 for a conventional machine of similar size. The .202 lbs/KVA weight is nearly an order of magnitude less than that for a conventional machine. The thermal capacity, as indicated by $I_2^2 t$, is at least 20 seconds compared to 8 to 10 seconds of present iron rotor design. The efficiency is about 99.8% compared to 98.7%, and the rotor natural frequencies are all high compared to conventional machines. Thus, the advantages associated with superconducting generators have been maintained while satisfying the criteria for survival of fault conditions.

CHAPTER III

Steady-State Effects Upon the Electrical and Thermal Shields1) Heating of the Rotor

A heat load is imposed upon the rotor of the generator by eddy currents, conduction through structure, and radiation. The heat load will be distributed among the electrical shield, the cryogenic thermal shield, the stainless steel can and supports, and the superconducting winding, depending on the design of the electrical and thermal shields. In chapters III and IV, the word "electrothermal shield" is sometimes used. This refers, in general, to the electrical and thermal shield combination. When considering mechanical stresses, attenuation, and eddy current heating, it refers to the electrical shield; for thermal radiation, it refers to the thermal (cryogenic) shield.

a) Sources of Heating1. Radiation

The heat flux due to radiation between two coaxial cylinders assuming diffuse reflection, is

$$\frac{Q}{A} = \sigma \frac{1}{\frac{1}{\epsilon_1} + \frac{A_1}{A_2} \left(\frac{1}{\epsilon_2} - 1 \right)} (T_2^4 - T_1^4) \quad (\text{III-1})$$

where ϵ_1, ϵ_2 are the emissivities of surfaces having areas $A_1 + A_2$ and temperatures $T_1 + T_2$. The areas $A_1 + A_2$ are nearly equal, and $T_2^4 \gg T_1^4$.

$$Q = \frac{A \sigma \epsilon_1 \epsilon_2}{\epsilon_2 + \epsilon_1 - \epsilon_1 \epsilon_2} T_2^4; \quad A = \text{area of thermal shield}$$

$$T_2 = \text{stator temperature}; \quad \sigma = 5.33 \times 10^{-8} \text{ watts/ft}^2 \text{ } ^\circ\text{K}$$

(2) Stator Phase Imbalance

The load supplied by most power system generators is not perfectly symmetric with respect to the three phases resulting in unbalanced current between the three phases. The imbalance of currents results in a negative sequence component of armature current, that is, one producing a magnetic field which rotates in the reverse direction to the rotor rotation. Formulae for determining the magnitude of the negative sequence current component are well known, and given in any power systems textbook. The newest standards for power system generators require that they be able to withstand 10% negative sequence, steady state.

The power dissipation in the shield due to a per-unit negative sequence current I_2 is obtained from Eq. (A-50) and Eq. (A-52), where

$$\omega = 2\omega_0 \text{ and } n = 1.$$

Negative Sequence Power Dissipation:

$$P_d = \begin{cases} \frac{2\pi}{\omega_0} \frac{R^2}{\left[1 \pm \left(\frac{R}{T}\right)^2\right]^2} \frac{1}{T_{s1}} \left(\frac{(2\omega_0 T_{s1})^2}{1 + (2\omega_0 T_{s1})^2} \right) \ell B_{I_2}^2 & \Delta < \delta \\ \frac{4\pi\ell}{\sigma\delta\mu_0^2} \frac{R}{\left[1 \pm \left(\frac{R}{T}\right)^2\right]^2} B_{I_2}^2 & \Delta > \delta \end{cases} \quad (\text{III-2})$$

$$\delta = \left(\frac{1}{\omega_0 \sigma \mu_0} \right)^{1/2}$$

$$B_{I_2} = \frac{\mu_0 S_0}{2} \left\{ 1 - x \pm \frac{1}{3} (1-x^3) \left(\frac{S_0}{T} \right)^2 \right\} \frac{3\sqrt{2} J_A I_2}{\pi}$$

$$J_A = \text{rated armature current density amp/m}^2 \text{ rms}$$

(3) Stator Harmonics

If all three phases of the generator are perfectly sinusoidally wound, a uniform magnetic field will be produced rotating at synchronous angular frequency by balanced phase currents. Spatial harmonics of order higher than the fundamental produce magnetic fields which rotate at different angular frequencies, some of which will induce currents in the shield and produce losses.

Harmonics which are multiples of three produce no rotating component; harmonics 5, 11, 17, $6m+1$ produce negative sequence fields rotating at angular frequency ω_o/n , or at $\omega_o(1 + \frac{1}{n})$ relative to the rotor; harmonics 7, 13, 19, ... $6m+1$ produce positive sequence fields at angular frequency $\omega_o(1 - \frac{1}{n})$ relative to the rotor; since the windings are symmetric odd distributions about their axes, there are no even harmonics.

The harmonics for a distributed winding between radii S_i and S_o with 60° phase winding angle are

$$J_n = - \frac{6 \sqrt{2} J_A}{n\pi} \cos \frac{2n\pi}{3}$$

$$P_{dn} = \begin{cases} \frac{2\pi}{\mu_o} \frac{R^2}{[1 \pm (\frac{R}{T})^{2n}]} \frac{1}{T_{sn}} \left(\frac{(\omega_{rn} T_{sn})^2}{1 + (\omega_{rn} T_{sn})^2} \right) \ell B_{on}^2 & \Delta < \delta_n \\ \frac{4\pi \ell}{\sigma \delta_n \mu_o} \left(\frac{R}{1 \pm (\frac{R}{T})^{2n}} \right) B_{on}^2 & \Delta > \delta_n \end{cases} \quad (\text{III-3})$$

$$\delta = \left(\frac{2}{\omega_{rn} \mu_o \sigma} \right)^{1/2}$$

The relative angular velocity of the n^{th} harmonic ω_{rn} is given by

$$\omega_{rn} = \begin{cases} 0 & n = 3, 6, 9, \dots \quad 3m \\ \omega_o (1 + \frac{1}{n}) & n = 5, 11, 17, \dots \quad 6m-1 \\ \omega_o (1 - \frac{1}{n}) & n = 7, 13, 19, \dots \quad 6m+1 \end{cases}$$

$$B_{on} = \left[\frac{\mu_o}{2} \right] \left[\frac{R^{n-1}}{2-n} S_o^{2-n} (1 - x^{2-n}) \pm \frac{R^{n-1}}{T^{2n}} \frac{S_o^{n+2}}{n+2} (1 - x^{n+2}) J_n \right] \quad (\text{III-4})$$

The armature is usually made up of discrete bars which yield large amplitude spatial harmonics for n near the number of bars per row. Some concern that losses due to these bar harmonics might be considerable led to the following analysis.

Each row of armature bars can be modeled as impulses of current at a constant radius. The magnitude of the n^{th} harmonic current sheet representing the row of bars shown is calculated from the formula

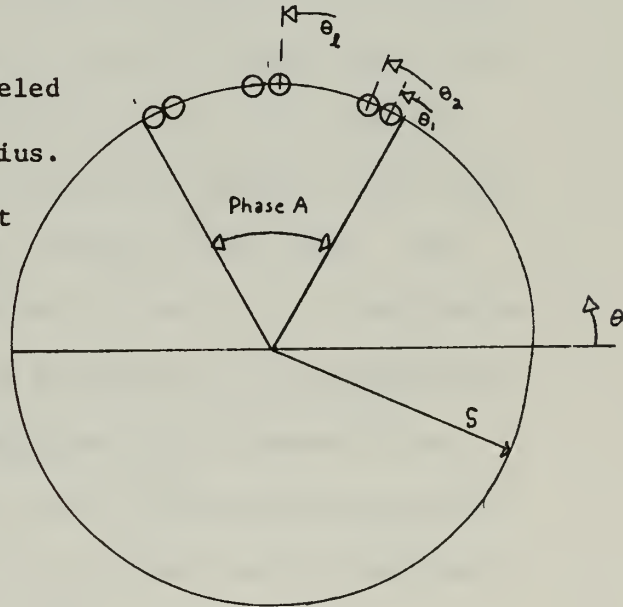
$$K_n = \frac{6 \sqrt{2} I}{\pi S} \sum_{i=1}^{\ell} \sin n\theta_i \quad (\text{III-5})$$

I = current in each bar rms

ℓ = one half the number of bars on one

side of the machine in the row at $r = S$.

$$B_{on} = \frac{\mu_o}{2} \left(\frac{R}{S} \right)^{n-1} \left[1 \pm \left(\frac{S}{T} \right)^2 \right] K_n \quad (\text{III-6})$$



The power dissipation due to each harmonic for each row of bars can be evaluated by Eq.s. (III-6) and (III-3) using the appropriate value of n

and S for each harmonic and row. The total time average power is the sum of the contributions of all harmonics for all rows, because the harmonics are orthogonal and the same harmonic for different rows are in phase.

b) Distribution of the Rotor Heat Load

The rotor of a superconducting generator will be arranged with the superconductor mounted upon a center spool, probably of stainless steel, a stainless steel containment vessel around the field winding to contain the liquid helium, with a thermal shield at approximately 20° K and an electrical shield at room temperature. If no electrical or thermal shield were included, the steady-state negative sequence component would induce currents in the stainless steel containment vessel and impose a heat load in the 4° K region. Since the stainless steel shell is a poor shield, due to its poor electrical conductivity, alternating currents would also be induced in the superconducting winding, producing loss there. The amount of dissipation within the superconducting wire and its consequences can be determined only with some operating experience with the experimental machine being built. However, the magnitude of the losses in the containment shell can be predicted, based on the electrical shield parameters, and the magnitude of the induced field current can be predicted.

1) Electrical Shield Heat Load

The total electrical shield heat load will be composed of the sum of negative sequence heating and stator harmonic heating. The calculation of these components is made using Eq. (III-2) for negative sequence and (III-3) for armature harmonics. The calculation of the resultant steady-state shield temperature must involve the cooling

mechanism for the shield. For example, the M.I.T. 2 MVA machine has a cryogenic shield cooled by conduction at the ends. Some heat will be lost by radiation to the colder region inside. This component of cooling is really more important in predicting the heat load on the radiation shield inside; it can be calculated from Eq. (III-1) after the approximate operating temperature of the electrical shield has been determined.

2) Stainless Steel Containment Vessel Heat Load

Radiant energy from the thermal shield and asynchronous magnetic fields which penetrate the electrical shield impose the heat load on the stainless steel vessel. If the shield is effective, none of these loads should be significant. The negative sequence heating will be the largest. The negative sequence magnetic field seen at the stainless steel vessel will be the negative sequence field seen by the electrical shield reduced by the attenuation factors presented in Appendix I.

$$B_{I2S} = B_I K_{att}$$

$$B_{I2S} = \text{flux density at stainless steel shell (assuming the shell is resistance-limited)}$$

$$B_{I2} = \text{from Eq. (III-2)}$$

$$K_{att} = \text{from Eq. (A-53) or Eq. (A-54)}$$

The time-average power dissipated in the stainless steel shell is summarized as

$$P_{d \text{ stainless steel}} = 4 \pi X^3 \omega_o^2 h \sigma_{ss} \ell B_{I2S}^2$$

$$B_{I2S} = \frac{\mu_o S_o}{2} \left\{ 1 - x \pm \frac{1}{3}(1-x^3) \left(\frac{S_o}{T} \right)^2 \right\} \frac{3\sqrt{2}}{\pi} J_A I_2 K_{att}$$

(III-7)

$$K_{att} = \frac{1}{\sqrt{1 + (2\omega_o T_{S1})^2}} \quad \Delta < \delta$$

$$2\sqrt{2} \frac{\delta}{R} e^{-\Delta/\delta} \quad \Delta > \delta$$

x = radius of stainless steel shell

h = thickness of " " "

σ_{ss} = electrical conductivity of stainless steel shell

T_{S1} = time constant of electrothermal shield

Δ = thickness of electrothermal shield

δ = skin depth in electrothermal shield at frequency $2\omega_o$

$$= \left(\frac{2}{2\omega_o \sigma \mu_o} \right)^{1/2}$$

σ = conductivity of electrothermal shield

Equation (III-7) appears to neglect the fact that the radial field at the stainless steel shell is reduced by the currents induced in the field winding. The flux produced by the ac field currents is oscillating, and can be resolved into two counter-rotating components relative to the stainless steel containment vessel. One of these components reduces the imposed negative sequence field, and hence reduces the losses; the other, of equal magnitude, rotates in the opposite direction relative to the shell, producing additional losses which are equal to the amount by which the losses due to the imposed field were reduced.

Hence, the total stainless steel vessel losses are as given by Eq. (III-7) even when the effect of the field winding is included.

III-(2) Alternating Currents in the Field Winding Due to Negative Sequence

The magnitude of the ac induced-field current depends on the ac direct-axis armature current, according to Eq. (A-18)

$$|i_{f_{ac}}| = \frac{M_{df}}{T'_{do} r_{ff}} \frac{1}{\sqrt{1 + (T''_{do}\omega_x)^2}} (I_{d_{ac}})$$

where ω_x is the frequency of the direct-axis ac current. For a steady-state negative sequence current, the direct-axis ac current equals the magnitude of the negative sequence current. This equation was derived for a single-time constant damper winding. The field current expression can be written in terms of the shell attenuation in order to generalize for thick as well as thin shells. The attenuation factor is evaluated at frequency $2\omega_o$.

For resistance-limited shells, ($2\omega_o I''_{do} \ll 1$),

$$|i_{f_{ac}}| = (x_d - x'_d) K_{att} I_2$$

For reactance-limited shells ($2\omega_o I''_{do} \gg 1$) (III-8)

$$|i_{f_{ac}}| = \frac{(x_d - x'_d)(x_d - x''_d)}{(x'_d - x''_d)} K_{att} I_2$$

The expressions for K_{att} are given in Eq. (III-7); all quantities in Eq. (III-8) are in per unit.

III-(3) Steady-State Mechanical Excitation of the Electrical Shield

The magnetic field produced by steady-state negative sequence currents will be excluded from the region inside the E.T. shield. The interaction of the imposed field and the induced shield currents will produce a traveling wave of normal force moving relative to the shield. The shield should be designed so that its ring frequencies as derived in Sec. A-3 are not near the driving frequency of these normal forces.

The normal electrical force per unit area is given in section A-2:

$$\begin{aligned}\sigma_r &= \hat{i}_r \mu_o \left[H_{\theta \text{ outside}} - H_{\theta \text{ inside}} \right] \left[\frac{H_{\theta \text{ outside}} + H_{\theta \text{ inside}}}{2} \right] \quad (\text{III-9}) \\ &= \hat{i}_r \frac{\mu_o}{2} \left[H_{\theta \text{ outside}} - H_{\theta \text{ inside}} \right]\end{aligned}$$

If the shield is effective in intercepting the negative sequence magnetic field, $H_{\theta \text{ inside}}$ will be much less than $H_{\theta \text{ outside}}$. This is equivalent to requiring that $\omega_{xsl}^T \gg 1$ where ω_x is the angular frequency of the traveling field with respect to the rotor. For negative sequence fields,

$$\omega_x = 2 \omega_o.$$

If $H_{\theta \text{ inside}}$ is neglected, the force can be written

$$\sigma_r = \hat{i}_r \frac{1}{2} \mu_o |H_{\theta}|^2 \cos^2 (\omega_x t - \theta) \quad (\text{III-10})$$

$$H_{\theta} = \frac{S_o}{1 \pm \left(\frac{R}{T}\right)^2} \left\{ 1 - x \pm \frac{1}{3} (1-x^3) \left(\frac{S_o}{T}\right)^2 \right\} \frac{3}{\pi} \sqrt{2} J_A I_2$$

At a fixed point on the shield in the rotor frame, the alternating component of force will vary with angular frequency $2 \omega_x$. For negative

sequence $\omega_x = 2\omega_o$ and the force will vary at frequency $4\omega_o$. Therefore, the lowest ring natural frequency should be above $4\omega_o$.

The maximum deflection of the shell for a constant load of the form $F \cos^2 \theta$ is calculated in Eq. (A-66). The steady-state deflection for a mechanical system with natural frequency ω_n and no damping, driven at frequency ω_d by a force $P_o \sin \omega_d t$ will be

$$x = x_o \frac{1}{1 - \left(\frac{\omega_d}{\omega_n}\right)^2} \sin \omega_d t$$

where x_o is the deflection for a constant force P_o . An upper bound on the steady-state deflection of the shell, due to imbalance, is obtained by assuming no damping of the ring vibrational motion. The radial deflection of the shell for negative sequence current I_2 is given by Eqs.

(III-11):

$$\begin{aligned} \sigma_{ro} &= \frac{1}{2} \mu_o H_\theta^2 \\ H_\theta &= \frac{3\sqrt{2} J_A}{\pi} \frac{S_o}{1 \pm \left(\frac{R}{T}\right)^2} \left\{ 1 - x \pm \frac{1}{3} (1 - x^3) \left(\frac{S_o}{T}\right) \right\} I_2 \\ \Delta r_o &= \frac{4 R^2}{\frac{1-v^2}{4} \left(\frac{\pi R}{\ell}\right)^4 + 3 \left(\frac{\Delta}{R}\right)^2} \left(\frac{1}{\Delta}\right) \left(\frac{1-v^2}{E}\right) \left(\frac{\sigma_{ro}}{2}\right) \\ \omega_n^2 &= \left(\frac{E}{1-v^2}\right) \left(\frac{1}{\rho_m}\right) \frac{3 \left(\frac{\Delta}{R}\right)^2 + \frac{1-v^2}{4} \left(\frac{\pi R}{\ell}\right)^4}{5 R^2} + 2.4 \omega_o^2 \\ \Delta r &= \Delta r_o \frac{1}{1 - \left(\frac{4\omega_o}{\omega_n}\right)^2} \sin 4\omega_o t \end{aligned} \quad (III-11)$$

Since the negative sequence magnetic field for a per-unit negative sequence of $I_s = .1$ is quite small, the maximum steady-state deflection Δr

should be negligible unless the ring natural frequency is very near

$$4 \omega_0.$$

Chapter IV

Electromechanical and Thermal Effects of Faults

The fault behavior of a superconducting generator as seen at its terminals (both electrical and mechanical) is essentially the same as for a conventional generator. The superconducting generator has the advantage of lower synchronous reactance, resulting in superior system stability. However, the effects internal to the machine produced by the large fault currents and forces may be more severe in the superconducting generator for the following reasons:

- (1) Alternating currents induced in the field winding could drive it normal.
- (2) Heating produced by induced currents in rotor parts can raise their temperature considerably, because of low thermal capacity at cryogenic temperatures.
- (3) Magnetic radial stresses upon the electrothermal shield can produce large deflections because of the lack of radial support between shield and inner rotor structure.
- (4) The thermal isolations of the rotor make it structurally more vulnerable to large transient torques.

None of these effects represents a fatal flaw of the superconducting generator concept. All can be overcome with proper design consideration of the effects. However, because of the critical competition between thermal isolation to minimize heat leak and structural integrity during faults, it is necessary to predict as well as possible the rotor stresses and heat loads during faults. Expressions for these stresses and heat loads are derived in Appendix III. In this chapter, the mechanical and

thermal model of the shell will be used to estimate the resulting motion of the shield, the temperature rise of the shield, and other determinantal effects upon the field winding.

1) The Effects of Fault Torques

The existence of large oscillating torques within a generator following a fault has been known for many years and studied in numerous papers. The most complete analysis including initial loading of the generator for three-phase short, line-to-line short, and synchronizing out of phase is included in Ref. [7], Woodson's Report to Consolidated Edison. Appendix I presents a derivation showing the applicability of the results to superconducting generators taking into account the constraint on the various mutual inductances imposed by the presence of the conducting electrothermal shield. The cases considered are appropriate for the superconducting machine, because the present armature configuration is a delta connection which precludes the possibility of line-neutral machine faults. Even when a machine is Y-connected, a large impedance is placed between neutral and ground to limit fault currents; the line-neutral fault can thereby be made less severe than the other faults in which such a simple current limitation is not possible.

The calculation of fault torques for conventional machines usually results in a total torque acting on the stator (or rotor). Since both the field windings and damper bars or windings are set in the rotor iron, the distribution of actual forces between field windings, damper bars, and rotor iron is not so important. However, in the superconducting generator, the damper winding is the electrical shield, which is a thin-walled tube supported only at the ends. The torque exerted upon this

tube can produce the following failure modes: shear off the shield if the yield stress of the material is exceeded; cause torsional buckling of the shield; produce large torsional oscillations of the shield if the natural torsional frequency is near the driving frequency of the torques. Oscillating torques are exerted upon the field winding also, to a lesser extent. The field winding must be mounted with sufficient rigidity to prevent excessive motion of the superconducting wire. There has been some concern as to the possibility of driving the superconductor normal because of motion during faults. The analysis shows, however, that most of the torque is taken by the shield. This fact lessens concern about the superconductor, but makes prediction of shield stresses more critical.

2) Torque Upon the Field Winding

The field winding is subjected to an oscillating torque, as given by Eq. (A-42):

$$T_f = \left(\frac{x_d - x_d'}{x_d'} \right) \left(\frac{1}{x_d - x_d''} \right) \frac{T_{do}''}{T_d''} \frac{x_d''}{\sqrt{1 + (T_{do}'' \omega)^2}} \left(I_{d_{ac}} \right) \psi_{q1} \quad (IV-1)$$

Inspection of Eqs. [A-32(a) thru (e)] shows that ψ_{q1} equals zero for faults from open circuit. Therefore, the alternating torque on the field winding is essentially zero for all shorts from open circuit. The second point to be observed from Eq. (IV-1) is that the factor $[1 + (T_{do}'' \omega)^2]^{-1/2}$ represents an attenuation factor due to the presence of the damper winding. For an electrical shield whose thickness is greater than a skin depth, the attenuation factor given by Eq. (A-53) must be used. The result is that, even for a loaded machine where ψ_{q1} is not zero, the torque upon the field winding is considerably less than the total rotor

torque. Another way to state this is to say that a shield which is effective in intercepting the asynchronous magnetic field seen on the rotor also intercepts the alternating torque which is exerted on the rotor.

Equation (IV-1) is evaluated for the cases of three-phase fault, line-line fault, and synchronizing out of phase, and the results are listed on the following pages. Inspection of these results indicates that the per-unit torque on the field winding is not large for reasonable values of attenuation factor.

Alternating Fault Torque Exerted Upon the Field Winding

1) Three-Phase Fault from Load

$$T_f = \left(\frac{x - x'}{x'} \right) \frac{T''_{do}}{T''_d} \frac{V_a I_a e^{-t/T_a}}{\sqrt{1 + (T''_{do} \omega)^2}} \cos(\delta + \theta) e^{-\frac{t}{T_q}} \sin \omega_o t$$

For a reactance-limited electrical shield $(T''_{do} \omega_o)^2 \gg 1$,

$$T_f = \left(\frac{x - x'}{x''} \right) \left(\frac{x - x''}{x' - x''} \right) K_{att}(\omega_o) V_a I_a \cos(\delta + \theta) e^{-t/T_a - t/T_q} \sin \omega_o t$$

$$K_{att}(\omega_o) = \begin{cases} \frac{1}{\omega_o T_{s1}} & \delta > \Delta \\ 2\sqrt{2} \frac{\delta}{R} e^{-\frac{\Delta}{\delta}} & \delta < \Delta \end{cases} \quad (IV-2)$$

$$\delta = \left(\frac{2}{\omega_o \sigma \mu} \right)^{1/2}$$

For a resistance-limited shield $(T''_{do} \omega_o)^2 \ll 1$

$$T_f = \frac{x - x'}{x''} V_a I_a \cos(\delta + \theta) e^{-\frac{t}{T_a} - \frac{t}{T_q}} \sin \omega_o t$$

2) Line-to-Line Fault from Load

The line-line fault produces two oscillating torque components, one at line frequency and one at double line frequency. The attenuation factor must be evaluated separately for each.

$$\psi_{q1} I_{d_{ac}} = \frac{V_{sa}^2}{2} \left(\frac{x - x''}{(x + x_s)(x'' + x_s)} \right) \sin \delta_s F_{ql} \cos(2\omega_o t - \delta_s) \\ + \frac{V_{sa} V_a}{x''} \left(\frac{x - x'}{x + x''} \right) \sin \delta_s \sin(\omega_o t - \delta) F_{ql} \sin \omega_o t$$

Reactance-Limited Electrothermal Shield $(T''_{do} \omega_o)^2 \gg 1$

$$T_f = \left(\frac{x - x'}{x' - x''} \right) \left(\frac{x''}{x'} \right) \left(\frac{x_s + 2x'}{x_s + 2x''} \right) \left[\frac{V_{sa}^2}{2} \frac{(x - x'')}{(x + x_s)(x'' + x_s)} \sin \delta_s F_{ql} K_{att}(2\omega_o) \cdot \right. \\ \left. \cos(2\omega_o t - \delta_s) + \frac{V_{sa} V_a}{x''} \left(\frac{x - x'}{x + x_s} \right) \sin \delta_s \sin(\omega_o t - \delta) F_{ql} K_{att}(\omega_o) \sin \omega_o t \right]$$

Resistance-Limited Electrothermal Shield $(T''_{do} \omega_o)^2 < 1$

$$T_f = \left(\frac{x - x'}{x - x''} \right) \left(\frac{x''}{x'} \right) \left(\frac{x_s + 2x'}{x_s + 2x''} \right) (\psi_{q1}) (I_{d_{ac}})$$

3) Closure Out-of-Phase by Angle θ_s

$$\psi_{q1} I_{d_{ac}} = \frac{e^{-t/T_d}}{x'' + x_s} [V_{sa} \cos(\omega t + \theta_s) - M_{df} I_{fo}] \left(\frac{x - x''}{x + x_s} \right) \left(1 - e^{-t/T_{qc}} \right)$$

Reactance-Limited Electrothermal Shield

$$T_f = \left(\frac{x - x'}{x' - x''} \right) \left(\frac{x''}{x'} \right) \left(\frac{x_s + x'}{x_s + x''} \right) K_{att}(\omega_o) (\psi_{q1} I_{d_{ac}})$$

Resistance-Limited Shield

(IV-4)

$$T_f = \left(\frac{x - x''}{x - x''} \right) \left(\frac{x''}{x'} \right) \left(\frac{x_s + x'}{x_s + x''} \right) (\psi_{q1} I_{dac})$$

b) Torque Upon the Electrical Shield

For an effective shield, the field winding torque has been shown to be small. For calculation of the effects of torques on the electrical shield, it is then slightly conservative to assume that the total resultant oscillating torques, as given for various faults in Eqs. (A-33) through (A-37), are applied to the shield.

If the shield is supported in torsion at both ends, the maximum torque along the shield, tending to shear it off azimuthally, is one-half the applied torque. If the natural frequency of the shell in torsion as given by Eq. (IV-3) is much higher than the oscillating torque frequency, the shield will yield in shear if the yield stress in shear of the material is exceeded. The frequency of the oscillating torques from Eq. (A-1-b) are fundamental line and second harmonic frequencies. The lowest torsional natural frequency is

$$f_t = \frac{1}{2\ell} \sqrt{\frac{G}{P}} \quad (IV-5)$$

The quantity $\sqrt{G/P}$ is roughly constant for most metals; evaluation of the equation shows that a shield nearly 10 meters long would be required to have a natural torsional frequency as low as 120 Hz. Even for the example 1000 MVA machine in section II-4, the shield length is only about 4.2 meters. The torsional natural frequency will almost always be well above the driving frequency of the oscillating torques. The

resultant state of stress in the shield must then be found by combining the shear stress due to torques with the centrifugal hoop stresses due to rotation of the shield.

The maximum shear stress due to torque of magnitude τ for a shield of inner and outer radii R_1 and R_o is given by the following equation:

$$\sigma_s = \frac{2 R_o \tau}{\pi(R_o^4 - R_1^4)} \quad (\text{IV-6a})$$

The tensile stress due to rotation of the shield is given by the following equation:

$$\sigma_T = \frac{\rho_m \omega_o^2 R_o^2}{2} \quad (\text{IV-6b})$$

where ρ_m is the mass density of the shield material. These stresses must be combined using Mohr's circle. For the ductile materials of which the shield will be composed, the most logical failure criterion is probably the maximum shear theory. The maximum shear stress resulting from σ_s and σ_T above must be less than the yield stress in shear. The yield stress in shear is about one-half the yield stress in tension.

The maximum torque τ to be used in Eq. (IV-6a) depends on the fault condition considered. Expressions for these torques are given by Eqs. (A-33) through (A-37). The most severe which is of practical interest is the line-to-line fault at the terminals, while operating loaded at rated power factor. The case of over-excited operation at zero power factor at rated reactive power is slightly worse, but is a more unusual condition of loading.

A second possible mode of failure is buckling of the shell due to torsion. The situation in which this mode of failure can occur before simple failure in shear is that for a very thin cylinder. Most calculations have shown that the critical torque for buckling is well above that for shearing off the shield; however, the criterion is reproduced here from Ref. [9] for completeness.

Buckling of a Shell in Torsion

$$\tau_{crit} = \frac{27.58 R^2 \Delta^2 E}{(1-\nu^2) \ell^2} \left[1 + .0257(1-\nu^2)^{3/4} \left(\frac{\ell}{\sqrt{R\Delta}} \right)^3 \right]^{1/2} \quad (IV-7)$$

$$\text{for } \frac{1}{\sqrt{1-\nu^2}} \frac{\ell^2 \Delta}{(2R)^3} < 7.8$$

$$\tau_{crit} = \frac{\pi \sqrt{2} E}{3(1-\nu^2)^{3/4}} \sqrt{R\Delta^5}$$

$$\text{for } \frac{1}{\sqrt{1-\nu^2}} \frac{\ell^2 \Delta}{(2R)^3} > 7.8$$

Unidirectional Shield Torques

Unidirectional torques or induction motor type torques are exerted upon the electrical shield during transients. In general, they are small compared to the peak values of the alternating torques. They can be evaluated from the power dissipation in the shield, due to the asynchronously rotating magnetic fields. The heating in the shield is itself a more important effect than the unidirectional torques, and is treated in section IV-3. The unidirectional torque can be evaluated from the value of P_{ac} , the power dissipated due to alternating currents

induced in the shield. Values of P_{ac} for the various fault conditions are derived in IV-3.

$$\text{Torque unidirectional} = \frac{1}{\omega_o} P_{ac}$$

IV-2 The Effects of Normal Mechanical Stresses of Electrical Origin

In Appendix I it is pointed out that, during an electrical transient, when a magnetic field is established external to a conducting shield in a time short compared to the shield time constant, a normal stress is exerted upon the shield. Inside the superconducting generator, this field is distributed sinusoidally in azimuth, producing a normal stress distribution which tends to flatten the shield. The magnitude of this stress is determined primarily by the machine reactances as shown in Appendix I. However, the duration of this transient is dependent on the time constant of current decay in the shield, and the maximum deflection of the shield will depend upon its ring natural frequencies as derived in Appendix I.

In this section will be presented expressions for the maximum radial deflection of the electrical shield under various fault conditions.

Three-Phase Fault

The normal stress resulting from a three-phase fault from open circuit is given by Eq. (A-61). In order to determine the flattening of the shield, the transient radial motion of a point on it can be solved as for a lumped-spring mass system subjected to a driving force whose time dependence is given by the normal stress equation. Equation (A-66) gives the radial deflection of a shell subjected to normal stress given by Eq. (A-65). The natural frequency of the shell is given by Eq. (A-65); with these expressions an equivalent spring constant and mass can be defined for radial motion of the shell at angle $\gamma = 0$. Evaluation of the second spatial harmonic terms of Eq. (A-61) gives the following stress distribution:

$$\begin{aligned}
\sigma_r = & \mu_o \left[\frac{\Delta H_{1f} \Delta H_{1i}}{2} \left(1 - e^{-\frac{t'}{T_d''}} \right) e^{-\frac{t'}{T_d''}} \cos 2\gamma + \frac{\Delta H_{1i}^2}{4} e^{-\frac{2t'}{T_d''}} \cos 2\gamma \right. \\
& + \frac{\Delta H_{1i}^2}{4} e^{-\frac{2t'}{T_a}} (\cos 2\omega t' \cos 2\gamma - \sin 2\omega t' \sin 2\gamma) \\
& - \frac{\Delta H_{1i}^2}{2} e^{-t' \left(\frac{1}{T_d''} + \frac{1}{T_a} \right)} (\cos \omega t' \cos 2\gamma - \sin \omega t' \sin 2\gamma) \quad (IV-8) \\
& \left. - \frac{\Delta H_{1f} \Delta H_{1i}}{2} e^{-\frac{t'}{T_a}} \left(1 - e^{-\frac{t'}{T_d''}} \right) (\cos \omega t' \cos 2\gamma - \sin \omega t' \sin 2\gamma) \right]
\end{aligned}$$

If we consider the deflection at $\gamma = 0$ as a function of time, the terms containing $\sin 2\gamma$ will produce no contribution; the $\cos 2\gamma$ will produce a deflection as given by Eq. (A-66). To solve for the transient shell deflection, the solution to the equation is given by

$$m\ddot{x} + kx = f(t')$$

where $f(t')$ is the time dependence of the $\cos 2\gamma$ terms in Eq. (IV-8).

Stress producing deflection at $\gamma = 0$ is expressed as

$$\begin{aligned}
\sigma_2(t') = & \mu_o \left[\frac{\Delta H_{1f} \Delta H_{1i}}{2} \left(1 - e^{-\frac{t'}{T_d''}} \right) e^{-\frac{t'}{T_d''}} + \frac{\Delta H_{1i}^2}{4} e^{-\frac{2t'}{T_d''}} \right. \\
& + \frac{\Delta H_{1i}^2}{4} e^{-\frac{2t'}{T_a}} \cos 2\omega_0 t' - \frac{\Delta H_{1i}^2}{2} e^{-t' \left(\frac{1}{T_a} + \frac{1}{T_d''} \right)} \cos \omega_0 t' \quad (IV-9) \\
& \left. - \frac{\Delta H_{1f} \Delta H_{1i}}{2} e^{-\frac{t'}{T_a}} \left(1 - e^{-\frac{t'}{T_d''}} \right) \cos \omega t' \right] \cos 2\gamma
\end{aligned}$$

From Eqs. (A-65) and (A-66), we obtain the following:

$$\text{For a load} \quad q = \frac{f}{2} \cos 2\phi$$

$$\text{Produce deflection} \quad x = \frac{4 R^2}{\frac{1 - \nu^2}{4} \left(\frac{\pi R}{L} \right)^4 + 3 \left(\frac{\Delta}{R} \right)^2} \frac{1}{\Delta} \frac{1 - \nu^2}{E} \frac{f}{2} \cos 2\phi$$

$$K = \frac{g}{x} \frac{\frac{1-v^2}{4} \left(\frac{\pi R}{l}\right)^4 + 3\left(\frac{\Delta}{R}\right)^2}{4R^2} \left(\frac{\Delta E}{1-v^2} \right) \quad (\text{IV-10})$$

The complete solution of the differential equation with the driving function (IV-9) requires much algebra. However, the result being sought is the maximum deflection of the shield during the transient. To obtain that result, we can make use of the fact that both the armature time constant and the subtransient time constants are at least several cycles of line frequency, and for most machines, even longer. Using this assumption, the differential equation can be written

$$\ddot{mx} + Kx = \frac{f_o}{4} + \frac{f_o}{4} \cos 2\omega_o t - \frac{f_o}{2} \cos \omega_o t$$

$$\frac{f_o}{2} = \frac{\mu_o \Delta H_{li}^2}{2}$$

The solution for x_{\max} depends on the relationship of the shell's natural frequency $\omega_n = \sqrt{K/m}$, as given by Eq. (A-67), and the driving frequencies ω_o and $2\omega_o$. Damping of these radial motions has been neglected; therefore, the deflection for $\omega_n = \omega_o$ or $\omega_n = 2\omega_o$ will become infinite. However, the limits for $\omega_n < \omega_o$ and $\omega_n > 2\omega_o$ can be estimated by the undamped case. The results are as follows:

$$\text{For } \omega_n > 2\omega_o, \quad \tau_a, T_d'' \gg \frac{2\pi}{\omega_o}$$

$$x_{\max} = 2 x_o$$

$$x_o = \frac{1}{K} \frac{f_o}{2}$$

(IV-11)

$$\text{For } \omega_n < \omega_o$$

$$x_{\max} = x_o$$

From Eq. (IV-11), it appears that the deflection is less for a shield with natural frequency below ω_0 ; however, this corresponds to a shield with a low value of K producing a larger x_0 . The stiffer high frequency shield produces the smaller deflection.

3) Rotor Heating During Faults

The effects of rotor heating during faults was studied extensively in the past [22] and criteria of $I_2^2 t$ for a generator was developed. The $I_2^2 t$ is essentially a measure of the amount of rotor heating due to transient negative sequence currents which can be tolerated without permanent damage to the machine. In a superconducting machine, this rotor heating effect must be accurately predicted for the following reasons:

- 1) Small specific heat of metals at cryogenic temperatures;
- 2) Relatively small thermal mass subjected to heating;
- 3) Possibility of driving the superconductor normal.

One of the most important functions of the electrical shield is to intercept the large negative sequence magnetic fields during faults. Since it is a relatively small thermal mass, considerable temperature rise can be experienced in the shield. Attempts to add thermal mass to the shield are difficult; materials such as stainless steel with low electrical conductivity also have low thermal conductivity; during the period of the transient, very little heat is conducted into them. A thicker shield of high electrical and thermal conductivity adds effective thermal mass, but increases the shield time constant and reduces the shield's effectiveness as a damper winding, as shown in Ref. [5].

The calculation of fault heating employs the results of Appendix I to obtain the armature fault currents, the magnetic field model to obtain

the heating, and the thermal model to calculate temperature rise of the shield, due to the nonlinear temperature dependence of the shield's electrical conductivity and specific heat.

Heating produced in the shield during faults results from the following sources:

- 1) The dc currents induced in the shell to maintain its flux linkage constant during the subtransient period;
- 2) Alternating currents induced by the trapped flux linkages in the armature which appear to rotate backward relative to the rotor at angular frequency ω_0 ;
- 3) Alternating currents induced by negative sequence fault currents resulting from unsymmetrical faults.

The most severe case is the line-line fault, which results in unbalanced currents even after the transient period. The results for this case can be used to determine the temperature rise occurring before the system circuit breakers interrupt the fault for a short-term fault, or the ultimate temperature rise for a sustained fault.

Three-Phase Fault Shield Heating

The magnitude of the increase in positive sequence armature current is given in Table IV-1. The resulting current induced in the shield to maintain constant flux linkage at the shield is derived from the magnetic field solution given in Appendix I. The resulting expression for power dissipation due to dc shell currents is

$$P_{dc} = \frac{\pi R \ell}{\sigma \Delta} \left(\frac{S_o}{1 \pm \left(\frac{R}{T}\right)^2} \right)^2 \left\{ 1 - x \pm \frac{1}{3}(1-x^3) \left(\frac{S_o}{T} \right)^2 \right\}^2 \left(\frac{3}{\pi} \sqrt{2} J_A \right)^2$$

$$\left[\left(\Delta i''_{d1} e^{-t/T''_d} \right)^2 + \left(\Delta i''_{q1} e^{-t/T''_q} \right)^2 \right] \quad (IV-13)$$

$\Delta i''_{d1}$, $\Delta i''_{q1}$ from Table IV-1.

The three-phase fault is symmetrical and no negative sequence armature currents are produced. The ac power loss in the shield results entirely from the trapped armature flux.

$$P_{ac} = \begin{cases} \frac{1}{\sigma \delta} \frac{4\pi \ell}{\mu_o^2} \frac{R}{1 \pm \left(\frac{R}{T}\right)^2} B_o^2 & \delta < \Delta \\ \frac{2\pi}{\mu_o} \frac{R^2}{1 \pm \left(\frac{R}{T}\right)^2} \frac{1}{T_{s1}} \frac{(\omega_o T_{s1})^2}{1 - (\omega_o T_{s1})^2} B_o^2 & \delta > \Delta \end{cases} \quad (IV-14)$$

$$\delta = \left(\frac{2}{\omega_o \sigma \mu_o} \right)^{1/2}$$

$$B_o = \mu_o \frac{3 \sqrt{2} J_A}{2\pi} S_o \left\{ 1 - x \pm \frac{1}{3}(1-x^3) \left(\frac{S_o}{T} \right)^2 \right\} i_o$$

$$i_o = \frac{V_a e^{-t/T_a}}{x''} \quad (\text{in per-unit})$$

The total dissipated power is the sum of P_{ac} and P_{dc} .

In calculating the shield temperature rise due to the fault, a step-by-step calculation is performed, taking account of the integrated power dissipated and the dependence of conductivity and specific heat on temperature. It can be shown that the power dissipated in a three-phase fault is independent of initial current; i.e., it depends only upon terminal voltage before the fault.

Line-to-Line Fault Shield Heating

The dc power for the line-line fault is given in Eq. (IV-13) if the appropriate time constants are used.

$$P_{dc} = \frac{\pi R \ell}{\sigma \Delta} \left(\frac{S_o}{1 \pm \left(\frac{R}{T}\right)^2} \right)^2 \left\{ 1 - x \pm \frac{1}{3}(1 - x^3) \left(\frac{S_o}{T} \right)^2 \left(\frac{3}{\pi} \sqrt{2} J_A \right)^2 \right. \\ \left. \left[\left(\Delta i''_{d1} e^{-\frac{t}{T''_{dl}}} \right)^2 + \left(\Delta i''_{q1} e^{-\frac{t}{T''_{ql}}} \right)^2 \right] \right\} \quad (IV-15)$$

T''_{dl} , T''_{ql} from Eq. (A-16)

$\Delta i''_{d1}$, $\Delta i''_{q1}$ from Table IV-1

The ac power is computed using Eq. (IV-14), using the appropriate value of magnetic flux density and angular frequency.

$$P_{ac} = \begin{cases} \frac{1}{\sigma \delta_x} \frac{4\pi \ell}{\mu_o^2} \frac{R}{1 \pm \left(\frac{R}{T}\right)^2} B_x^2 & \delta_x < \Delta \\ \frac{2\pi}{\mu_o} \frac{R^2}{1 \pm \left(\frac{R}{T}\right)^2} \frac{1}{T_{s1}} \frac{(\omega_x T_{s1})^2}{1 + (\omega_x T_{s1})^2} B_x^2 & \delta_x > \Delta \end{cases} \quad (IV-16)$$

$$\delta_x = \left(\frac{2}{\omega_x \sigma \delta} \right)^{1/2}$$

Equation (IV-16) must be evaluated for both trapped armature flux and negative sequence armature currents:

$$B_x = \mu_o \frac{3\sqrt{2} J_A}{2\pi} S_o \left\{ 1 - x \pm \frac{1}{3}(1 - x^3) \left(\frac{R_o}{T} \right)^2 \right\} J_x$$

Trapped Flux:

$$i_o = \frac{\lambda_{BO}}{x''}$$

Negative Sequence (2 components):

$$J_{2A} = \frac{1}{2(x'' + x_s)} \left[\frac{x_s}{x''} \psi_{d1} + V_{sa} \cos \delta_s \right]$$

$$J_{2B} = \frac{1}{2(x'' + x_s)} \left[\frac{x_s}{x''} \psi_{q1} + V_{sa} \sin \delta_s \right]$$

ψ_{d1} , ψ_{q1} , λ_{BO} from Eq. (A-32a)

The total ac power is evaluated as the sum of the result of letting J_x be equal to i_{2A} , i_{2B} , and i_o . The total dissipation is then the sum of P_{dc} and P_{ac} .

IV-4 The Field Current During Faults

During the period immediately following a fault, the field current level rises due to the demagnetizing effect of the armature currents, and an alternating component of current is induced due to trapped armature flux and unbalanced conditions of the fault.

The rise in the direct current level is not affected by the presence of the electrical shield; the rate of rise will, however, depend on the electrical shield time constant. The peak direct current level depends only on the increase in the direct-axis current during the transient period, that is, when the shield currents have decayed, but the field winding is still linking a constant flux. In per-unit notation,

$$\Delta i_{f_{dc}} = (x - x') \Delta i_{d1}'$$

The expressions for $\Delta i_{d1}'$ are summarized for three-phase and line-to-line fault in Table IV-1. The largest rise occurs for a line-to-line fault on a generator operating at zero power factor over-excited.

The alternating current induced in the field winding depends upon the attenuation of asynchronous magnetic field provided by the electrical shield. The equations are given as Eqs. (A-19) relating alternating field current and alternating direct-axis current. They are repeated below in per-unit notation, giving peak values.

Resistance-Limited Shield $(\omega_x T_{do}'')^2 \ll 1$

$$|i_{f_{ac}}| = (x - x') K_{att} |i_{d_{ac}}|$$

Reactance-Limited Shield $(\omega_x T_{do}'')^2 \gg 1$

$$|i_{f_{ac}}| = \frac{(x - x')(x - x'')}{(x' - x'')} K_{att} |i_{d_{ac}}|$$

The expressions for $i_{d_{ac}}$ are given in Table IV-2 for three-phase short and line-to-line short circuit where $i_{d_{ac}}$ is given by i_0 for a three-phase short circuit, and i_0 and i_2 for a line-to-line short circuit.

Table IV-1

Increase in Positive Sequence Direct-Axis Armature Current
Following Fault

- 1) Three-Phase Short Circuit (same for loaded or unloaded)

$$\Delta i_{d1}' = \frac{V}{x''} \left[\left(1 - \frac{x''}{x'}\right) e^{-\frac{t}{T_d''}} + \left(\frac{x''}{x'} - \frac{x''}{x}\right) e^{-\frac{t}{T_d'}} + \frac{x''}{x} \right]$$

$$\Delta i_{d1}'' = \frac{V}{x''} \quad t \ll T_d''$$

$$\Delta i'_{d1} = \frac{V_t}{x'} \quad T''_d \ll t \ll T'_d$$

2) Line-Line Short Circuit:

(a) From Open Circuit:

$$\Delta i'_{d1} = \frac{V_t}{2x''} \left\{ \left(1 - \frac{2x''}{x'' + x'} \right) e^{-\frac{t-t_0}{T'_{dl}}} + \left(\frac{2x''}{x'' + x'} - \frac{2x''}{x'' + x} \right) e^{-\frac{t-t_0}{T''_{dl}}} + \frac{2x''}{x'' + x} \right\}$$

$$\Delta i''_{d1} = \frac{V_t}{2x''} \quad t \ll T''_{dl}$$

$$\Delta i'_{d1} = \frac{V_t}{x'' + x}, \quad T''_{dl} \ll t \ll T'_{dl}$$

(b) From Load:

$$\Delta i_{d1} = \frac{1}{2(x'' + x_s)} \left\{ \left(\frac{2x'' + x_s}{x''} \right) \left[\left(\frac{x'' + x_s}{x + x_s} \right) E_f F_{dl1} + \left(\frac{x - x''}{x + x_s} \right) V_{sa} \cos \delta_s F_{dl2} \right] - V_{sa} \cos \delta_s \right\} - I_a \sin(\delta + \theta_p)$$

F_{dl1}, F_{dl2} given in Eq. (III-24).

$$\Delta i''_{d1} = \frac{1}{2(x'' + x_s)} \left\{ \left(\frac{2x'' + x_s}{x''} \right) \left[\left(\frac{x'' + x_s}{x + x_s} \right) E_f + \left(\frac{x - x''}{x + x_s} \right) V_{sa} \cos \delta_s \right] - I_a \sin(\delta + \theta_p) \right\}$$

for $t \ll T''_{dl}$

$$\Delta i'_{d1} = \frac{1}{2(x'' + x_s)} \left\{ \left(\frac{2x'' + x_s}{x''} \right) \left[\left(\frac{x'' + x_s}{x + x_s} \right) \left(\frac{2x''(x' + x_s)}{x''(x' + x_s) + x'(x'' + x_s)} \right) E_f \right. \right. \\ \left. \left. + \left(\frac{x - x''}{x + x_s} \right) \left(\frac{2x''(x'' + x_s)}{x''(x' + x_s) + x'(x'' + x_s)} \right) \left(\frac{x - x'}{x - x''} + \frac{(x + x_s)(x' - x'')}{2(x'' + x_s)(x - x'')} \right) \right] \right. \\ \left. - V_{sa} \cos \delta_s \right\} - I_a \sin(\delta + \theta_p)$$

for $T''_{d\ell} \ll t \ll T'_{d\ell}$

$$\Delta i_{d1} = \frac{1}{2(x'' + x_s)} \left\{ \left(\frac{2x'' + x_s}{x''} \right) \left(\frac{x'' + x_s}{x + x_s} \right) \left(\frac{2x''(x + x_s)}{x''(x + x_s) + x(x'' + x_s)} \right) E_f - V_{sa} \right. \\ \left. \cos \delta_s \right\} - I_a \sin(\delta + \theta_p)$$

for $t \gg T'_{d\ell}$

Table IV-2Magnitude of Direct-Axis Alternating Current Following Fault

- 1) Three-Phase Short Circuit (same for loaded or unloaded):

$$\frac{\omega_x = \omega_o}{|i_o| = \frac{V_a}{x''} e^{-\frac{t}{T_a}}}$$

- 2) Line-to-Line Short Circuit

- (a) From Open Circuit:

$$\frac{\omega_x = \omega_o}{|i_o| = \frac{V_a \sin(\omega_o t_o - \delta)}{x''} e^{-t/T_a}}$$

$$\frac{\omega_x = 2 \omega_o}{|i_2| = \frac{V_t}{2x''} \left\{ \left(1 - \frac{2x''}{x'' + x'} \right) e^{-\frac{t-t_o}{T''_{do}}} + \left(\frac{2x''}{x'' + x'} - \frac{2x''}{x'' + x} \right) e^{-\frac{t-t_o}{T'_{dl}}} \frac{2x''}{x'' + x} \right\}}$$

$$|i_2'| = \frac{V_t}{2x''} \quad t \ll T''_{dl}$$

$$|i_2'| = \frac{V_t}{x'' + x'} \quad T''_{dl} \ll t \ll T'_{dl}$$

$$|i_2| = \frac{V_t}{x'' + x} \quad T'_{dl} \ll t$$

- (b) From Load:

$$\frac{\omega_x = \omega_o}{|i_o| = \frac{V_a \sin(\omega_o t_o - \delta)}{x''} e^{-\frac{t}{T_a}}}$$

$$\frac{\omega_x = 2\omega_o}{|i_2| = \frac{V_t}{2x''} \left\{ \left(1 - \frac{2x''}{x'' + x'} \right) e^{-\frac{t-t_o}{T''_{do}}} + \left(\frac{2x''}{x'' + x'} - \frac{2x''}{x'' + x} \right) e^{-\frac{t-t_o}{T'_{dl}}} \frac{2x''}{x'' + x} \right\}}$$

$$|i_2| = (i_{2A}^2 + i_{2B}^2)^{1/2}$$

$$i_{2A} = \frac{1}{2(x'' + x_s)} \left(\frac{x_s}{x''} \psi_{d1} + V_{sa} \cos \delta_s \right)$$

$$i_{2B} = \frac{1}{2(x'' + x_s)} \left(\frac{x_s}{x''} \psi_{q1} + V_{sa} \sin \delta_s \right)$$

ψ_{d1}, ψ_{q1} from Eq. (III-24).

$$|i_2''| = \frac{1}{2(x'' + x_s)} \left\{ \left[\frac{x_s}{x''} \left(\frac{x'' + x_s}{x + x_s} E_f + \frac{x - x''}{x + x_s} V_{sa} \cos \delta_s \right) + V_{sa} \cos \delta_s \right]^2 + \left[\frac{x_s}{x''} \left(\frac{x - x''}{x + x_s} \right) V_{sa} \sin \delta_s + V_{sa} \sin \delta_s \right]^2 \right\}^{1/2}$$

for $t \ll T_{dl}''$

$$|i_2'| = \frac{1}{2(x'' + x_s)} \left\{ \left[\frac{x_s}{x''} \left(\frac{x'' + x_s}{x + x_s} \right) \left(\frac{2x''(x' + x_s)}{x''(x' + x_s) + x'(x'' + x_s)} \right) E_f + \left(\frac{x - x''}{x + x_s} \right) \left(\frac{2x''(x'' + x_s)}{x''(x' + x_s) + x'(x'' + x_s)} \right) \left(\frac{x - x'}{x - x''} + \frac{(x + x_s)(x' - x'')}{2(x'' + x_s)(x - x'')} \right) \right]^2 + \left[V_{sa} \cos \delta_s + V_{sa} \cos \delta_s \right]^2 + \left[\frac{x_s}{x''} \left(\frac{x - x''}{x + x_s} \right) \left(\frac{x''(x + x_s)}{x''(x + x_s) + x(x'' + x_s)} \right) V_{sa} \sin \delta_s + V_{sa} \sin \delta_s \right]^2 \right\}^{1/2}$$

for $T_{dl}'' \ll t \ll T_{dl}'$

CHAPTER V

Experiments

Several experiments were performed during the course of this study to confirm intermediate results of the analysis. Some experiments were also performed upon the existing superconducting generator. These were to confirm prediction of performance, and to observe whether or not any unexpected developments should occur.

The first experiments were done to confirm predictions of armature-produced flux density, time constants of conducting shields, attenuation factors of shields, and power dissipation in shields. The experiments on the existing machine were to record performance for a sudden three-phase and line-to-line short circuit. Also, the generator was run as an induction motor with the shield acting as the rotor winding, to measure shield dissipation and to observe the effect on the field winding. The results of these experiments with explanations of the setup and comments on the results are given in the sections of this chapter.

V-1 Armature-Produced Magnetic Field

The magnetic flux density produced by the armature of the 80 KVA generator was measured while the rotor had been removed for repairs. The armature currents were produced by a bank of three-phase transformers connected through an autotransformer to the line. The rms flux density was measured on the axis of the machine in the active region, and through the end-turn region. The results are plotted in Fig. V-1.

From Eq. (A-48), the predicted rms flux density using the distributed armature current model was 140.5 gauss for armature current of 200 amps. Using the discrete bar model with the Fourier analysis from Eqs.

(III-5) and (III-6) plus Eq. (A-48), the predicted value was 141 gauss.

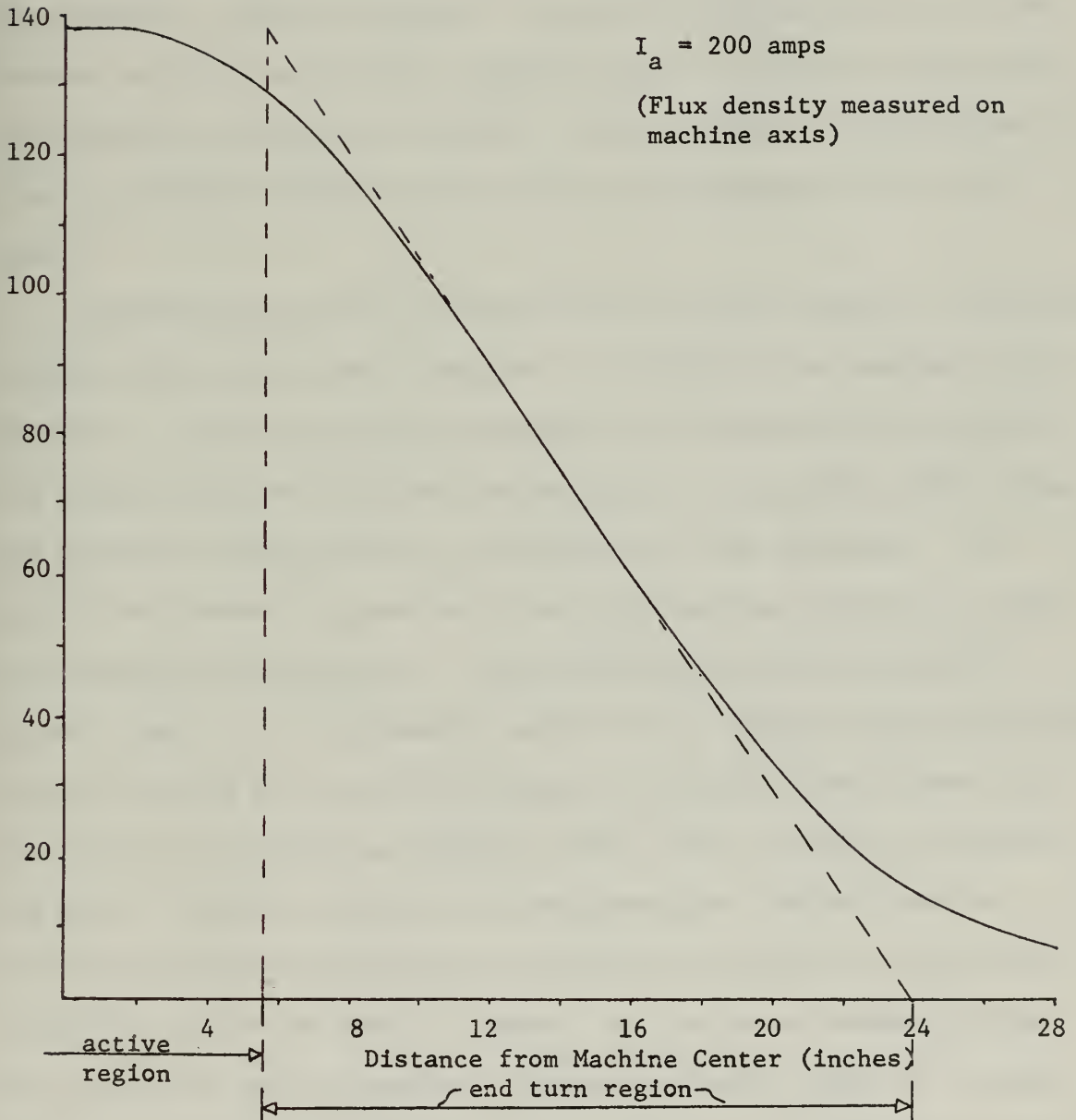
The measured value at the center of the active region was 139 gauss.

FIGURE V-1

Flux Density vs. Axial Position

80 KVA Machine Stator

Y connected

 $I_a = 200$ amps(Flux density measured on
machine axis)

V-2 Shield Time Constants

A number of experiments were performed to confirm the expressions for shield time constants which are developed in section A-2-C. Conducting shields were used, whose thicknesses were about 30% of their outer radius, so that the diffusion time constants, as well as the lowest shield time constant, could be observed. The shield conductivities were first measured with dc, and the time constants predicted from the conductivity and dimensions, using Eqs. (A-60,60'). The experiments were performed by placing the shield inside a motor stator and suspending a flux probe inside.

Resistance was placed in series with the motor armature, to make the armature time constant short compared to the shield time constants to be measured. A step of voltage was applied to the armature and the resulting voltage upon the flux probe was recorded. The recorded probe voltage was plotted on semilog paper, to determine the time constants. The shield time constant T_{s1} and the first diffusion time constant T_{s2} could be determined from the plots. The predicted and measured results are given in Table V-1. The measured values are all slightly smaller than the predicted values for the thicker shields. There are three reasons for this: first, the shield was slightly shorter than the overall length of the motor armature, therefore the two-dimensional analysis does not take into account the resistance contributed by the path of the currents around the ends of the shield. Second, the iron outer boundary of the motor had teeth for the armature windings; the inner radius of the teeth was used for the iron boundary in the equations, but the effective boundary is slightly larger, and would predict a slightly lower time constant.

Third, it was difficult to make the armature time constant too much less than T_{s2} , because the resulting flux inside the shield became very small. Although the armature time constant is too small to separate by the plotting technique, it provides an additional delay in the rise of the flux inside the shell, and appears to make observed time constants slightly larger.

Table V-1

Shield	R_o (in)	Δ (in)	σ	T_{s1} (ms)		T_{s2} (ms)	
				Pred.	Meas.	Pred.	Meas.
Al	1.75	.5	2.28×10^7	7.0	6.8	.47	.58
Al (N temp)	1.75	.5	5.67×10^7	17.7	17.4	1.19	1.45
Bronze	1.75	.5	$.65 \times 10^7$	2.0	1.92	.134	.139
Al	2.25	.116	2.11×10^7	3.3	3.0	not measured	

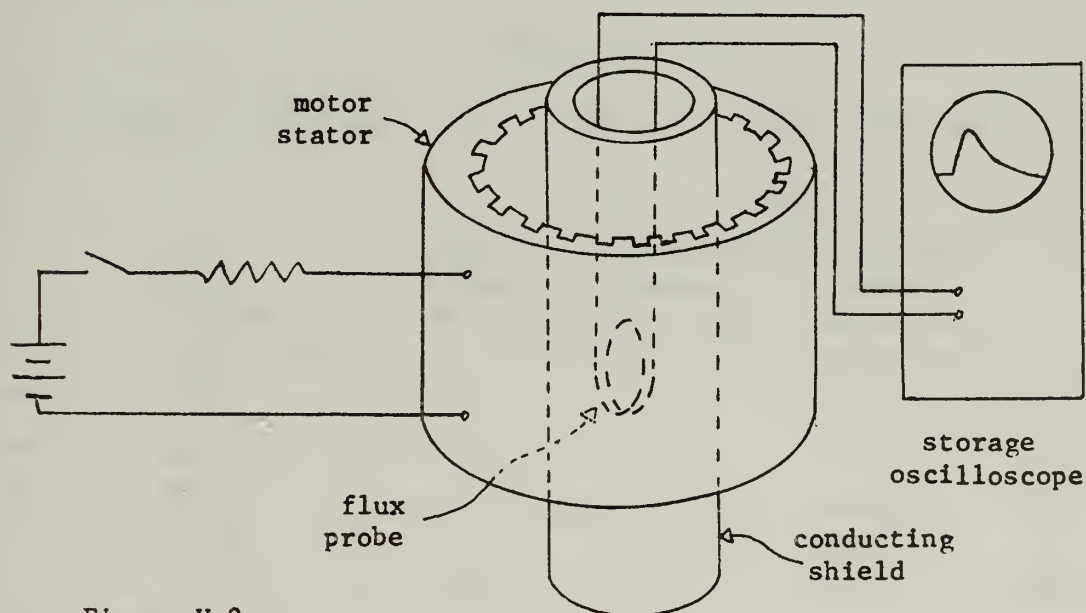


Figure V-2

Shield Time Constant Experimental Setup

V-3 Attenuation Factor of Thick and Thin Shields

An aluminum shield with dimensions 3.5 inches OD and 2.5 inches ID was placed inside a motor stator while the stator windings were excited with variable-frequency currents. The flux density inside the stator was first recorded as a function of frequency and current without the shield. The shield was placed inside the stator and the flux density measured inside the shield at the same frequencies and currents as without the shield. The range of frequencies was such that the magnetic skin depth ran from much greater to much less than the shield thickness.

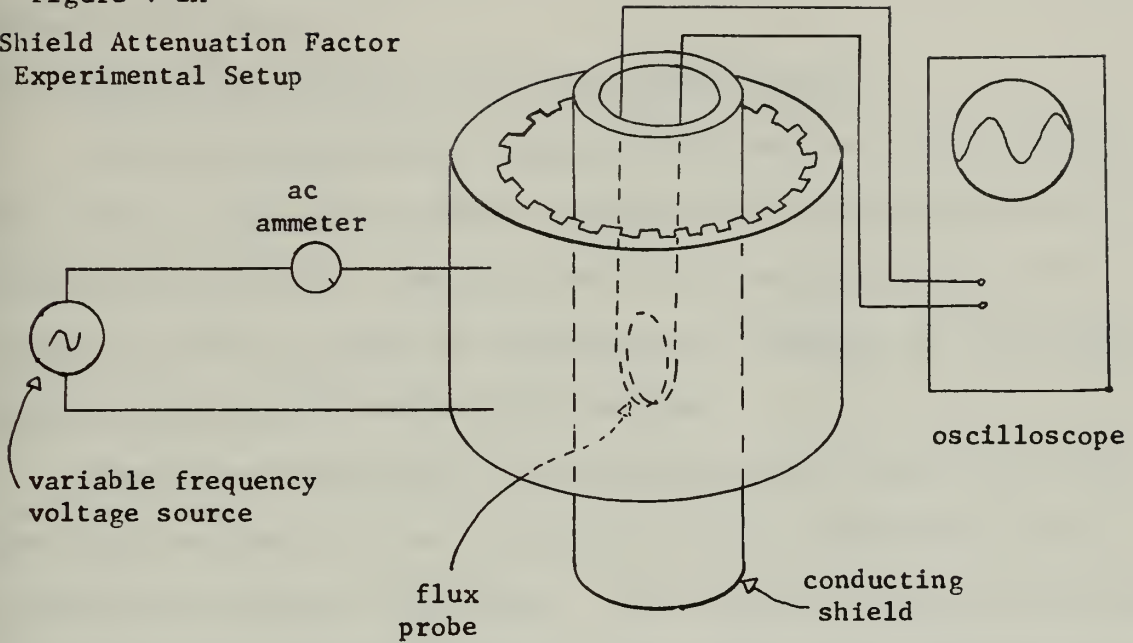
The attenuation factor reciprocals predicted by Eq. (A-54) for a thin shield, Eq. (A-53) for a thick shield, Eq. (A-52') using the Bessel functions, and the measured values, are recorded in Table V-2. For skin depths greater than the physical thickness, the thin shield attenuation factor is fairly accurate. For thickness greater than about two skin depths, the approximate expression given by Eq. (A-53) is quite accurate.

Table V-2

$$R_1 = 1.25'' = 31.75 \text{ mm}, \quad R_0 = 44.45 \text{ mm}, \quad \sqrt{R_1 R_0} = 37.6 \text{ mm}, \quad \Delta = 12.7 \text{ mm}$$

f	δ (mm)	$1/K_{att}$			Exper.
		Bessel Function Eq. A-52'	Thick Shell Approx. Eq. A-53	Thin Shell Approx. Eq. A-54	
40	16.67	2.46	1.71	1.99	1.75
80	11.78	4.52	4.68	3.58	3.8
100	10.54	5.65	5.72	4.42	4.5
200	7.45	12.20	12.14	8.66	8.7
500	4.72	47.2	47.6	21.42	47.0
1000	3.33	196.7	197.6	43.0	200.0

Figure V-2A
Shield Attenuation Factor
Experimental Setup



V-4 Power Dissipation in a Shield

The power dissipated in a conducting, stationary shield inside a three-phase induction motor stator excited by balanced, three-phase currents was measured. The flux density as a function of stator current was measured without the shield and armature i^2r losses were recorded. The shield was placed inside the stator and the increase in power at the stator terminals recorded for the same armature current as without the shield. The time constant of the shield had been determined independently by the experiment of section V-2, but was also checked by recording the attenuation factor of flux inside the shield.

The flux density without the shield was recorded as a function of axial position through the end-turn region in order to determine the effective length of the stator. The power dissipation was predicted from Eq. (A-50), using the flux density without the shield, the shield time

constant, and the geometric factors to be 191 watts. The measured dissipation was 196 watts.

V-5 Sudden Short Circuits of MIT Experimental Generator

The MIT first-generation superconducting machine (nominal rating, 86.5 KVA) was subjected to sudden three-phase and line-to-line short circuits from open circuit. Oscillograms of the resulting currents were recorded in order to check the expressions for transient and subtransient reactance, and for subtransient time constant.

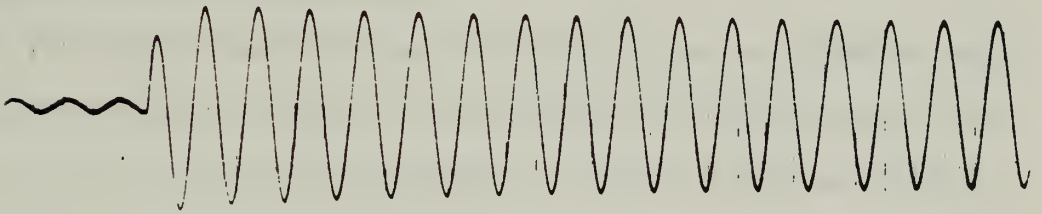
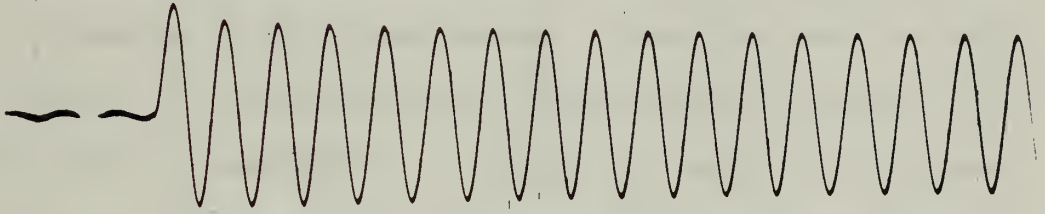
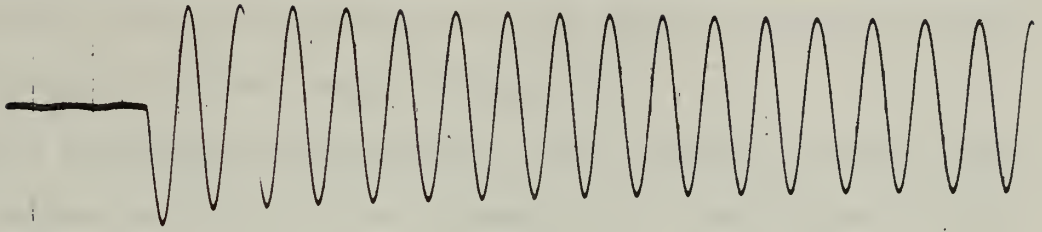
Several runs were made of the three-phase short circuit test. All gave about the same value for reactances, but the later values of subtransient time constant were longer. This, probably, is because the shield was below nitrogen temperature for the later runs, since nitrogen was not used after the initial cool down. Tests made in September, 1969, were done at about 3% of what was then considered rated field current; results of the three-phase tests are stated below. The impedance bases results from the nominal machine rating of 64 volts, line to neutral, phase current of 450 amps, and power rating of 86.5 KVA. The theoretical impedances are predicted from reference [6], and the time constants for equations in Appendix I.

Table V-3

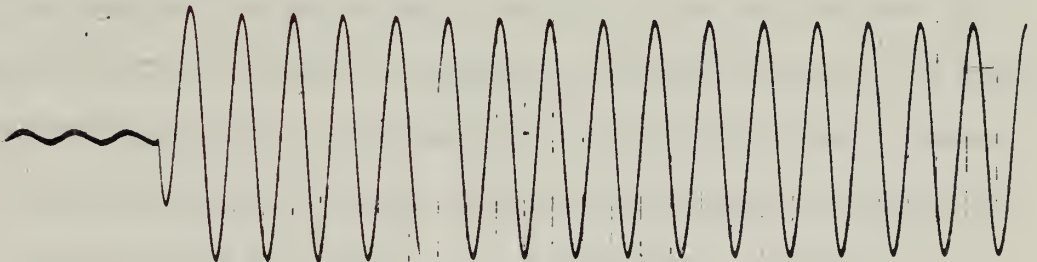
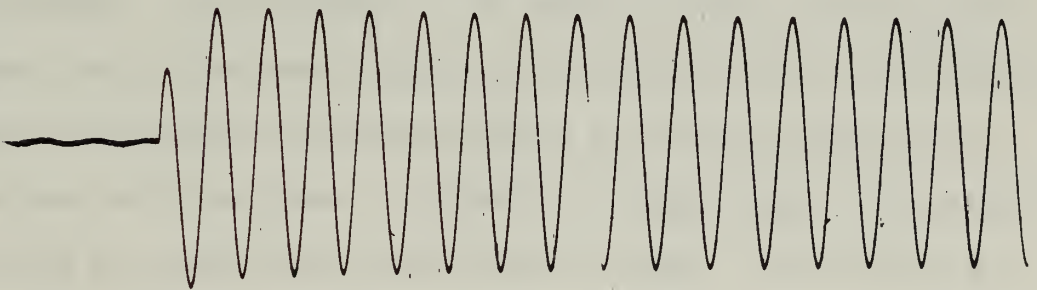
<u>Quantity</u>	<u>Theory</u>	<u>Measured (per unit)</u>	
x		.0133 Ω	.0865
x'	.0188 Ω	.0104 Ω	.0675
x''	.0054 Ω	.0070 Ω	.0455
T'' _d	.0116 sec.	.015 sec.	
Δi_f	.061 amp.	.063 amp.	

FIGURE V-3

Oscillograms of Sudden Short Circuits upon 80 KVA Generator



Three Phase Short Circuit



Line to Line Short Circuit

The field current rise was measured for the three-phase short circuit and was found to be consistent with the measured reactances and the equation for field current surge in Chapter II.

Later experiments have shown that a more realistic voltage rating for the machine is 45 volts, line to neutral, at a field current of 56 amps. Another set of sudden short circuit tests was run with the field current at 6 amps or 10.7% of rated voltage. These tests were run with similar results. No adverse effect upon the machine was observed, and superconductivity was maintained. A line-to-line short circuit from the same open circuit voltage was also performed, with no adverse effects.

V-6 Induction Motor Loss Experiment

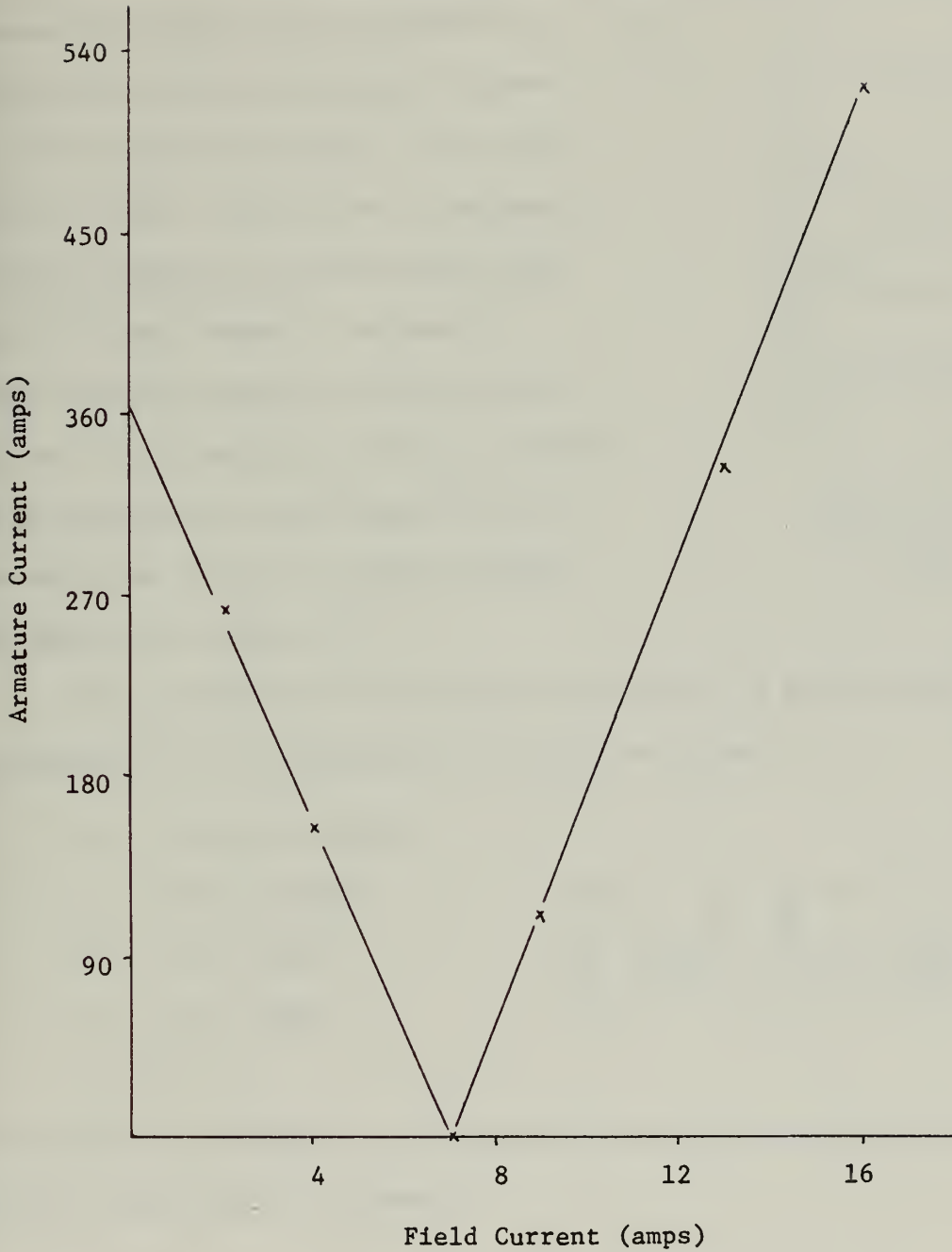
The 80 KVA superconducting generator was run as an induction motor by driving the armature through a three-phase autotransformer and a set of specially built step-down transformers. The electrothermal shield served as the induction motor rotor. The power into the armature terminals was measured. From knowledge of the armature losses and the bearing and windage losses, the power dissipation in the shield can be calculated. The shield time constant was measured before the run was started, and after the last point was taken, by imposing a voltage step on the armature and recording the open-circuit field winding voltage. The shield time constant had changed from beginning of the run to the end, because of the dissipation, but at least the conditions for the first and last point of the run were determined. From knowledge of the shield time constant, armature currents, and rotor speed, the power dissipation in the shield could be predicted from Eq. (A-50). The experimental and predicted results are given below.

<u>RPM</u>	<u>T_{sl}</u>	<u>I_a (amp)</u>	<u>P_{totmeas.}</u>	<u>P_{losses}</u>	<u>P_{shield}</u>	<u>P_{shield (A-50)}</u>
2400	.012	160	53	22	31	32.1
600	.0062	160	115	15	100	90.0

The machine was run to 3,550 rpm as an induction motor, voltage was applied to the field winding, and the machine was synchronized with the 60 Hz. system. Armature current as a function of field current was then recorded with the machine running as a synchronous condensor. The resulting V curve of armature current vs field current is shown below.

FIGURE V-4

"V" Curve for 80 KVA Generator

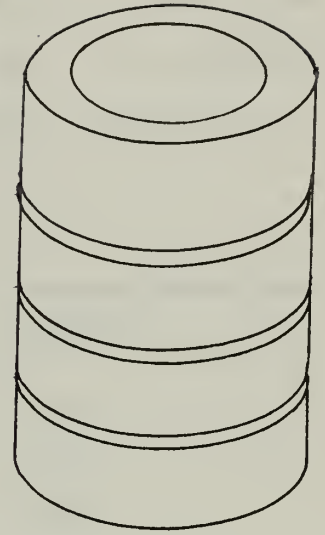


Terminal Voltage = 9.7 volts line-line

Rated Armature Current = 450 amps

V-7 Slotted Electrical Shield

The shield time constant of a conducting shield can be decreased by cutting circumferential slots as shown in the figure at the right. The resistance to axial current flow is increased without affecting the inductance, thus the L/R time constant is decreased. This technique permits a shield designer to use a thick shield for thermal capacity while keeping the time constant to a low enough value to achieve optimum damping, as explained in Chapter II.



Slotted Electrical
Shield

The cross section of one side of the shield is shown below, giving definitions of the parameters of the slots as follows:

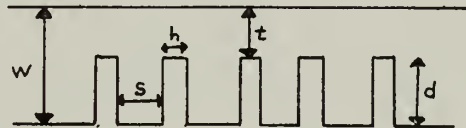
w = shield thickness

s = slot spacing

h = slot width

d = slot depth

t = w - d



The effective thickness Δ_e of the shield for use in calculating the shield time constant is given by

$$\Delta_e = \frac{h + s}{h/w + 2 \ln(1 + \frac{s}{2t})} \quad \text{for } s < d$$

The time constant of the slotted shield can then be calculated using Eq.

(A-56) with Δ_e substituted for Δ .

Experiments were performed using conducting paper with different numbers of slots and spacing. The resistance increase in the paper from one end to the other was measured as the slots were made. The results of the experiment are given below, comparing the resistance predicted by the formulae and the measured values.

<u>Number of slots</u>	<u>Predicted Resistance KΩ/inch</u>	<u>Measured Resistance KΩ/inch</u>
1	8.69	8.65
2	10.80	10.60
3	12.60	12.50
5	14.55	14.70
9	16.33	16.50
17	17.68	17.90

CHAPTER VI

Conclusions and Suggestions for Further Study

The purpose of this study is to identify the critical considerations in the design of a superconducting generator rotor, to insure that it can survive fault conditions. The classes of fault conditions and criteria for survival are as follows:

- 1) A short-term fault of from five to 15 cycles which is cleared by the system circuit breaker.

Criterion: Superconductivity must be maintained.

- 2) A sustained fault inside the system circuit breaker which cannot be cleared.

Criterion: Structural integrity of the rotor must be maintained such that permanent damage does not result.

Chapter II has presented a discussion of the critical effects with a proposed design for a 1000 MVA machine which satisfies the above criteria, while maintaining satisfactory steady-state performance with the inherent advantages of a superconducting generator. Chapter III, IV and V have presented the analytical tools and experimental verification used to develop the design in a form which can be used to evaluate fault effects upon future designs. The conclusions which can be drawn from this study concerning the critical considerations in design of a superconducting generator to survive fault conditions are presented in the following section.

VI-1 Conclusions

- 1) To insure the maintenance of superconductivity through a short-term fault, the following design considerations will be critical:
 - (a) An attenuation factor no greater than .01 at line frequency must be provided to limit temperature rise in the 4.2° K region.
 - (b) The superconductor operating point must be established with anticipation of the field current rise which results during the period prior to breaker interruption of the fault.
 - (c) It is possible to provide a shield which will produce nearly optimum damping consistent with the attenuation requirement of (a). The dynamic stability should therefore be superior to that of a conventional machine, where it is more difficult to tailor the damping coefficient.
- 2) To maintain structural integrity of the rotor, the following design considerations are established:
 - (a) For a shield with an adequate attenuation factor, most of the transient torques are taken by the shield. To provide adequate support for the shield, it should be run at room temperature. A cryogenic shield with adequate structural support will have an intolerable heat leak.
 - (b) The thermal capacity of the shield can be made large compared to the thermal capacity of conventional machines of comparable rating. Values of $I_2^2 t$ up to 20 seconds are possible without excessive shield temperature rise.

- (c) Provision for shield structure to support torques will also provide sufficient support for transient normal mechanical stresses upon the shield.
- (d) Mechanical natural frequencies of the rotor will be high enough not to cause problems for a shield with sufficient structure to withstand the transient mechanical stresses.

In summary, it is possible to design a rotor for a 1000 MVA superconducting generator which can survive short-term faults without loss of superconductivity and sustain faults without damage. This can be done while retaining the advantages of lower weight, lower synchronous reactance, improved efficiency, better damping characteristics, larger $I_2^2 t$, and higher rotor natural frequencies than for a comparable conventional machine.

VI-2 Suggestions for Further Study

- 1) The most important question which is yet to be answered is exactly how to relate short sample characteristics of superconducting wire to the transient conditions in the field winding. Just how much alternating current, what rate of current rise, and how much of a temperature increase will drive the winding normal, must be determined experimentally. With this kind of information, the analytical tools developed in this study can be used to arrive at a shield design which will permit best use of the superconducting winding.
- 2) A restudy of weight optimization should be done, taking into account the rotor structure necessary to support the transient electromechanical stresses.

- 3) A complete study of the refrigeration and shield cooling requirements should be done. It may turn out that the optimum shield temperature is somewhat below room temperature, if the rotor exit gas is used to cool the shield. Otherwise, conventional gas cooling of the shield at room temperature would probably be best.
- 4) The specifications for the secondary or thermal shield should be more exactly determined, once its optimum operating temperature is determined.

A-1 The Lumped-Parameter Machine Model

Generators are conventionally modeled as shown in Fig. A-1, where each winding has a lumped inductance and resistance plus mutual inductance to the other windings. Three identical windings 120° apart in space represent the stationary armature, two orthogonal moving windings represent the damper windings, and a moving winding represents the field winding.

Use of such a model with appropriate engineering approximations and mathematical transformations yields

expressions for transient reactances and time constants describing the behavior of a machine following a fault.

A superconducting generator can likewise be modeled as in Fig. A-1. However, the damper windings for the superconducting machine consist of the electrothermal shield. During transients, the process of magnetic diffusion through the E.T. shield (and the stainless steel dewar shells and metal structure), as well as the decay of currents in the shield's equivalent L-R circuit, affects the observed behavior. The adequacy of representing the electrothermal shield as a lumped L-R circuit, i.e., as one time constant, is investigated in section A-2-c. The result of that analysis shows that the first diffusion time constant is less than the decay time constant by a factor of approximately Δ/R , i.e., the thickness-to-

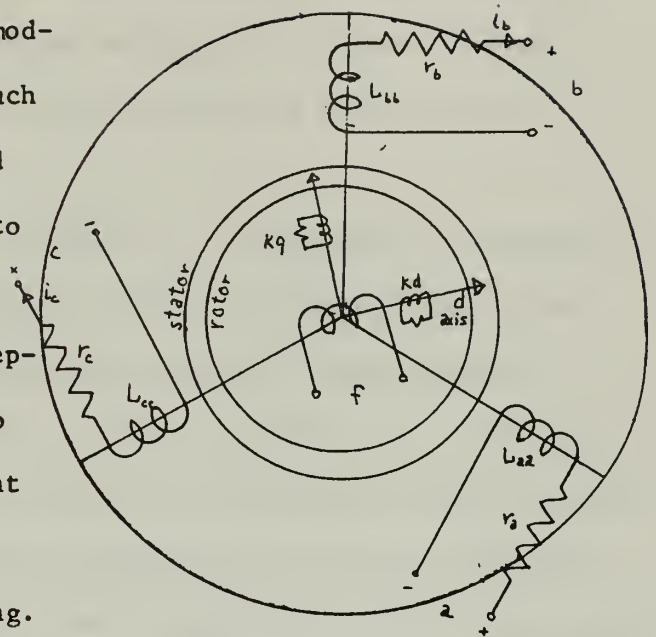


Figure A-1

radius ratio of the E.T. shield. For the thickness-to-radius ratios being used, the determination of stator currents and torques following faults will be sufficiently modeled by neglecting the diffusion time constants.

The ultimate aim of this investigation is to determine the electromechanical and thermal effects within the rotor of a superconducting generator following a fault. The purpose for using the lumped-parameter model is to determine the magnitudes of armature currents following various types of faults based upon the values of reactances analogous to those for conventional machines, but defined appropriately for superconducting machines. Out of this same analysis comes magnitudes of total fault torques exerted upon the armature. The total rotor torques must, of course, be equal and opposite, but their distribution between electrothermal shield and field winding must also be determined. The resulting armature fault currents are used in the magnetic field model, as developed in A-2, to determine the electrical forces and electrical heat loads to which the electrothermal shield and the field winding are subjected during fault conditions.

A-1(a) The Lumped-Parameter Model Including Resistances

A lumped-parameter model as shown in Fig. A-1 can be used in two ways. If the resistances are included in each winding, the differential equations describing the circuit behavior, even after appropriate transformations, can be solved correctly only by using a step-by-step numerical integration with a digital computer. Such investigations are necessary for system performances and stability studies, and have been carried out in reference [5]. However, for determination of internal

effects within the machine itself, it is felt that more insight into the important aspects of fault behavior can be obtained by use of approximate analytical solutions.

The approximate solution of a six-winding model of a generator for fault currents and torques is by no means unique. In fact, the Park's transformation idea which led to many papers on the subject was published over 40 years ago. The one unique aspect of applying such analyses to superconducting generators results from the absence of iron in the rotor; that is, the fact that the generator is an air-core machine. Conventional analyses have normally assumed that all windings of a common axis are coupled by a common mutual flux. In an air-core machine, this is obviously not true. However, the physical placement of the E.T. shield and its continuum nature lead to another simplifying assumption. This is that all flux which links the armature phases and the field winding must also link the E.T. shield (or the damper winding representing the E.T. shield for the lumped-parameter model). This assumption leads directly to a relationship between the mutual and self-inductances of the model shown in Fig. A-1, and is stated algebraically in Eq. (A-10).

The assumption produces a simplification similar to the common mutual flux assumption for conventional machines, and makes an approximate solution of the machine equations possible. This assumption was used by Einstein [5] in preparation of his computer model, and is demonstrated algebraically by Kirtley [6] from a magnetic fields model to determine mutual and self-inductance.

The effect of resistances in the lumped-parameter model is to cause a decay of fault currents; the magnitudes of the fault currents are

practically independent of the resistances. Therefore, once the appropriate time constants for decay of currents are determined, the model excluding resistances can be used. This provides considerable simplification, especially for non-symmetrical faults which are in some ways most severe upon the machine.

In the present section, the resistances are included to determine the appropriate definitions of the transient reactances, time constants, and attenuation of asynchronous fluxes.

The lumped-parameter model for the superconducting generator is shown in Fig.

A-2. The E.T. shield is modeled as two R-L circuits, one in the d axis and one in the q axis. A general relationship between the fluxes linked by the windings and the currents is given by Eq. (A-1).

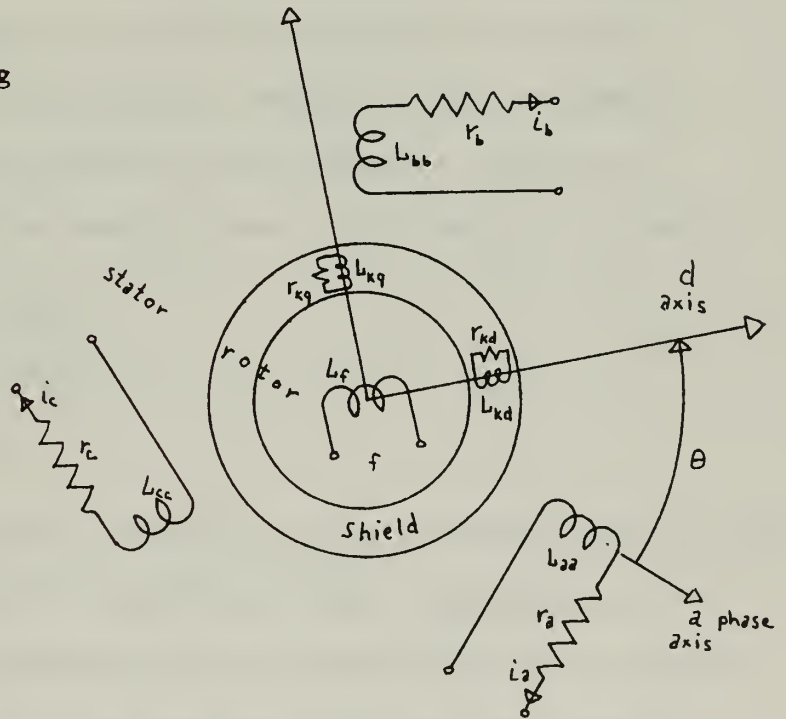


Figure A-2

$$\begin{bmatrix} \lambda_a \\ \lambda_b \\ \lambda_c \\ \lambda_f \\ \lambda_{kd} \\ \lambda_{kq} \end{bmatrix} = \begin{bmatrix} -L_{aa} & -M_{ab} & -M_{ac} & M_{af} & M_{akd} & M_{akq} \\ -M_{ba} & -L_{bb} & -M_{bc} & M_{bf} & M_{bkd} & M_{bkq} \\ -M_{ca} & -M_{cb} & -L_{cc} & M_{cf} & M_{ckd} & M_{ckq} \\ -M_{fa} & -M_{fb} & -M_{fc} & L_f & M_{fkd} & 0 \\ -M_{kda} & -M_{kdb} & -M_{kdc} & M_{kdf} & L_{kd} & 0 \\ -M_{kqa} & -M_{kqb} & -M_{kqc} & 0 & 0 & L_{kq} \end{bmatrix} \begin{bmatrix} i_a \\ i_b \\ i_c \\ i_f \\ i_{kd} \\ i_{kq} \end{bmatrix} \quad (A-1)$$

Most of the inductance coefficients are functions of the angular position of the rotor ϕ . Use of the Park's transformation will yield a considerable simplification of the matrix. However, first the number of coefficients can be reduced by reciprocity and symmetry. Reciprocity implies that the matrix must be symmetric about the diagonal; for example,

$$|M_{ab}| = |M_{ba}|$$

$$|M_{akq}| = |M_{kqa}|$$

etc.

The stator self- and mutual inductances will be a constant because of no rotor saliency. By symmetry, the magnitudes of these inductances must be equal. The rotor-to-stator mutuals must be dependent on the rotor angular position. As in conventional machine analysis, only the first spatial harmonic of flux will be considered in the lumped-parameter representation. All angular dependences must be sinusoidal. By physical symmetry, the magnitudes of the sinusoidal dependences must be equal for similar sets of windings. Mutual and self-inductances within the rotor are constant. By symmetry

Stator

$$L_{aa} = L_{bb} = L_{cc} \equiv L_a$$

$$M_{ab} = M_{ac} = M_{bc} \equiv L_{ab}$$

Stator-to-Rotor

$$|M_{akd}| = |M_{akq}| = |M_{bkd}| = \text{etc.} \equiv M_{kd}$$

$$|M_{af}| = |M_{bf}| = |M_{cf}| \equiv M_{fd}$$

Rotor

$$M_{fkd} \equiv M_{fk}$$

$$L_{kq} = L_{kd} \equiv L_k$$

Park's transformation from a,b,c variables to dqo variables is defined below for the dummy variable, u:

$$\begin{bmatrix} u_d \\ u_q \\ u_o \end{bmatrix} = \begin{bmatrix} 2/3 \cos \theta & 2/3 \cos(\theta - \frac{2\pi}{3}) & 2/3 \cos(\theta + \frac{2\pi}{3}) \\ -2/3 \sin \theta & -2/3 \sin(\theta - \frac{2\pi}{3}) & -2/3 \sin(\theta + \frac{2\pi}{3}) \\ 1/3 & 1/3 & 1/3 \end{bmatrix} \begin{bmatrix} u_a \\ u_b \\ u_c \end{bmatrix}$$

When applied to Eq. (A-1), the result is as follows:

$$\begin{bmatrix} \lambda_d \\ \lambda_q \\ \lambda_o \\ \lambda_f \\ \lambda_{kd} \\ \lambda_{kq} \end{bmatrix} = \begin{bmatrix} -L_d & 0 & 0 & M_{fd} & M_{kd} & 0 \\ 0 & -L_d & 0 & 0 & 0 & M_{kd} \\ 0 & 0 & L_o & 0 & 0 & 0 \\ -3/2 M_{fd} & 0 & 0 & L_f & M_{fk} & 0 \\ -3/2 M_{kd} & 0 & 0 & M_{fk} & L_k & 0 \\ 0 & -3/2 M_{kd} & 0 & 0 & 0 & L_k \end{bmatrix} \begin{bmatrix} i_d \\ i_q \\ i_o \\ i_f \\ i_{kd} \\ i_{kq} \end{bmatrix}$$

$$L_d = L_a = -L_{ab} \quad , \quad L_o = L_o + 2L_{ab}$$

The inductances L_a , L_{ab} , L_f , L_k , M_{kd} , M_{fd} , and M_{fk} are defined in terms of the geometric parameters of the superconducting generator in Ref. [13].

The voltage equations associated with the dqo transformed flux equations are well known, and are given below.

direct axis

$$v_d = -r_a i_d + p \lambda_d - \omega_m \lambda_q$$

$$v_{kd} = 0 = r_k i_{kd} + p \lambda_{kd}$$

$$e_f = r_f i_f + p \lambda_f$$

quadrature axis

$$v_q = -r_a i_q + p \lambda_q + \omega_m \lambda_d$$

$$v_{kq} = 0 = r_k i_{kq} + p \lambda_{kq}$$

$$p = d/dt$$

The next step in any machine analysis of this type is to convert to a dimensionless set of parameters called the "per unit system". Base values of current and voltage are chosen, usually the rated machine values in the armature, and the corresponding base values for the other windings are derived. In determining base currents for rotor circuits, account must be taken of the fact that the direct and quadrature axis armature circuits are 3/2 times as effective in producing armature flux as the rotor circuits, even when the turns ratio has been accounted for. This is because a three-winding armature is now being represented by two windings in the d and q axes. The derivation is carried out in most machine theory texts and is also given in Ref. [5]. The exact expressions for the base values of flux and inductance are not important to the results here. However,

after the appropriate normalization has been done, the per unit flux and voltage equations can be written as follows:

Per Unit Machine Equations

flux

$$\begin{bmatrix} \lambda_d \\ \lambda_{dk} \\ \lambda_f \end{bmatrix} = \begin{bmatrix} -L_d & M_{dk} & M_{df} \\ -M_{dk} & L_k & M_{kf} \\ -M_{df} & M_{kf} & L_f \end{bmatrix} \begin{bmatrix} i_d \\ i_{dk} \\ i_f \end{bmatrix} \quad (\text{A-2})$$

$$\begin{bmatrix} \lambda_q \\ \lambda_{kq} \end{bmatrix} = \begin{bmatrix} -L_d & M_{dk} \\ -M_{dk} & L_k \end{bmatrix} \begin{bmatrix} i_q \\ i_{qk} \end{bmatrix} \quad (\text{A-3})$$

voltage

$$\begin{aligned} v_d &= -r_a i_d + \frac{p}{\omega_o} \lambda_d - \frac{\omega_m}{\omega_o} \lambda_q \\ v_{dk} &= r_k i_{dk} + \frac{p}{\omega_o} \lambda_{dk} = 0 \\ e_f &= r_f i_f + \frac{p}{\omega_o} \lambda_f \\ v_q &= -r_a i_q + \frac{p}{\omega_o} \lambda_q + \frac{\omega_m}{\omega_o} \lambda_d \\ v_{kq} &= r_k i_{kq} + \frac{p}{\omega_o} \lambda_{kq} = 0 \end{aligned} \quad (\text{A-4})$$

All voltage, current, and flux quantities in Eqs. (A-2,3,4) are per unit, ω_o is the angular line frequency, and ω_m is the machine mechanical angular frequency. For example, a value of $i_f = 1.0$ would produce rated open-circuit armature voltage.

At this point, it would be useful to derive the constraint upon the mutual and self-inductances imposed by the presence of the E.T. shield. This result was referred to as the "shell constraint" in Reg. [5]. It will be derived differently here, but will yield the same result.

In Fig. A-2', we have placed three windings on a common axis. We assume that all flux linking windings f and d must also link winding k. An alternating current i_d is imposed in winding d and the flux linked by d, i.e., the alternating open-circuit voltage upon d is measured.

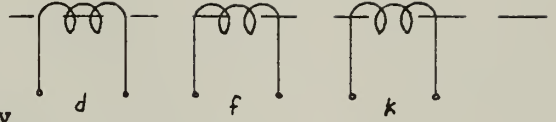


Figure A-2'

$$L_d = \frac{\lambda_d}{I_d}$$

The amplitudes of the alternating quantities are given by λ_d and I_d . At the same time, we measure the flux linked by k, with k open circuit and f open circuit:

$$\lambda_k = M_{dk} I_d$$

The fraction of flux produced by d which is linked by k is

$$\frac{\lambda_k}{\lambda_d} = \frac{M_{dk}}{L_d}.$$

Since all flux produced in d and linking f must also link k, we can express the ratio of λ_f to λ_k similarly to the above equation,

$$\frac{\lambda_f}{\lambda_k} = \frac{M_{fk}}{L_k}$$

In other words, since no flux produced external to k can link f without linking k, the effect is just as if the flux in k were produced by a current in k. We can solve the above equation for λ_f in terms of i_d

$$\lambda_f = \frac{M_{fk} M_{dk}}{L_k} i_d$$

But, by definition, $\lambda_f = M_{df} i_d$

$$\text{Therefore, } M_{df} = \frac{M_{fk} M_{dk}}{L_k} .$$

The relationship can also be expressed as

$$C = M_{df} L_k - M_{fk} M_{dk} = 0 . \quad (\text{A-5})$$

The expression for C appears in later derivations and can be set equal to zero by the above assumption.

Machine transients are conventionally studied in terms of subtransient and transient reactances. These are the reactances of the armature during the period during which the damper windings and the field windings maintain constant flux linkages after a short in the armature. To determine the definitions of these quantities and definitions for the decay time constants of currents during these periods, Eqs. (A-2,4) will be solved for a symmetrical three-phase short circuit upon the armature.

Using (A-2,3,4) we can write the following matrix of equations:

$$\begin{bmatrix} -L_d & M_{df} & M_{dk} \\ -M_{df} \frac{p}{\omega_o} & r_f + L_f \frac{p}{\omega_o} & M_{kf} \frac{p}{\omega_o} \\ -M_{dk} \frac{p}{\omega_o} & M_{kf} \frac{p}{\omega_o} & r_k + L_k \frac{p}{\omega_o} \end{bmatrix} \begin{bmatrix} i_d \\ i_f \\ i_{dk} \end{bmatrix} = \begin{bmatrix} \lambda_d \\ e_f \\ 0 \end{bmatrix} .$$

We can solve for i_d using Cramer's Rule:

$$i_d = -\frac{\lambda_d}{L_d} \frac{\left[1 + p \left(\frac{L_f r_k + L_k r_f}{\omega_o r_f r_k} \right) + p^2 \left(\frac{L_f L_k - M_{kf}^2}{\omega_o^2 r_f r_k} \right) \right]}{D} - \frac{e_f M_{df}}{r_f L_d} \frac{\left(1 + p \frac{C}{\omega_o r_k M_{df}} \right)}{D} \quad (\text{A-6})$$

$$D = 1 + p \left(\frac{L_f r_k}{\omega_o r_k r_f} - \frac{M_{df}^2 r_k}{\omega_o L_d r_k r_f} \right) + p^2 \left(\frac{L_f L_k - M_{kf}^2}{r_k r_f \omega_o^2} - \frac{M_{dk} (M_{dk} L_f - M_{df} M_{kf})}{r_f r_k \omega_o^2} + \frac{M_{df} C}{L_d \omega_o^2 r_f r_k} \right)$$

We define the time constants as follows:

$$\begin{aligned} T_1 &= \frac{L_f}{\omega_o r_f} \\ T_2 &= \frac{L_k}{\omega_o r_k} \\ T_3 &= \frac{L_k}{\omega_o r_k} \left[1 - \frac{M_{kf}^2}{L_k L_f} \right] \\ T_5 &= \frac{L_f}{\omega_o r_f} \left[1 - \frac{M_{df}^2}{L_d L_f} \right] \\ T_6 &= \frac{L_k}{\omega_o r_k} \left[1 - \frac{M_{dk}^2}{L_d L_k} \right] \\ T_7 &= \frac{L_k}{\omega_o r_k} \frac{\left[1 - \frac{M_{kf}^2}{L_f L_k} \right] \left[1 - \frac{M_{dk}^2}{L_k L_d} \right]}{\left[1 - \frac{M_{df}^2}{L_f L_d} \right]} \end{aligned} \quad (\text{A-7})$$

Equation (A-6) can be solved for λ_d and rewritten, using (A-7) and $C = 0$:

$$\lambda_d = -\frac{1+p(T_5+T_6) + p^2 T_5 T_7}{1+p(T_1+T_2)+p^2 T_1 T_3} L_d i_d - \frac{1}{1+(T_1+T_2)p+T_1 T_3 p^2} \frac{M_{df}}{r_f} e_f \quad (\text{A-8})$$

Inspection of Eq. (A-7) shows that

$$T_6, T_7 < T_5$$

and $T_2, T_3 < T_1$

since T_1, T_5 are related to the field winding time constant, and T_6, T_7, T_2 , and T_3 are all related to the E.T. shield time constant;

$$\therefore 1 + (T_5 + T_6)p + T_5 T_7 p^2 \approx (1 + T_5 p)(1 + T_7 p)$$

$$\text{and } 1 + (T_1 + T_2)p + T_1 T_3 p^2 \approx (1 + T_1 p)(1 + T_3 p).$$

$$\lambda_d = - \frac{(1 + T_5 p)(1 + T_7 p)}{(1 + T_1 p)(1 + T_3 p)} L_d i_d - \frac{1}{(1 + T_1 p)(1 + T_3 p)} \frac{M_{df}}{r_f} e_f \quad (\text{A-9})$$

From (A-9), the open-circuit and short-circuit time constants are obtained and listed below.

$$T'_{do} = T_1 = \frac{L_f}{\omega_o r_f}$$

$$T''_{do} = T_3 = \frac{L_k}{\omega_o r_k} \left[1 - \frac{M_{kf}^2}{L_k L_f} \right]$$

$$T'_d = T_5 = \frac{L_f}{\omega_o r_f} \left[1 - \frac{M_{df}^2}{L_d L_f} \right] \quad (\text{A-10})$$

$$T''_d = T_7 = \frac{L_k}{\omega_o r_k} \frac{\left[1 - \frac{M_{kf}^2}{L_f L_k} \right] \left[1 - \frac{M_{dk}^2}{L_k L_d} \right]}{\left[1 - \frac{M_{df}^2}{L_f L_d} \right]}$$

The general operational inductance can be written as follows:

$$L_d(p) = L_d \frac{(1 + T'_d p)(1 + T''_d p)}{(1 + T'_{do} p)(1 + T''_{do} p)} \quad (\text{A-11})$$

For times short compared to T_3 , i.e., $1/T_3 < p < \infty$, the inductances reduce to L_d'' , the subtransient inductance.

$$L_d'' = L_d \frac{T_d' T_d''}{T_{do}' T_{do}''}$$

$$L_d'' = L_d \left(1 - \frac{M_{kd}^2}{L_k L_d} \right) \quad (A-12)$$

For times $T_3 < t < T_5$, i.e., $\frac{1}{T_1} < p < \frac{1}{T_3}$, the operational inductance becomes the transient inductance, L_d' .

$$L_d' = L_d \frac{T_d'}{T_{do}'}$$

$$L_d' = L_d \left(1 - \frac{M_{df}}{L_d L_f} \right) \quad (A-13)$$

In per-unit notation, inductances and reactances are numerically equal because the machine is operating at rated frequency, that is, for $\omega = \omega_o$, $\omega_{\text{per unit}} = 1$. The more conventional notation is to use per-unit reactances rather than inductances.

Per-Unit Reactances

$$x_d = L_d$$

$$x_d'' = x_d \left(1 - \frac{M_{kd}^2}{L_k L_d} \right) \quad (A-14)$$

$$x_d' = x_d \left(1 - \frac{M_{df}^2}{L_d L_f} \right)$$

More useful forms for the time constant expressions are in terms of the reactances as follows:

$$\begin{aligned}
 T'_{do} &= T_f \\
 T''_{do} &= T_{s1} \left(\frac{x'_d - x''_d}{x_d - x''_d} \right) \\
 T'_d &= T_f \frac{x'_d}{x_d} \\
 T''_d &= T''_{do} \frac{x''_d}{x_d}
 \end{aligned}
 \begin{array}{l}
 \text{Symmetrical fault} \\
 \text{time constants}
 \end{array}
 \quad (A-15)$$

where T_f is the field time constant, and T_{s1} is the E.T. shield decay time constant.

For non-symmetrical (line-line) fault, one phase of the machine remains connected to the system through a system reactance, x_s . Transformation of flux equations for this case shows that the effective direct axis armature inductance is increased by one-half the system inductance. Therefore, the same definitions of time constants can be used if, in Eqs.(A-15), the value of x_d is replaced by $x_d + \frac{x_s}{2}$. The resulting time constants for line-line short circuit written in form similar to Eqs. (A-15) are as follows:

$$\begin{aligned}
 T'_{d\ell} &= T_f \left[1 - \frac{x_d - x'_d}{x_d + \frac{x_s}{2}} \right] \\
 T''_{d\ell} &= T_{s1} \left[\frac{x'_d - x''_d}{x'_d - x''_d} \right] \left[\frac{\frac{x_s}{2} + x''_d}{\frac{x_s}{2} + x'_d} \right] \\
 T''_{q\ell} &= T_{s1} \left[1 - \left(\frac{x'_d - x''_d}{x_d + \frac{x_s}{2}} \right) \right]
 \end{aligned}
 \begin{array}{l}
 \text{Line-Line} \\
 \text{Fault}
 \end{array}
 \quad (A-16)$$

For transient following synchronizing of the machine to a system through a reactance x_s , the effective value of x_d must be replaced by $x_d + x_s$ with the resulting time constants:

$$T'_{dcl} = T_f \left[1 - \frac{x_d' - x_d'}{x_d' + x_s'} \right]$$

$$T''_{dcl} = T_s \left[\frac{x_d' - x_d''}{x_d' - x_d''} \right] \left[\frac{x_s + x_d''}{x_s + x_d'} \right]$$

Synchronizing
at arbitrary
phase angle

(A-17)

$$T''_{qcl} = T_s \left[1 - \frac{x_d - x_d''}{x_d + x_s} \right]$$

Field Current During Transient

The determination of distribution of transient torques between field winding and electrothermal shield as developed in section A-1-b requires that field current during transient be determined. This obviously can be determined only from the model including winding resistance, because of the shielding effect of the damper windings. This shielding effect is a function of only the damper winding time constant in the lumped-parameter model. For an electrothermal shield thick compared to an appropriate skin depth, the shielding expression must be determined from the magnetic fields model in section A-2-b. The lumped-parameter determination of field current will indicate how the thick shield attenuation should be used for shields for which the thin shield, or single time constant attenuation, is no longer adequate.

To determine the induced alternating field currents, we write the direct axis voltage and flux equations.

$$v_d = -r_a i_d + \frac{p}{\omega_o} \lambda_d - \frac{\omega_m}{\omega_o} \lambda_q$$

$$0 = r_k i_{dk} + \frac{p}{\omega_o} \lambda_{dk}$$

$$e_f = r_f i_f + \frac{p}{\omega_o} \lambda_f$$

$$\begin{bmatrix} \lambda_d \\ \lambda_{dk} \\ \lambda_g \end{bmatrix} = \begin{bmatrix} -L_d & M_{dk} & M_{df} & i_d \\ -M_{dk} & L_k & M_{kf} & i_{dk} \\ -M_{df} & M_{kf} & L_f & i_f \end{bmatrix}$$

We can reduce the above six equations to one equation in i_f , i_d , e_f using the same time constant approximations as in deriving the direct-axis operational impedance:

$$i_f = \frac{1 + T_2 p}{(1 + T'_{do} p)(1 + T''_{do} p)} \left(\frac{e_f}{r_f} \right) + \frac{M_{df} p}{(1 + T'_{do} p)(1 + T''_{do} p)} \left(\frac{1}{r_f} \right) i_d$$

To find the induced ac field current due to an alternating i_d , we let

$i_d = -I_d \cos \omega_x t$ and $e_f = \text{constant}$, and solve for i_f with the assumption that $T'_{do} \omega_x \gg 1$.

$$i_{f_{ac}} = - \frac{M_{df}}{T'_{do} r_f} \frac{I_d}{\sqrt{1 + (T''_{do} \omega_x)^2}} \cos(\omega_x t - \alpha), \quad \alpha = \tan^{-1} \frac{\omega_x T''_{do}}{\sqrt{1 + (T''_{do} \omega_x)^2}} \quad (\text{A-18})$$

The square root factor in the denominator represents the damper attenuation. Further simplification results for the assumptions of resistance- and reactance-limited E.T. shields (equations in per-unit).

Resistance-Limited E.T. Shield

$$|i_{f_{ac}}| = (x_d - x'_d) |I_d| \quad (\text{A-19a})$$

$$\left| i_{f_{ac}} \right| = \frac{(x_d - x'_d)(x_d - x''_d)}{(x'_d - x''_d)} K_{att} |I_{d_{ac}}| \quad (A-19b)$$

A-1(b) The Lumped-Parameter Model Neglecting Resistance

The magnitudes of transient torques and currents are affected very little by the resistance of the windings. By solving for these magnitudes in a model neglecting resistances, and applying appropriate decrement factors using time constants developed in the last section, the electromechanical effects on the rotor can be determined. In order to include the possibility of an unsymmetrical fault, an α - β transformation will be used instead of the dq transformation. The α - β stator windings are the two windings equivalent to the three armature windings fixed in space, rather than the d-q windings which rotate with the rotor.

The per-unit d-q inductance matrix given by Eqs. (A-2,3) can be transformed directly to the α , β notation. Equations (A-2,3) are rewritten below within one matrix.

$$\begin{bmatrix} -\lambda_d \\ \lambda_q \\ \lambda_f \\ \lambda_{kd} \\ \lambda_{kq} \end{bmatrix} = \begin{bmatrix} -L_d & 0 & M_{fd} & M_{kd} & 0 & i_d \\ 0 & -L_d & 0 & 0 & M_{kd} & i_q \\ -M_{df} & 0 & L_f & M_{fd} & 0 & i_f \\ -M_{kd} & 0 & M_{fk} & L_k & 0 & i_{kd} \\ 0 & -M_{kd} & 0 & 0 & L_k & i_{kq} \end{bmatrix}$$

The α , β to dq and the dq to α , β transformations are as follows:

$$\begin{bmatrix} i_d \\ i_q \end{bmatrix} = \begin{bmatrix} \cos \theta & \sin \theta \\ -\sin \theta & \cos \theta \end{bmatrix} \begin{bmatrix} i_\alpha \\ i_\beta \end{bmatrix}, \quad \begin{bmatrix} i_\alpha \\ i_\beta \end{bmatrix} = \begin{bmatrix} \sin \theta & \cos \theta \\ \cos \theta & -\sin \theta \end{bmatrix} \begin{bmatrix} i_d \\ i_q \end{bmatrix}$$

The dq inductance matrix in α, β notation is as follows:

$$\begin{bmatrix} \lambda_{\alpha} \\ \lambda_{\beta} \\ \lambda_f \\ \lambda_{kd} \\ \lambda_{kq} \end{bmatrix} = \begin{bmatrix} -L_d & 0 & M_{fd} \cos \theta & M_{kd} \cos \theta & M_{kd} \sin \theta & i_{\alpha} \\ 0 & -L_d & M_{fd} \sin \theta & M_{kd} \sin \theta & M_{kd} \cos \theta & i_{\beta} \\ -M_{fd} \cos \theta & -M_{fd} \sin \theta & L_f & M_{fd} & 0 & i_f \\ -M_{kd} \cos \theta & -M_{kd} \sin \theta & M_{fd} & L_k & 0 & i_{kd} \\ M_{kd} \sin \theta & -M_{kd} \cos \theta & 0 & 0 & L_k & i_{kq} \end{bmatrix}$$

Assume a short on phase β at $t = 0$, $\lambda_{kq0} = \lambda_{kq}(t=0)$ and solve for i_{kq} :

$$i_{kq} = \frac{\lambda_{kq0}}{L_{kd}} + \frac{M_{kd}}{L_{kd}} i_q$$

We define the quantity ψ_{q1} as follows:

$$\psi_{q1} = \frac{M_{kd}}{L_{kd}} \lambda_{kq0} \quad (\text{A-21})$$

$$i_{kq} = \frac{\psi_{q1}}{M_{kd}} + \frac{M_{kd}}{L_{kd}} i_q$$

We solve in Eq. (A-20) for $M_{kd} i_{kd} + M_{fd} i_f$ with $\lambda_{fo} = \lambda_f(t=0)$, $\lambda_{kdo} = \lambda_{kd}(t=0)$.

$$M_{kd} i_{kd} = \left(\frac{1}{M_{fk}^2 - L_k L_f} \right) [M_{kd} M_{fk} \lambda_{fo} - M_{kd} L_f \lambda_{kdo} + M_{kd} (M_{fd} M_{fk} - L_f M_{kd}) i_d]$$

$$M_{fd} i_f = - \left(\frac{1}{M_{fk}^2 - L_k L_f} \right) [M_{fd} L_k \lambda_{fo} - M_{fd} M_{fk} \lambda_{kdo} + M_{kd} \underbrace{(M_{fd} L_k - M_{kd} M_{fd})}_C i_d]$$

Since the electrothermal shield completely surrounds the field winding and is a continuum of conducting material which permits currents to

flow such that its total flux linked must remain constant, a sudden change in direct axis current will produce no sudden change in i_f . Therefore, the coefficient of i_d must be zero. This is equivalent to the assumption expressed in Eq. (A-5).

$$M_{fd}L_k - M_{kd}M_{fk} = C = 0$$

The assumption that $C = 0$ leads to a more simple result for the sum of direct-axis rotor currents:

$$M_{kd}i_{kd} + M_{fd}i_f = \left(\frac{M_{fd}M_{fk} - M_{kd}L_f}{M_{fk}^2 - L_kL_f} \right) \lambda_{kdo} + \frac{M_{kd}(M_{fd}M_{fk} - L_fM_{kd})}{M_{fk}^2 - L_kL_f} i_d$$

We define the quantity ψ_{d1} as follows:

$$\psi_{d1} = \frac{M_{kd}}{L_k} \lambda_{kdo} \quad (A-22)$$

Use of the constraint $C = 0$ and the definitions of i_α and i_β lead to the solution for λ_α and λ_β :

$$M_{kd}i_{kd} + M_{fd}i_f = \psi_{d1} + \frac{M_{kd}^2}{L_k} i_d$$

$$\lambda_\alpha = -L_d \left(1 - \frac{M_{kd}^2}{L_dL_k} \right) i_\alpha + \psi_{d1} \cos \theta - \psi_{q1} \sin \theta$$

$$\lambda_\beta = -L_d \left(1 - \frac{M_{kd}^2}{L_dL_k} \right) i_\beta + \psi_{d1} \sin \theta + \psi_{q1} \cos \theta \quad (A-23)$$

Equations (A-23) are now in a form which can be used to calculate the effects of unbalanced (or balanced) transients from loaded (or unloaded) conditions.

The machine configuration is as shown below with the α and β phase connected to an infinite bus $v_{s\alpha}$, $v_{s\beta}$ through a system reactance x_s .

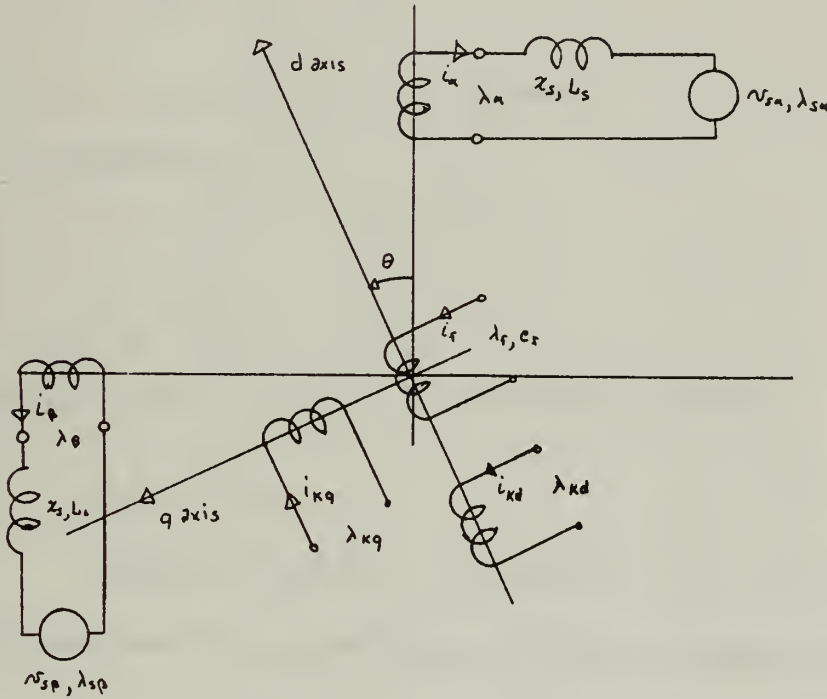


Figure A-3

The steady state of the system before the fault is represented by the phasor diagram below:

$$\theta = \omega t$$

$$\psi_f = M_{fd} I_f \cos \omega t$$

$$v_\alpha = -v_a \sin(\omega t - \delta)$$

$$v_{s\alpha} = -v_{sd} \sin(\omega t - \delta_s)$$

$$i_\alpha = -I_a \sin(\omega t - \delta - \theta_p)$$

$$i_\beta = I_a \cos(\omega t - \delta - \theta_p)$$

$$i_d = I_a \sin(\delta + \theta_p)$$

$$i_q = I_a \cos(\delta + \theta_p)$$

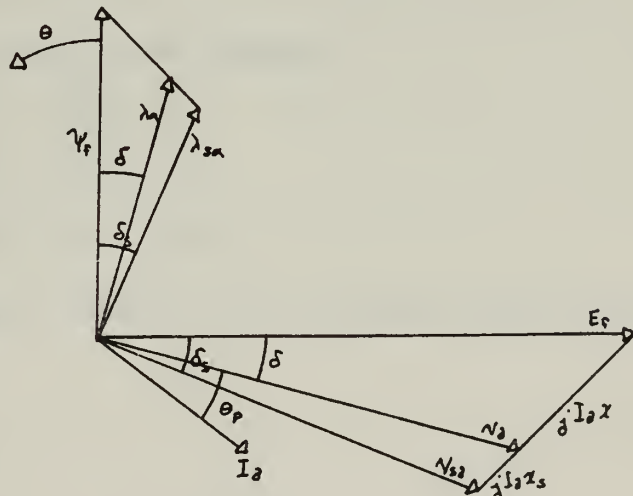


Figure A-4

Equations (A-23) can also be written using (A-12,13) and reactance notation, as (in per-unit):

$$\lambda_{\alpha} = -x_d'' i_{\alpha} + \psi_{d1} \cos \theta - \psi_{q1} \sin \theta \quad (\text{A-24})$$

$$\lambda_{\beta} = -x_d'' i_{\beta} + \psi_{d1} \sin \theta + \psi_{q1} \cos \theta$$

and in dq components as

$$\psi_d = \psi_{sd} + i_d L_s = -x_d'' i_d + \psi_{d1} \quad (\text{A-25})$$

$$\psi_q = \psi_{sq} + i_q L_s = -x_d'' i_q + \psi_{q1}$$

The torque acting on the stator is given by Eq. (A-26):

$$\begin{aligned} \tau &= \psi_d i_q - \psi_q i_d \\ &= (M_{kd} i_{kd} + M_{fd} i_f) i_q - (M_{kd} i_{kd}) i_d \end{aligned} \quad (\text{A-26})$$

From the equations for i_{kq} and $M_{kd} i_{kd} + M_{fd} i_f$, we obtain in the quadrature axis the following equations:

$$\begin{aligned} M_{kd} i_{kq} &= \psi_{q1} + \frac{M_{kd}^2}{L_{kd}} i_q \\ &= \psi_{q1} + (L_d - L_d'') i_q \end{aligned}$$

In the direct axis, similar results are obtained.

$$\begin{aligned} M_{kd} i_{kd} + M_{fd} i_f &= \psi_{d1} + \frac{M_{kd}^2}{L_k} i_d \\ &= \psi_{d1} + (L_d - L_d'') i_d \end{aligned}$$

The torque equation can then be reduced to the following simple result:

$$\tau = \psi_{d1} i_q - \psi_{q1} i_d \quad (\text{A-27})$$

The following equations relate torque angles, terminal voltage, system voltage, and voltage behind synchronous reactance.

$$\delta = \tan^{-1} \frac{I_a x \cos \theta_p}{V_t + I_a x \sin \theta_p}$$

$$\delta_s = \delta + \tan^{-1} \frac{x_s I_a \cos \theta_p}{V_t - x_s I_a \sin \theta_p}$$

$$V_t = x_s I_a \sin \theta_p + [V_{sa}^2 - (x_s I_a)^2 (1 - \sin^2 \theta_p)]^{1/2}$$

$$E_f^2 = (V_t + x I_a \sin \theta_p)^2 + (x I_a \cos \theta_p)^2$$

$$\lambda_\alpha = \lambda_{s\alpha} + i_\alpha x_s = -x_d'' i_\alpha + \psi_{d1} \cos \theta_p - \psi_{q1} \sin \theta_p$$

$$\lambda_\beta = \lambda_{s\beta} + i_\beta x_s = -x_d'' i_\beta + \psi_{d1} \sin \theta_p + \psi_{q1} \cos \theta_p$$

Eliminating λ_α , λ_β , we obtain the following expressions for $\lambda_{s\alpha}$ and $\lambda_{s\beta}$:

$$\lambda_{s\alpha} = - (x'' + x_s) + \psi_{d1} \cos \omega t - \psi_{q1} \sin \omega t \quad (\text{A-28})$$

$$\lambda_{s\beta} = - (x'' + x_s) + \psi_{d1} \sin \omega t + \psi_{q1} \cos \omega t$$

We solve for the currents in (A-28) with the following results:

$$i_\alpha = - \frac{\psi_{s\alpha}}{x'' + x_s} + \frac{\psi_{d1}}{x'' + x_s} \cos \omega t - \frac{\psi_{q1}}{x'' + x_s} \sin \omega t \quad (\text{A-29})$$

$$i_\beta = - \frac{\psi_{s\beta}}{x'' + x_s} + \frac{\psi_{d1}}{x'' + x_s} \sin \omega t + \frac{\psi_{q1}}{x'' + x_s} \cos \omega t$$

Line-Line Short Circuit from Load

At $t = 0$, the β winding is shorted, trapping flux $\psi_{\beta 0}$. Equations

(A-29) become:

$$\begin{aligned} i_{\alpha} &= \frac{\psi_{s\alpha}}{x'' + x_s} + \frac{\psi_{d1}}{x'' + x_s} \cos \omega t - \frac{\psi_{q1}}{x'' + x_s} \sin \omega t \\ i_{\beta} &= -\frac{\psi_{\beta 0}}{x''} + \frac{\psi_{d1}}{x''} \sin \omega t + \frac{\psi_{q1}}{x''} \cos \omega t \end{aligned} \quad (A-30)$$

The currents can also be expressed as i_d and i_q :

$$\begin{aligned} i_d &= -\frac{\psi_{s\alpha}}{x'' + x_s} \cos \omega t - \frac{\psi_{\beta 0}}{x''} \sin \omega t + \frac{\psi_{d1}(2x'' + x_s)}{2x''(x'' + x_s)} \\ &\quad - \frac{\psi_s}{2x''(x'' + x_s)} (\psi_{d1} \cos 2\omega t - \psi_{q1} \sin 2\omega t) \\ i_q &= \frac{\psi_{s\alpha}}{x'' + x_s} \sin \omega t - \frac{\psi_{\beta 0}}{x''} \cos \omega t + \frac{\psi_{q1}(2x'' + x_s)}{2x''(x'' + x_s)} \\ &\quad + \frac{\psi_s}{2x''(x'' + x_s)} (\psi_{d1} \sin 2\omega t + \psi_{q1} \cos 2\omega t) \end{aligned} \quad (A-31)$$

We substitute the above into the torque equation:

$$\begin{aligned} \tau &= \frac{\psi_{s\alpha}}{x'' + x_s} (\psi_{d1} \sin \omega t + \psi_{q1} \cos \omega t) \\ &\quad - \frac{\psi_{\beta 0}}{x''} (\psi_{d1} \cos \omega t - \psi_{q1} \sin \omega t) \\ &\quad + \frac{\psi_s}{2x''(x'' + x_s)} [2\psi_{d1}\psi_{q1} \cos 2\omega t + (\psi_{d1}^2 - \psi_{q1}^2) \sin 2\omega t] \end{aligned} \quad (A-32)$$

Equations for ψ_{d1} , ψ_{q1} as functions of t following various faults were derived in Ref. [7] by Woodson; these expressions are reproduced on the following pages.

Line-to-Line Short From Load

$$\psi_{d1} = \frac{x'' + x_s}{x + x_s} M_{df} I_{fo} F_{dl1} + \frac{x - x''}{x + x_s} V_{sa} \cos \delta_s F_{dl2} \quad (A-32-1)$$

$$\psi_{q1} = - \frac{x - x''}{x + x_s} V_{sa} \sin \delta_s F_{ql}$$

$$F_{dl1} = 1 - \frac{2x''(x' + x_s)}{x''(x' + x_s) + x'(x'' + x_s)} e^{-t/T''_{dl}} \\ + \frac{2x''(x' + x_s)}{x''(x' + x_s) + x'(x'' + x_s)} - \frac{2x''(x + x_s)}{x''(x + x_s) + x(x'' + x_s)} e^{-t/T'_{dl}} \\ + \frac{2x''(x + x_s)}{x''(x + x_s) + x(x'' + x_s)}$$

$$F_{dl2} = 1 - \frac{2x''(x'' + x_s)}{x''(x'' + x_s) + x'(x'' + x_s)} \frac{x - x'}{x - x'} + \frac{(x + x_s)(x' - x'')}{2(x'' + x_s)(x - x'')} e^{-t/T''_{dl}} \\ + \frac{2x''(x'' + x_s)}{x''(x'' + x_s) + x'(x'' + x_s)} \frac{x - x'}{x - x'} + \frac{(x + x_s)(x' - x'')}{2(x'' + x_s)(x - x'')} \frac{x''(x + x_s)}{x''(x + x_s) + x(x'' + x_s)} e^{-t/T'_{dl}} \\ + \frac{x''(x + x_s)}{x''(x + x_s) + x(x'' + x_s)}$$

$$F_q = 1 - \frac{x''(x + x_s)}{x''(x + x_s) + x(x'' + x_s)} e^{-\frac{t}{T''_{ql}}} + \frac{x''(x + x_s)}{x''(x + x_s) + x(x'' + x_s)}$$

$$\psi_{s\alpha} = V_{sa} (\omega t - \delta_s)$$

$$\psi_{\beta 0} = V_a \sin (\omega t_0 - \delta) A_\beta$$

$$A_\beta = e^{-t/\tau_{al}}$$

Line-Line Short from Open Circuit

In the preceding, let $x_s \rightarrow \infty$. Equation (A-32) for torque becomes:

$$\tau = -\frac{\psi_{\beta 0} A_{\beta}}{x''} \psi_{d1} \cos \omega t + \frac{\psi}{2x''} \sin 2\omega t \quad (\text{A-32-2})$$

$$\psi_{\beta 0} = V_a \sin \omega t_0$$

$$A_{\beta} = e^{-t/\tau_a} l$$

$$\psi_{d1} = M_{df} I_{fo} F_{dlo}$$

$$F_{dlo} = \left(1 - \frac{2x''}{x' + x''} e^{-t/\tau_{d\ell}} + \left(\frac{2x''}{x' + x''} - \frac{2x''}{x + x''}\right) e^{-t/\tau_{d\ell}'} + \frac{2x''}{x + x''}\right)$$

$$i_{\alpha} = 0$$

$$i_{\beta} = -\frac{\psi_{\beta 0}}{x''} + \frac{\psi_{d1}}{x''} \sin \omega t$$

Three-Phase Short Circuit from Load

The three-phase short circuit is independent of time of application of the short; therefore we apply it when flux linking α is zero - i.e., when $\omega t_0 = \delta + \pi/2$.

$$\text{Let } \psi_{s\alpha} = 0$$

$$\psi_{\beta 0} = V_a$$

$$x_s = 0$$

From Equations (26),

$$i_{\alpha} = \frac{\psi_{d1}}{x''} \cos \omega t - \frac{\psi_{q1}}{x''} \sin \omega t \quad (\text{A-32-3})$$

$$i_{\beta} = -\frac{V_a A_{\beta}}{x''} + \frac{\psi_{d1}}{x''} \sin \omega t + \frac{\psi_{q1}}{x''} \cos \omega t.$$

From Eq. (A-28),

$$\tau = -\frac{V_a A_\beta}{x''} (\psi_{d1} \cos \omega t - \psi_{q1} \sin \omega t)$$

From Ref. [7],

$$\psi_{d1} = M_{fd} I_{fo} F_{d1} - (x - x'') I_a \sin (\delta + \theta) F_{d2}$$

$$\psi_{q1} = - (x - x'') I_a \cos (\delta + \theta) F_q$$

$$F_d = \left(1 - \frac{x''}{x'}\right) e^{-\frac{t-t_o}{T_d''}} + \left(\frac{x''}{x'} - \frac{x}{x}\right) e^{-\frac{t-t_o}{T_d'}} + \frac{x''}{x}$$

$$F_d = 1 - \frac{x''(x-x')}{x'(x-x'')} e^{-t-t_o/T_d''} + \frac{x''(x-x')}{x'(x-x'')} e^{-t-t_o/T_d'}$$

$$A_\beta = e^{-t-t_o/T_a}$$

Three-Phase Short Circuit from Open Circuit at $\omega t = \pi/2$

$$I_a = 0 \text{ before fault}$$

(A-32-4)

$$i_\alpha = \psi_{d1}/x'' \cos \omega t$$

$$i_\beta = \frac{V_a}{x''} + \frac{\psi_{d1}}{x''} \sin \omega t$$

$$\tau = -\frac{V_a A}{x''} \psi_{d1} \cos \omega t$$

$$\psi_{d1} = M_{fd} I_{fo} F_{d1} \text{ where } M_{fd} I_{fo} = V_a$$

Closing at Arbitrary Phase from Open Circuit

We assume the generator is out of phase with system by angle θ_s .

$$v_\alpha = -M_{fd} I_{fo} \sin \omega t, \quad v_\beta = M_{fd} I_{fo} \cos \omega t \quad (A-32-5)$$

$$\psi_\alpha = M_{fd} I_{fo} \cos \omega t, \quad \psi_\beta = M_{fd} I_{fo} \sin \omega t \quad \text{before}$$

$$v_{s\alpha} = -V_{sa} \sin(\omega t - \theta_s), \quad v_{s\beta} = V_{sa} \cos(\omega t - \theta_s) \quad \text{closing}$$

$$\psi_{s\alpha} = V_{sa} \cos(\omega t - \theta_s), \quad \psi_{s\beta} = V_{sa} \sin(\omega t - \theta_s)$$

$$i_\alpha = i_\beta = i_{kd} = i_{kq} = 0$$

$$i_f = I_{fo}$$

Closure occurs at $t = 0$.

$$i_d = \frac{1}{x'' + x_s} \{ \psi_{d1} - V_{sa} \cos \theta_s - [M_{fd} I_{fo} \cos \omega t - V_{sa} \cos(\omega t + \theta_s)] A_c \}$$

$$i_q = \frac{1}{x'' + x_s} \{ \psi_{q1} + V_{sa} \sin \theta_s + [M_{fd} I_{fo} \sin \omega t - V_{sa} \sin(\omega t + \theta_s)] A_c \}$$

$$\tau = \frac{1}{x'' + x_s} \psi_{d1} V_{sa} \sin \theta_s + \psi_{q1} V_{sa} \cos \theta_s + M_{fd} I_{fo} A_c [\psi_{d1} \sin \omega t + \psi_{q1} \cos \omega t] \\ - V_{sa} A_c [\psi_{d1} \sin(\omega t + \theta_s) + \psi_{q1} \cos(\omega t + \theta_s)]$$

$$A_c = e^{-t/T_{ac}} \quad T_{ac} = \frac{x_s + x''}{(r_s + r_a)}$$

$$\psi_{d1} = M_{fd} I_{fo} F_{dc1} + V_{sa} \cos \theta_s F_{dc2}$$

$$\psi_{q1} = -V_{sa} \sin \theta_s F_{qc}$$

$$F_{dc1} = 1 - \frac{x'' + x_s}{x' + x_s} e^{-\frac{t}{T_{dc}''}} + \frac{x'' + x_s}{x' + x_s} - \frac{x'' + x_s}{x + x_s} e^{-t/T_{dc}'} + \frac{x'' + x_s}{x + x_s}$$

$$F_{dc2} = -\frac{x' - x''}{x' + x_s} e^{-\frac{t}{T_{dc}''}} + \frac{x' - x''}{x' + x_s} - \frac{x - x''}{x + x_s} e^{-\frac{t}{T_{dc}'}} + \frac{x - x''}{x + x_s}$$

$$F_{qc} = \frac{x - x'}{x + x_s} \left(1 - e^{-\frac{t}{T_{qc}''}} \right)$$

The preceding equations give the time dependence of trapped fluxes and torques following faults; they will be used later in developing calculations of rotor heating following faults. However, the peak torque occurs during the subtransient period, and is the critical value for predicting failure of the mechanical structure. Simplified expressions for the subtransient torques are given on the following pages.

Torques During Subtransient Period

Three-Phase Short Circuit from Open Circuit at $t = \pi/2$

$$\begin{aligned} \tau &= - \frac{V_a M_{fd} I_{fo}}{x''} \cos \omega t \\ &= - \frac{V_a^2}{x''} \cos \omega t \quad \tau_{\max} = - \frac{V_a^2}{x''} \text{ at } \omega t = \pi \end{aligned} \quad (A-33)$$

Three-Phase Short Circuit from Load at $\omega t = \pi/2 + \delta$

$$\tau = - \frac{V_a}{x''} \{ [M_{fd} I_{fo} - (x - x'') I_a \sin(\delta + \theta)] \cos \omega t + [(x - x'') I_a \cos(\delta + \theta)] \sin \omega t \} \quad (A-34)$$

Line-Line Short Circuit from Open Circuit at $t = \omega t_o$

$$\tau = - \frac{V_a \sin \omega t_o}{x''} M_{df} I_{fo} \cos \omega t + \frac{(M_{df} I_{fo})^2}{2x''} \sin 2\omega t$$

$$V_a = M_{df} I_{fo} ; \quad \tau_{\max} \text{ for } \omega t_o = \pi/2$$

$$\tau = - V_a^2 / x'' \cos \omega t + V_a^2 / 2x'' \sin 2\omega t \quad (A-35)$$

$$\tau_{\max} = V_a^2 / x'' \frac{3\sqrt{3}}{4} = \frac{1.3 V_a^2}{x''}$$

Torques during Subtransient Period, (cont'd)

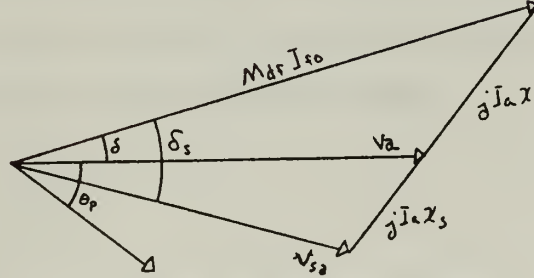
Line-Line Short Circuit from Load at ωt_0

$$\tau = \frac{V_{sa} \cos(\omega - \delta_s)}{x'' + x_s} [\psi_{d1} \sin \omega t + \psi_{q1} \cos \omega t] - \frac{V_a \sin(\omega t_0 - \delta)}{x''} [\psi_{d1} \cos \omega t - \psi_{q1} \sin \omega t] \quad (A-36)$$

$$+ \frac{x_s}{2x''(x'' + x_s)} [2 \psi_{d1} \psi_{q1} \cos 2 \omega t + (\psi_{d1}^2 - \psi_{q1}^2) \sin 2 \omega t]$$

$$\psi_{d1} = \frac{x'' + x_s}{x + x_s} M_{df} I_{fo} + \frac{x - x''}{x + x_s} V_{sa} \cos \delta_s$$

$$\psi_{q1} = - \frac{x - x''}{x + x_s} V_{sa} \sin \delta_s$$



Closing Out of Phase by Angle θ_s at $t = 0$

$$\tau = \frac{1}{x'' + x_s} \{ \psi_{d1} V_{sa} \sin \theta_s + \psi_{q1} V_{sa} \cos \theta_s + M_{fd} I_{fo} [\psi_{d1} \sin \omega t + \psi_{q1} \cos \omega t] - V_{sa} [\psi_{d1} \sin(\omega t + \theta_s) + \psi_{q1} \cos(\omega t + \theta_s)] \}$$

$$\text{Voltages matched } V_{sa} = M_{fd} I_{fo}$$

$$\psi_{d1} = V_{sa}, \quad \psi_{q1} = 0$$

$$\tau = \frac{V_{sa}^2}{x'' + x_s} [\sin \theta_s (1 - \cos \omega t) + \sin \omega t (1 - \cos \theta_s)] \quad (A-37)$$

Rotor Torques

The total torque acting upon the stator is given by the following equations.

$$\tau = \psi_{d1} i_q - \psi_{q1} i_d \quad (A-38)$$

To determine the distribution of the reaction rotor torque between the shield and field winding, the shield torque may be written as follows:

$$\tau_s = \psi_{kd} i_{kq} - \psi_{kq} i_{kd} \quad (A-39)$$

If we use the constraint upon inductances and the definitions of the previous section, Eq. (A-39) can be resolved into the difference of total torque and a component depending only on field current.

$$\tau_s = \tau - \left(\frac{L_k M_{fd}}{M_{kd}^2} i_f \psi_{q1} \right)$$

The field winding torque is given by the second term above:

$$\tau_f = - \frac{L_k M_{fd}}{M_{kd}^2} i_f \psi_{q1} \quad (A-40)$$

The alternating field winding torques can then be found by solving for the induced field winding ac currents since ψ_{q1} has no ac component. For all short circuits from open circuit, $\psi_{q1} = 0$; therefore, $\tau_f = 0$.

The largest component of field winding fault torque will be alternating, since unidirectional torques are associated with resistance losses which are extremely small for a superconducting winding.

In Eq. (A-18), the alternating component of field current as a function of alternating direct-axis current was derived:

$$|i_{f_{ac}}| = \frac{M_{df}}{T'_{do} r_{ff}} \frac{I_{d_{ac}}}{\sqrt{1 + (T''_{do} \omega)^2}} \quad (A-41)$$

The alternating field winding torque is given by the following equation:

$$\tau_f = \frac{x_d - x_d'}{x_d'} \frac{1}{x_d' - x_d''} \frac{T''_{do}}{T'_d} \frac{x_d''}{[1 + (T''_{do} \omega)^2]^{1/2}} I_{d_{ac}} \psi_{q1} \quad (A-42)$$

Use of the Lumped-Parameter Model Results

The lumped-parameter models have yielded expressions for the per-unit currents, total torques, and field winding torques following short circuits. However, for use in calculating the heating and normal forces to which the shield is subjected, it is more convenient to write the armature currents in forms which identify the traveling waves of current which move forward, backward, and are stationary with respect to the stator. This can be done by assuming first harmonic spatial distribution of the current.

$$i(\theta, t) = i_{\alpha}(t) \cos \theta + i_{\beta}(t) \sin \theta \quad (A-43)$$

When the fault currents are written in this manner, the currents can be resolved into component waves which move relative to the stator. Current components with $\cos(\omega_0 t + \theta)$ move backward, relative to the stator, at frequency ω_0 and backward relative to the rotor at angular frequency $2\omega_0$; they will be designated i_2 and referred to as "negative

sequence". Components stationary with respect to the stator move backward relative to the rotor at angular frequency ω_0 ; they will be designated i_0 and referred to as a "zero sequence".

Current components with dependence $\cos(\omega_0 t - \theta)$ will exist before the short circuit if the machine is initially loaded, but will increase in value following the short circuit; these current components are stationary with respect to the rotor, and create the magnetic field which is initially excluded from the electrothermal shield. The increase in these currents over the value before the short circuit will be designated Δi_1 ; this corresponds to increase in positive sequence currents.

Three-Phase Short Circuit

From load at $\omega_0 t_0 = \pi/2 + \delta$

$$i(\theta, t) = \frac{\psi_{d1}}{x''} \cos(\omega_0 t - \theta) - \frac{\psi_{q1}}{x''} \sin(\omega_0 t - \theta) - \frac{V_a \beta}{x''} \sin \theta$$

$$\Delta i_{d1} = \frac{V_a}{x''} F_d \quad (A-44)$$

$$i_0 = \frac{V_a}{x''} A$$

Line-to-Line Short Circuit

From open circuit at $t = t_0$

$$i(\theta, t) = \frac{\psi_{d1}}{2x''} \cos(\omega t - \theta) - \frac{\psi_{\beta 0}}{x''} \sin \theta - \frac{\psi_{d1}}{2x''} \cos(\omega t + \theta)$$

$$\Delta i_{d1} = \frac{V_a}{2x''} \left(1 - \frac{2x''}{x'' + x'}\right) e^{-\frac{t-t_0}{T_d l}} + \left(\frac{2x''}{x'' + x'} - \frac{2x''}{x'' + x}\right) e^{-\frac{t-t_0}{T_d l}} + \frac{2x''}{x'' + x}$$

$$i_0 = \frac{V_a \sin(\omega_0 t_0 - \delta)}{x''} e^{-\frac{t}{T_d l}}$$

$$i_2 = \frac{V_a}{2x''}$$

From load at $t = t_0$

$$\begin{aligned}
 i(\theta, t) = & \frac{1}{2(x'' + x_s)} \left(\frac{2x'' + x_s}{x''} \psi_{d1} - V_{sa} \cos \delta_s \right) \cos(\omega t - \theta) \\
 & - \left(\frac{2x'' + x_s}{x''} \psi_{q1} + V_{sa} \sin \delta_s \right) \sin(\omega t - \theta) \\
 & - \frac{\psi_{\beta 0}}{x''} \sin \theta \\
 & - \frac{1}{2(x'' + x_s)} \left(\frac{x_s}{x''} \psi_{d1} + V_{sa} \cos \delta_s \right) \cos(\omega t + \theta) \\
 & - \frac{x_s}{x''} \psi_{q1} - V_{sa} \sin \delta_s \sin(\omega t + \theta)
 \end{aligned}$$

$$\Delta i_{d1} = \frac{1}{2(x'' + x_s)} \left(\frac{2x'' + x_s}{x''} \psi_{d1} - V_{sa} \cos \delta_s - I_a \sin(\delta + \theta_p) \right)$$

(A-46)

$$i_0 = \frac{\psi_{\beta 0}}{x''}$$

$$|i_2| = (i_{2A}^2 + i_{2B}^2)^{1/2}$$

$$i_{2A} = \frac{1}{2(x'' + x_s)} \left(\frac{x_s}{x''} \psi_{d1} + V_{sa} \cos \delta_s \right)$$

$$i_{2B} = \frac{1}{2(x'' + x_s)} \left(\frac{x_s}{x''} \psi_{d1} - V_{sa} \sin \delta_s \right)$$

A-2 The Quasistatic Magnetic Field Model

The armature currents which result when a generator is subjected to various fault conditions have been derived in section A-1-b. They were resolved into traveling waves of current moving relative to the electrothermal shield and a positive sequence component which appears to remain stationary. In order to determine the electromechanical effects upon the shield, a two-dimensional magnetic field model of the armature-electrothermal shield will be developed with traveling waves of armature current as the source of magnetic field.

Two types of effects are of interest in this model. One is a quasi-steady-state effect produced by a traveling wave of armature current which decays slowly relative to its angular frequency, producing induced currents in the moving conducting shield. Heating of the shield results, and normal forces due to the interaction of the induced current with the armature field tend to produce ring vibration of the shell. The second effect results from the sudden increase in the positive sequence component of armature current. Currents are induced in the shield to keep its total flux linked constant, and exclude the demagnetizing effect of the armature currents. The currents induced in the shield decay with a time constant which depends upon shield parameters, but a large magnetic pressure is exerted upon the shield during this transient.

In section A-2-a, the steady-state magnetic fields model will be derived for E.T. shields both thin and thick compared to skin depth. The results of these models will be used to predict heating and attenuation of the magnetic fields inside the shield. Experimental results are presented in Chapter V to verify the analytical results. In section

and (3) the magnetic field inside the E.T. shield as a function of shield parameters.

The problem is solved by replacing the distributed armature current by a current sheet. The effect of the distributed current is obtained by integrating the current sheet solution.

Definitions for an annular region
with outer radius α and inner
radius β are as follows:

$$B_r^\alpha = \mu H_r(r=\alpha)$$

$$B_r^\beta = \mu H_r(r=\beta)$$

$$K_{\alpha} = -H_{\theta}(r=\alpha)$$

$$K_{\beta} = H_{\theta}(r=\beta)$$

The α and β notation are replaced by a-b, c-d, e-f for the three annular regions in Fig. A6.

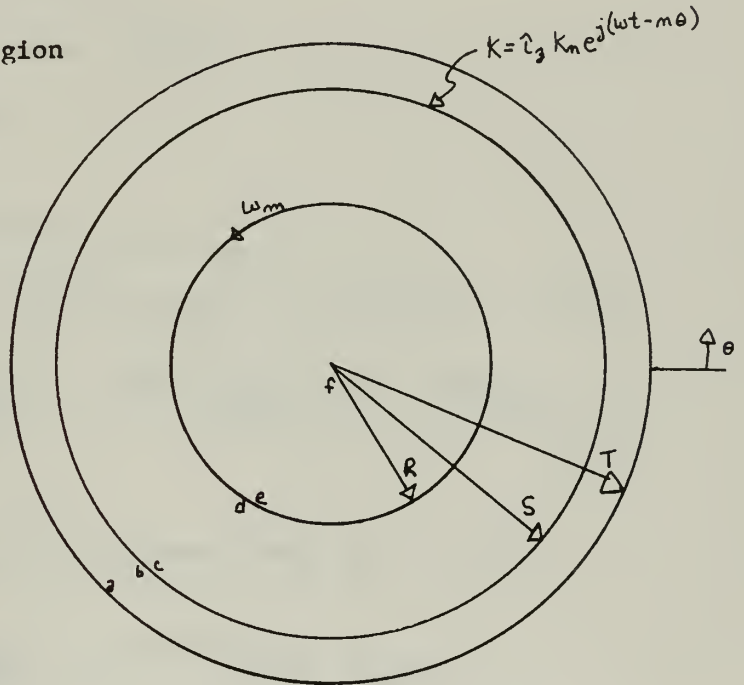


Figure A-6

The solutions for Laplace's equation for each of the annular regions a-b, c-d, e-f are combined according to the following boundary conditions:

Boundary Conditions

$$\begin{aligned} r = T \quad B_r^a &= 0 & \text{for } \mu \rightarrow \infty & \quad r > T \\ \text{or } K^a &= 0 & \text{for } \sigma \rightarrow \infty & \quad r > T \end{aligned}$$

(wherever a double sign appears in the solution (\pm),
the top sign applies for the iron ($\mu \rightarrow \infty$) outer shield,

and the bottom sign for the image ($\sigma \rightarrow \infty$) shield.

$$r = S \quad B_r^b = B_r^c$$

$$K_b + K_c = K_n$$

$$r = R \quad B_r^d = B_r^e$$

$$K_e + K_d = \Delta\sigma R \left(\omega_m - \frac{\omega}{n} \right) B_r^d$$

$$r = 0 \quad K_f = 0$$

The solution is as follows, with $\omega_x = \omega_m - \frac{\omega}{n}$.

The tangential magnetic field outside E.T. shield ($r = R^+$) is"

$$H_{\theta o} = \frac{-\sqrt{1 + (\Delta\sigma\mu R\omega_x)^2}}{\sqrt{1 + (T_{sn}\omega_x)^2}} e^{j(\tan^{-1} T_{sn}\omega_x - \tan^{-1} \Delta\sigma\mu R\omega_x)} H_{w/o n}$$

The tangential magnetic field inside shell ($r = R^-$) is:

$$H_{\theta i} = - \frac{1}{\sqrt{1 + (\omega_x T_{sn})^2}} e^{-j \tan^{-1} T_{sn}\omega_x} H_{w/o n}$$

$H_{w/o n}$ is the magnitude of the magnetic field intensity which would exist at the shell surface if the shell were removed and the stator currents held constant.

$$H_{w/o n} = \frac{1}{2} \left(\frac{R}{S} \right)^{n-1} \left[1 \pm \left(\frac{S}{T} \right)^{2n} \right] K_n \quad \text{current sheet as (A-48)} \\ \text{in Fig. A-6.} \\ \frac{1}{2} \frac{R^{n-1}}{2-n} S_o^{2-n} (1-x^{2-n}) \pm \frac{R^{n-1}}{T^{2n}} \frac{S_o^{n+2}}{n+2} (1-x^{n+2}) J_n \quad \text{distributed stator} \\ \text{current, as in Fig. A-5.}$$

Current induced in shield

$$K_s = \frac{\Delta\sigma\mu R\omega_x}{\sqrt{1 + (\omega_x T_{sn})^2}} e^{j(\pi + \tan^{-1} \frac{1}{T_{sn}\omega_x})} H_{w/o\ n} \quad (A-49)$$

The time-average power dissipated in the shell is calculated from

$P_{av} = \frac{|K_s|^2}{2\sigma\Delta^2}$. The attenuation factor is the ratio of magnetic field inside the E.T. shield to magnetic field intensity without a field, but with the same armature current.

Time-Average Power Dissipation (Thin E.T. Shield)

$$P_{dn} = \mu_o 2\pi \frac{R^2}{[1 \pm (\frac{R}{T})^2]} \frac{1}{T_{sn}} \frac{[(\frac{\omega}{n} - \omega_m)T_{sn}]^2}{1 + [(\frac{\omega}{n} - \omega_m)T_{sn}]^2} \ell H_{w/o\ n}^2 \quad (A-50)$$

where $T_{sn} = \frac{1}{2} \Delta\sigma\mu_o R[1 \pm (\frac{R}{T})^{2n}]$

$\ell = \ell_{ac+} + \ell_{end\ turn}$

Attenuation (Thin E.T. Shield)

$$K_{att} = \frac{|H_{\theta i}|}{|H_{w/o\ n}|} = \frac{1}{\{1 + [(\frac{\omega}{n} - \omega_m)T_{sn}]^2\}^{1/2}} \quad (A-51)$$

A-2-b The Thick Shield, Steady-State Model

The electrothermal shield can be considered thick if the skin depth of the induced currents is small compared to the shell thickness. This definition applied only for one frequency and the meaning of a thick shield is less apparent for transients. For steady-state power dissipation, the problem can be solved by simply replacing the electrothermal shield in Fig. A-5 by a solid cylinder of conductivity $\sigma \rightarrow \infty$ and radius R . The boundary conditions are changed such that now $B_r^d = 0$ at $r = R$. The result is familiar, and shows that the induced surface current is twice the magnitude of $H_{w/o n}$. The total power dissipation is then the same as would be dissipated by the surface current distributed uniformly over one skin depth. The result is:

Power Dissipation (Thick E.T. Shield)

$$P_{dn} = \frac{4\pi\ell}{\sigma\delta} \frac{R}{\left[1 \pm \left(\frac{R}{T}\right)^{2n}\right]^2} H_{w/o n}^2 \quad (A-52)$$

$$\text{where } \delta = \left(\frac{2}{\omega_x \sigma \mu_o} \right)^{1/2}$$

The attenuation factor for a thick shield is much harder to obtain. It involves solution of the diffusion equation in cylindrical coordinates, which results in Bessel functions. The result can be simplified to the following equation:

Attenuation (Thick Shield)

$$K_{att} = 2 \sqrt{2} \frac{\delta}{R} e^{-\frac{\Delta}{\delta}}$$

The complete solution for the thick E.T. shield is presented in the following section.

Solution of the Diffusion Equation for an Annular Region

In section A-2-a, the solution for the induced currents in a thin conducting shield produced by armature currents was developed by combining solutions to Laplace's equation for an annular region. For a thick conducting shield, the appropriate equation is the diffusion equation which can be derived from the Maxwell's equation neglecting displacement current and assuming that current density and electric field intensity are related by a constant conductivity. The resulting form of the diffusion equation is

$$\frac{1}{\sigma\mu} \nabla^2 \bar{H} = \left(\frac{\partial}{\partial t} + v \cdot \nabla \right) \bar{H}$$

The problem is to solve the diffusion equation for an annular region as in Fig. A-7, and find a relationship among B_r^o , B_r^i , K^o , K^i which are defined below, to represent the radial and tangential components of the magnetic field intensity at the outer and inner radii of the annular region.

$$\hat{B}_r^o = \mu \hat{H}_r(r=R_o)$$

$$\hat{B}_r^i = \mu \hat{H}_r(r=R_i)$$

$$\hat{K}^o = -\hat{H}_\theta(r=R_o)$$

$$\hat{K}^i = \hat{H}_\theta(r=R_i)$$

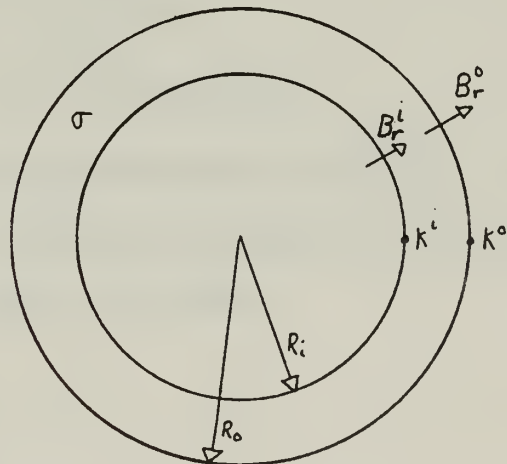


Fig. A-7

In two-dimensional cylindrical coordinates, the diffusion equation can be written for the radial component

$$\frac{1}{\mu\sigma} \left(\frac{1}{r} \frac{\partial}{\partial r} \left(r \frac{\partial H_r}{\partial r} \right) + \frac{1}{r^2} \frac{\partial^2 H_r}{\partial \theta^2} \right) = \left(\frac{\partial}{\partial t} + \frac{r\omega_m}{r} \frac{\partial}{\partial \theta} \right) H_r$$

$$\text{where } \bar{v} = \hat{i}_\theta v_\theta = \hat{i}_\theta \omega_m r.$$

Assume $H_r = \hat{H}_r(r) e^{j(\omega t - n\theta)}$ solve for $\hat{H}_r(r)$ and obtain H_θ from

$$\nabla \cdot \mu \bar{H} = 0.$$

$$r^2 \frac{\partial^2 \hat{H}_r}{\partial r^2} + r \frac{\partial \hat{H}_r}{\partial r} - (n^2 + jq^2 r^2) \hat{H}_r = 0$$

$$q^2 = \mu\sigma(\omega - n\omega_m)$$

The solution can be written as follows:

$$\hat{H}_r = C_1 j^n I_n(\sqrt{j} q r) + C_2 j^{-n} K_n(\sqrt{j} q r)$$

Since we are interested primarily in the attenuation of the first spatial harmonic, we will let $n = 1$.

$$\hat{H}_r = C_1 j I_1(\sqrt{j} q r) + C_2 j^{-1} K_1(\sqrt{j} q r)$$

$$\text{and } \hat{H}_\theta = C_1 \sqrt{j} q r I_0(\sqrt{j} q r) - C_2 j^{-\frac{3}{2}} r q K_0(\sqrt{j} q r)$$

The boundary conditions are given in the definitions of B_r^0 , B_r^1 , ... etc. above. After much manipulation, a relationship among the field components at the edges of the annular region is obtained.

$$\begin{bmatrix} \hat{B}_r^0 \\ \hat{B}_r^1 \end{bmatrix} = \frac{\mu}{w} \begin{bmatrix} \delta' & \gamma' \\ \beta' & \alpha' \end{bmatrix} \begin{bmatrix} \hat{K}^0 \\ \hat{K}^1 \end{bmatrix}$$

$$\alpha' = (AF - BE)$$

$$\beta' = (CF - DE) = -j$$

$$\gamma' = (AH - BG)$$

$$\delta' = (CH - DB) = -j$$

$$w = AD - CB$$

$$A = \sqrt{j} q R_o I_o(\sqrt{j} q R_o) \quad , \quad E = j I_1(\sqrt{j} q R_1)$$

$$B = \sqrt{j} q R_o K_o(\sqrt{j} q R_o) \quad , \quad F = j^{-1} K_1(\sqrt{j} q R_1)$$

$$C = \sqrt{j} q R_1 I_o(\sqrt{j} q R_1) \quad , \quad G = j J_1(\sqrt{j} q R_o)$$

$$D = \sqrt{j} q R_1 K_o(\sqrt{j} q R_1) \quad , \quad H = j^{-1} K_1(\sqrt{j} q R_o)$$

The above expressions can be simplified by making assumptions about the magnitude of the skin depth of currents in the conducting annulus.

$$\delta = \left(\frac{2}{|\omega - \omega_m| \sigma \mu} \right)^{1/2} = \frac{\sqrt{2}}{q}$$

For $\delta < R_1, R_o$

$$w = \frac{\sqrt{R_1 R_o}}{\sqrt{2} \delta} e^{j \frac{\pi}{4}} \left[e^{\frac{\Delta}{\delta}} e^{j \frac{\Delta}{\delta}} - e^{\frac{\Delta}{\delta}} e^{-j \frac{\Delta}{\delta}} \right]$$

$$\alpha' = -\frac{j}{2} \left(\frac{R_o}{R_1} \right)^{1/2} \left[e^{\frac{\Delta}{\delta}} e^{j \frac{\Delta}{\delta}} + e^{-\frac{\Delta}{\delta}} e^{-j \frac{\Delta}{\delta}} \right]$$

$$\delta' = -\frac{j}{2} \left(\frac{R_o}{R_1} \right)^{1/2} \left[e^{\frac{\Delta}{\delta}} e^{j \frac{\Delta}{\delta}} + e^{-\frac{\Delta}{\delta}} e^{-j \frac{\Delta}{\delta}} \right]$$

$$\Delta = R_o - R_1$$

To find the attenuation of an alternating magnetic field by a thick shield, i.e., one for which $\Delta > \delta$, we assume a uniform magnetic field far

from the thick shield alternating in magnitude at frequency ω . This, of course, is equivalent to two counter-rotating magnetic fields rotating at frequency ω . The solution for the ratio of field inside to outside is given by

$$\frac{\hat{B}_i}{B_o} = K_{att} = \frac{-2}{(j\omega - \delta')(j\omega - \alpha') + 1} \quad (A-52')$$

Further assumptions lead to increased simplification of ω , α' , and δ' .

Thick Shield $\Delta > \delta$

$$w = \frac{\sqrt{R_i R_o}}{\sqrt{2} \delta} e^{j\frac{\pi}{4}} e^{\frac{\Delta}{\delta}} e^{j\frac{\Delta}{\delta}}$$

$$\alpha' = \delta' = -j\omega \frac{\delta}{\sqrt{2R_i R_o}} e^{-j\frac{\pi}{4}}$$

$$\frac{1}{K_{att}} = \frac{1}{2\sqrt{2}} \frac{\sqrt{R_i R_o}}{\delta} e^{\frac{\Delta}{\delta}} \left[1 + \frac{\delta}{\sqrt{R_i R_o}} + \left(\frac{\delta}{\sqrt{R_i R_o}} \right)^2 \right] e^{j\left(\frac{\Delta}{\delta} + \frac{\pi}{4}\right)}$$

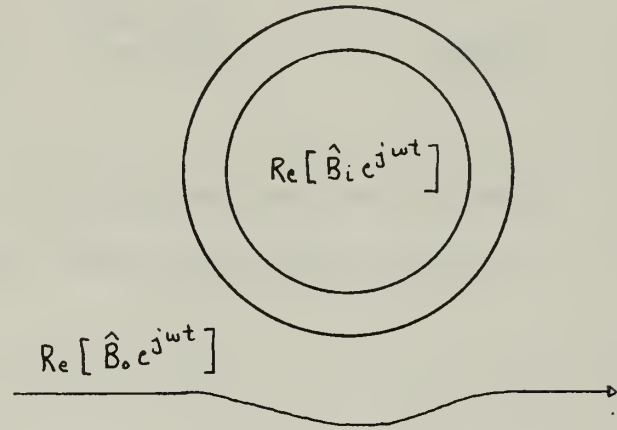
The attenuation magnitude is given by

$$|K_{att}| = 2\sqrt{2} \frac{\delta}{\sqrt{R_i R_o}} e^{-\frac{\Delta}{\delta}} \quad (A-53)$$

Thin Shield $\nabla < \delta$

In the thin shield case, the solution must reduce to that obtained in the previous section.

$$w = 2j \frac{\sqrt{R_i R_o}}{\delta} \frac{\Delta}{\delta} = j\Delta\sigma\mu \sqrt{R_i R_o} \omega_x \quad \omega_x = \omega_m - \omega$$



$$\alpha' = \delta' = -j$$

$$K_{att} = \left(1 + \frac{1y}{\omega} + \frac{\omega}{2} - \frac{x^2 + y^2}{2\omega} \right)^{-1}$$

$$x = \frac{\Delta}{2 R_1} \approx \frac{\Delta}{2 R_o} \quad y = \left(\frac{\Delta}{\delta} \right)^2$$

$$K_{att} \approx \frac{1}{1+j \frac{\Delta \sigma \mu \sqrt{R_1 R_o} \omega}{2}}$$

$$|K_{att}| = \frac{1}{[1 + (\omega T_{s1})^2]^{1/2}} \quad T_{s1} = \frac{\Delta \sigma \mu \sqrt{R_1 R_o}}{2} \quad (A-54)$$

Equation (A-54) is identical with Eq. (A-51) obtained from the thin shell model. Experimental verification of Eqs. (A-53) and (A-54) is given in Chapter V.

A-2-c Transient Magnetic Fields Model

Thin Shield

The time constant associated with decay of a sinusoidally distributed current sheet in a cylindrical shell of surface conductivity σ_s can be calculated as follows:

$$K_z = K_n \cos n\theta \quad \text{at } t = 0$$

$$E_z = \frac{K_x}{\sigma_s} = \frac{K_n \cos n\theta}{\sigma_s}$$

$$\nabla \times E = -\mu_o \frac{\partial H}{\partial t}$$

We assume time dependence of E, H to be $e^{-\alpha t}$ and substitute into the curl equation.

$$\frac{1}{r} \frac{\partial E_z}{\partial \theta} = -\mu_o \alpha H_r$$

$$\text{at } r = R, \quad H_r = \frac{Kz}{2}$$

$$T_{sn} = \frac{1}{\alpha} = \frac{\mu_o \sigma_s R}{2}$$

The value of σ_s in terms of the bulk conductivity of a thin shell of thickness Δ is $\sigma_s = \Delta\sigma$

$$T_{sn} = \frac{\mu_o \sigma \Delta R}{2} \quad (\text{A-55})$$

If the conducting shell is placed inside a boundary of $\mu \rightarrow \infty$ or $\sigma \rightarrow \infty$ at $r = T$, the result will be

$$T_{sn} = \frac{1}{2} \mu_o \sigma \Delta R \left[1 \pm \left(\frac{R}{T} \right)^{2n} \right]$$

It should be emphasized that the n refers to the harmonic of the initial current distribution. The longest time constant is for $n = 1$. The time constants associated with higher harmonics should not be confused with time constants associated with diffusion of the current through the thickness of the material when a magnetic field is suddenly established outside the shield. The diffusion time constants are derived in the next section. The result is that the first diffusion time constant is smaller than the decay time constant by a factor of the thickness-to-radius ratio.

Thick Shield

The terms "thick" and "thin" as applied to an electrothermal shield have significance only in terms of some steady-state frequency of induced eddy currents. However, it is clear that, for a shield whose thickness is larger than a small fraction of its radius, magnetic diffusion will result in time lags of the establishment of a magnetic field inside the

shield after a field has been established outside. This transient problem has been investigated [8, 18] and the solution for the time constants has been shown to reduce to the solution of the transcendental equation of Bessel functions

$$\frac{Y_2(\alpha_n R_i)}{J_2(\alpha_n R_i)} = \frac{Y_0(\alpha_n R_o)}{J_0(\alpha_n R_o)} \quad (A-57)$$

where R_i and R_o are the inner and outer radii of the shield, and α_n are related to the time constants of the field inside by

$$T_n = \frac{\mu\sigma}{\alpha_n^2} \quad (A-58)$$

The magnetic field outside is uniform a long distance from the shield, and is established in a time short compared to the shield time constants. The resulting magnetic field intensity inside is then

$$H_i(t) = H_o - \sum_{n=1}^{\infty} H_i e^{-\frac{t}{T_n}}$$

To determine the solutions for the T_n approximations for the Bessel functions from Ref. [19] are used.

$$\begin{aligned} J_0(x) &= \left(\frac{2}{\pi x}\right)^{1/2} \left[\cos\left(x - \frac{\pi}{4}\right) + \frac{1}{x} \sin\left(x - \frac{\pi}{4}\right)\right] \\ J_2 &= \left(\frac{2}{\pi x}\right)^{1/2} \left[\cos\left(x - \frac{5\pi}{4}\right) - \frac{15}{8x} \sin\left(x - \frac{5\pi}{4}\right)\right] \\ Y_0 &\approx \left(\frac{2}{\pi x}\right)^{1/2} \left[\sin\left(x - \frac{\pi}{4}\right) - \frac{1}{8x} \cos\left(x - \frac{\pi}{4}\right)\right] \\ Y_2 &= \left(\frac{2}{\pi}\right)^{1/2} \left[\sin\left(x - \frac{5\pi}{4}\right) + \frac{15}{8x} \cos\left(x - \frac{5\pi}{4}\right)\right] \end{aligned} \quad 0 \leq x < 2\pi$$

Using the above approximations, Eq. (A-57) reduces to

$$\sin(\alpha_n \Delta + \pi) - \frac{15}{9\alpha_n R_i} \cos(\alpha_n \Delta + \pi) - \frac{1}{8\alpha_n R_o} \cos(\alpha_n \Delta + \pi) = 0 \quad (A-59)$$

The maximum value of $\alpha_n \Delta$ is related to the longest shield time constant and the shield thickness. If we assume $\alpha_n \ll 1$, and solve for T_n , the assumption can then be checked for typical dimensions of electrothermal shields. This has been done, and the value of $\alpha_n \Delta$ is usually less than .34. Using the assumption $\alpha_1 \Delta < 1$, we can expand the sines and cosines and obtain

$$\alpha_1^2 = \frac{15 R_o + R_1}{8 \Delta R_1 R_o}$$

which gives the result for the time constant

$$T_1 = \frac{\Delta \sigma \mu R_1}{2} \left(1 + \frac{\Delta}{2 R_o} \right) \quad (\text{A-60})$$

For $\Delta \ll R_o$, this reduces to the result of the thin shield assumption obtained in the previous section.

The higher order time constants are obtained from Eq. (A-59) by observing that, for larger n , the magnitudes of α_n become smaller; i.e., α_n are larger and the second and third terms can be neglected in Eq. (A-59). This gives

$$\alpha_n = \frac{\pi (n-1)}{R_o - R_1} \quad n \geq 2$$

and

$$T_n = \frac{\Delta^2 \mu \sigma}{(n-1)^2 \pi^2} \quad n \geq 2 \quad (\text{A-60})'$$

Therefore, the first diffusion time constant ($n=2$) is smaller than the L/R shield time constant ($n=1$) by a factor less than the thickness-to-radius ratio. Experimental verification of these results is presented in Chapter V.

A-2-d Transient Normal Forces on a Conducting Shield

When a magnetic field is established external to a conducting shield in a time short compared to the eddy current decay time of the shield, normal forces are exerted upon the surface. These forces result from the interaction of the external tangential magnetic field and the surface currents which are induced to prevent instantaneous change in the flux linked by the shield. In Fig. A-8, the external field which is uniform far from the conducting shield has been established in a time short compared to the shield time constant. The currents in the shield are uniformly distributed across the thickness of a time long compared to the diffusion time constant. That

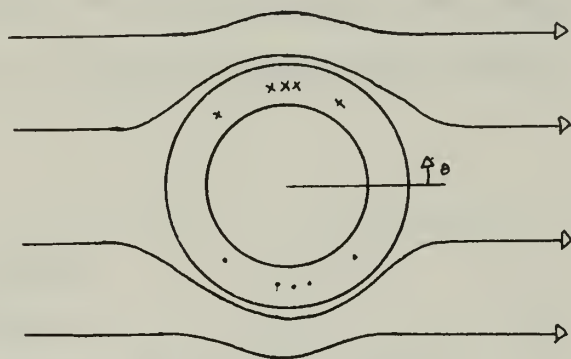


Figure A-8

is, if the field were established at $t = 0$, the observation is made at $t = t_0$ where $\frac{\Delta^2 \sigma \mu}{\pi^2} < t_0 < \frac{1}{2} \Delta \sigma \mu R$. It is clear from the figure that an inward radial force is being exerted upon the surface, the spatial dependence of which is $\cos^2 \theta$.

During transients in a generator, an increase in the positive sequence component of armature current will produce a demagnetizing field which will initially be excluded from the electrothermal shield. As the induced currents in the shield decay, the armature produced field will penetrate the shield. During this transient, radially-directed forces are exerted which are stationary with respect to the shield. The trapped dc

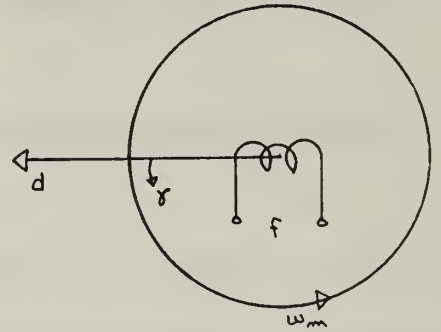
flux in the armature produces a traveling wave of normal stress upon the shield. Unbalanced faults such as line-to-line result in negative sequence magnetic field, which also produces traveling waves of normal stress.

The magnitude and distribution of the normal stress is derived by calculating the distribution of magnetic field inside and outside the shell during the transient. The magnitude of the normal stress for a three-phase short circuit is independent of loading condition. The line-to-line fault is dependent upon loading, but the maximum normal stress which occurs one-half cycle after the fault is calculated for the open-circuit fault case.

Normal Stress

Three-Phase Fault from Open Circuit

The stresses are independent of time of application of the fault. For simplification, let $t_0 = \pi/2$ where t_0 is time of application of fault, and t' equals time of the fault,



$$\begin{aligned}
 t' &= t - t_0 \\
 \sigma_r(t', r) &= \mu_0 \left[\frac{\Delta H_{1f} \Delta H_{1i}}{2} \left(1 - e^{-\frac{t'}{T_d}} \right) e^{-\frac{t}{T_d}} \cos 2\gamma + \frac{H_i^2}{4} e^{-\frac{2t'}{T_d}} \cos 2\gamma \right. \\
 &\quad + \frac{\Delta H_{1i}^2}{4} e^{-\frac{2t'}{T_a}} \cos 2(\omega t' + \gamma) - \frac{\Delta H_{1i}^2}{2} e^{-t' \left(\frac{1}{T_a} + \frac{1}{T_a} \right)} \cos(\omega t' + 2\gamma) \\
 &\quad \left. - \frac{\Delta H_{1f} \Delta H_{1i}}{2} e^{-\frac{t'}{T_a}} \left(1 - e^{-\frac{t'}{T_a}} \right) \cos(\omega t' + 2\gamma) \right] \quad (A-61)
 \end{aligned}$$

$$+ \mu_o - \frac{\Delta H_{1f} \Delta H_{1i}}{2} \left(1 - e^{-\frac{t'}{T_d''}} \right) e^{-\frac{t'}{T_d''}} - \frac{\Delta H_{1i}^2}{4} e^{-\frac{2t'}{T_d''}} - \frac{\Delta H_{1i}^2}{4} e^{-\frac{2t'}{T_a}} \\ + \frac{\Delta H_{1i}^2}{2} e^{-\frac{t'}{T_a}} \frac{1}{T_a} + \frac{1}{T_a} \cos \omega t' + \frac{\Delta H_{1f} \Delta H_{1i}}{2} e^{-\frac{t'}{T_a}} \left(1 - e^{-\frac{t'}{T_d''}} \right) \cos \omega t'$$

$$\Delta H_{1i} = \frac{3\sqrt{2} J_A}{\pi} \frac{S_o}{1 \pm \left(\frac{R}{T}\right)^2} \left\{ 1 - x \pm \frac{1}{3}(1-x^3) \frac{S_o}{T} \right\} \Delta J_d''$$

$$\Delta H_{1f} = \frac{3\sqrt{2} J_A}{2\pi} S_o \left\{ 1 - x \pm \frac{1}{3}(1-x^3) \frac{S_o}{T} \right\} + \frac{2J_f}{3\pi} \sin \frac{\theta_{wf}}{2} \cdot$$

$$R \left\{ \left(\frac{F_o}{R}\right)^3 (1-y^3) \left[1 \pm \left(\frac{R}{T}\right)^2 \right] \right\} (x_d - x_d') \Delta J_d'$$

$\Delta J_{d1}''$ = increase in direct-axis, positive sequence current following fault

$\Delta J_{d1}'$ = increase in direct-axis, positive sequence current for time t such that $T_d'' \ll t' \ll T_d'$

The normal stress given by Eq. (A-61) is made up of a component independent of angular position, and one having a $\cos 2\gamma$ dependence. Since the shell is much less resistant to the $\cos 2\gamma$ stress, its maximum value is important. This occurs for $\omega_o t' = \pi$, i.e., one-half cycle after the fault. The second spatial harmonic normal stress is given by

$$\sigma_{r2\max}(t' = \frac{\pi}{\omega_o}, \gamma) = \mu_o \frac{\Delta H_{1f} \Delta H_{1i}}{2} \left(1 - e^{-\frac{t'}{T_d''}} \right) e^{-\frac{t'}{T_d''}} + \frac{\Delta H_{1i}}{4} e^{-\frac{2t'}{T_d''}} \\ + \frac{\Delta H_{1i}}{4} e^{-\frac{2t'}{T_a}} + \frac{\Delta H_{1i}}{2} e^{-\frac{1}{T_d''} + \frac{1}{T_a}} + \frac{\Delta H_{1f} \Delta H_{1i}}{2} e^{-\frac{t'}{T_a}} \left(1 - e^{-\frac{t'}{T_d''}} \right) \cos 2\gamma$$

$$\Delta J_{d1}'' = \frac{V_{oc}}{x''}$$

$$\Delta J_{d1}' = \frac{V_{oc}}{x'}$$

(A-62)

A-3 The Thin Shell Mechanical Model

During transients following machine faults, large normal forces are exerted upon the electrothermal shield. These forces consist of a dc or stationary force relative to the shield distributed with a $\cos^2 \theta$ angular dependence, and a traveling wave or alternating normal force. The magnitudes of these forces were derived in the previous sections. In order to predict the mechanical motion of the shell when subjected to these normal forces, the thin shell elasticity equations are solved for the given loading. Steady-state deflections are calculated as a function of loading, and ring natural frequencies are derived by the energy method.

The Thin Shell with Hinged Ends Radially Supported

The shell is loaded as shown in Fig.

A-9.

$$\sigma_r = \sum_{m=0}^{\infty} \sum_{n=0}^{\infty} \sigma_{rnm} \cos n\phi \sin \frac{m\pi x}{\ell} \quad (\text{A-64})$$

The loading due to the armature-produced magnetic flux occurs primarily for $n = 1$ and $n = 0, 1$ which can be written as

$$\sigma_r = \sigma_0 \cos^2 \phi \sin \frac{\pi x}{\ell}$$

The distribution of loading was shown in section A-2-c to have the $\cos^2 \phi$ dependence. The loading distribution along the axial length of the shield depends upon the armature active length and end turns

relative to the end supports of the E.T. shield. Fourier analysis of the

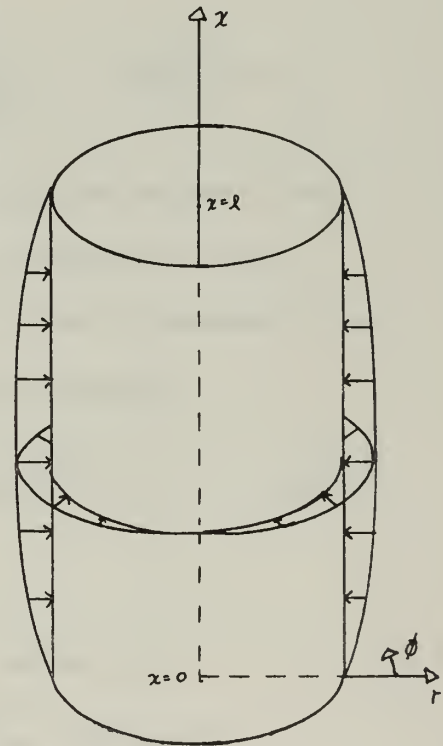


Fig. A-9

flux distributions for armatures of the machines being built, and the geometries of larger machines, has shown that the $\sin \pi x/\ell$ term very closely represents the axial flux distribution. Higher harmonics in the axial distribution are very small relative to the fundamental.

The partial differential equations which govern the deflection of a thin shell, when loaded by a normal stress on the surface, are given in Ref. [15] and reproduced here:

$$\frac{1+\nu}{2R} \frac{\partial^2 v}{\partial x \partial \phi} - \frac{\nu}{R} \frac{\partial \omega}{\partial x} + \frac{\partial^2 u}{\partial x^2} + \frac{1-\nu}{2R^2} \frac{\partial^2 u}{\partial \phi^2} = 0$$

$$\frac{1+\nu}{2} \frac{\partial^2 u}{\partial x \partial \phi} + R \frac{1-\nu}{2} \frac{\partial^2 v}{\partial x} + \frac{1}{R} \frac{\partial^2 v}{\partial \phi^2} - \frac{1}{R} \frac{\partial \omega}{\partial \phi} = 0$$

$$\nu \frac{\partial u}{\partial x} + \frac{1}{R} \frac{\partial v}{\partial \phi} - \frac{\omega}{R} - \frac{\Delta^2}{12} \left(R \frac{\partial^4 \omega}{\partial^4} + \frac{2}{R} \frac{\partial^4 \omega}{\partial z^2 \partial \phi^2} + \frac{1}{R^3} \frac{\partial^4 \omega}{\partial \phi^4} \right) = - \frac{R(1-\nu^2)}{E h} \sigma_r$$

where u , v , ω are the axial, azimuthal, and radial deflections, respectively, and σ_r is the radial load which is a function of x and ϕ .

The primary loading due to magnetic pressure has a $\cos^2 \phi$ dependence, as shown in the previous section. The loading is then assumed

$$\sigma_r = \sigma_o \cos^2 \phi \sin \frac{\pi x}{\ell} = \sigma_o \left(\frac{1}{2} + \frac{1}{2} \cos^2 \phi \right) \sin \frac{\pi x}{\ell} \quad (\text{A-65})$$

Assume solutions of the form

$$u = \cos \frac{\pi x}{\ell} \sum A_n \cos n\phi \quad \text{axial deflection}$$

$$v = \sin \frac{\pi x}{\ell} \sum B_n \sin n\phi \quad \text{azimuthal deflection ,}$$

$$w = \sin \frac{\pi x}{\ell} \sum C_n \cos n\phi \quad \text{radial deflection}$$

The shell is assumed to be hinged, with radial support at the ends $x = 0$, but is free to move axially.

After substitution of the assumed solutions into the equations, application of approximations concerning relative dimensions, and solution for the coefficients, the resulting radial deflection is

$$w = \sin \frac{\pi x}{\ell} \frac{R^2}{E\Delta} \frac{\sigma_0}{2} + \frac{1-\nu^2}{4} \frac{4R}{\left(\frac{\pi R}{\ell}\right)^4 + 3\left(\frac{\Delta}{R}\right)^2} \left(\frac{1}{\Delta}\right) \left(\frac{1-\nu^2}{E}\right) \frac{\sigma_0}{2} \cos 2\phi \quad (\text{A-66})$$

$$\frac{\ell}{R} > \pi$$

R = shield radius

ℓ = length between shield and support

Δ = shield thickness

E = Young's modulus

ν = Poisson's ratio

The ratio of C_0 to C_2 gives the relative magnitude of the uniform radial deflection to the second harmonic deflection.

$$\frac{C_0}{C_2} = \frac{\left(\frac{1-\nu^2}{4}\right)\left(\frac{\pi R}{\ell}\right)^2 + 3\left(\frac{\Delta}{R}\right)^2}{4(1-\nu^2)}$$

which is clearly less than 1. Even for the limiting case of $\ell = \pi R$, the uniform deflection is only about 1/16 the second harmonic amplitude.

Shell Mechanical Natural Frequencies

The natural frequency of ring vibrations having radial deflections of the lowest mode

$$w(r, \phi, x) = w_{\max} \cos \omega t \cos 2\phi \sin \frac{\pi x}{\ell}$$

can be determined by equating the maximum kinetic energy of the motion to the maximum energy of bending.

To calculate the potential energy stored in a ring mode deflection, we use Castigliano's theorem [16] which states that $U = \frac{1}{2} P_1 \delta_1 + \frac{1}{2} P_2 \delta_2 + \dots$ where P_1 is the load in the 1 direction and δ_1 is the deflection in the 1 direction, etc.

$$\delta_r = w = dr \cos 2\phi \sin \frac{\pi x}{\ell}$$

$$P = \frac{f_0}{2} \cos 2\phi$$

$$U = \frac{1}{2} \int_0^{2\pi} \int_0^{\omega_{\max}} \int_0^{\ell} R \sin^2 \frac{\pi x}{\ell} dx \cos^2 \phi dr \frac{f_0}{2} d\phi.$$

The kinetic energy maximum is calculated by assuming deflection time dependence as

$$\delta_r = w_{\max} \cos 2\phi \sin \frac{\pi x}{\ell} \sin \omega_1 t \quad \text{radial deflection}$$

$$\dot{\delta}_{r_{\max}} = w_{\max} \omega_1 \cos 2\phi \sin \frac{\pi x}{\ell}$$

$$v = \frac{\omega_{\max}}{2} \sin 2\phi \sin \frac{\pi x}{\ell} \sin \omega_1 t \quad \text{azimuthal deflections}$$

$$\dot{v}_{\max} = \frac{\omega_{\max}}{2} \omega_1 \sin 2\phi \sin \frac{\pi x}{\ell}$$

The contribution of the axial deflections to kinetic energy is neglected, since for a long shield, they are much smaller than radial deflections:

$$K.E._{\max} = \frac{1}{2} \int_0^{2\pi} R \ell \omega_1^2 \omega_{\max}^2 \cos^2 2\phi \rho_m \Delta \sin^2 \frac{\pi x}{\ell} d\phi dx$$

$$= \frac{5}{16} R \ell \omega_1^2 \omega_{\max}^2 \rho_m \Delta$$

The energy change due to motion in centrifugal force field of a shield rotating at frequency ω_m [17] is:

$$U_c = \frac{3\pi}{2} \rho_m \Delta R^2 \omega_m^2 \omega_{\max}^2 \ell$$

If the sum of the maximum potential and kinetic energies are equated, the natural frequency of the shield is obtained for the assumed mode of vibration:

$$\omega_c^2 = 2.4 \omega_m^2 + \omega_1^2$$

$$\omega_1^2 = \frac{E}{1-\nu^2} \left(\frac{1}{\rho_m} \right) \frac{3 \left(\frac{\Delta}{R} \right)^2 + \frac{1-\nu^2}{4} \left(\frac{\pi R}{\ell} \right)^4}{5 R^2} \quad (\text{A-67})$$

ω_c = natural frequency of rotating shield

ω_m = angular frequency of rotation

ρ_m = density of shield material (kg/m^3).

BIBLIOGRAPHY

1. Thullen, P., Smith, J. L., and Woodson, H. H., "Economic and Operational Aspects of the Application of Superconductors in Steam Turbine Generator Field Windings", Paper No. 70 CP211-PWR, presented at the 1970 IEEE Winter Power Meeting.
2. Woodson, H. H., Smith, J. L., Thullen, P., and Kirtley, J. L., "The Application of Superconductors in the Field Windings of Large Synchronous Machines", IEEE Trans., Power Apparatus and Systems, Vol. PAS-90, # 2, March/April, 1971.
3. Thullen, P., Dudley, J. C., Greene, D. L., Smith, J. L., and Woodson, H. H., "An Experimental Alternator with a Superconducting Rotating Field Winding", IEEE Trans., Power Apparatus and Systems, Vol. PAS-90, #2, March/April, 1971.
4. Thullen, P., and Smith, J. L., "Mechanical Design Concept for 1000 MVA Superconducting Turboalternator", ASMW Paper No. 69-WA/PID-3.
5. Einstein, T. H., "Excitation Requirements and Dynamic Performance of a Superconducting Alternator for Electric Utility Power Generation", M.I.T. Thesis, Sc.D., Department of Mechanical Engineering, 1970.
6. Kirtley, J. L., "Basic Formula for Air Core Synchronous Machines", Paper No. 71 CP 155-PWR, Presented at the 1971 IEEE Winter Power Meeting.
7. Woodson, H. H., Private communication.
8. Jaeger, J. C., "Magnetic Screening by Hollow Circular Cylinders", Phil. Mag., Vol. 29, p. 18 (1940).
9. Timoshenko, S. P., and Gere, J. M., Theory of Elastic Stability, McGraw-Hill Book Co., New York, 1961.
10. Rogers, E. C., "The Nature of the 50 c/s Phase Transition in Type II Superconductors", Phys. Letters, Vol. 22, No. 4.

Bibliography (continued)

11. Rocher, Y.A., and Septfonds, J., "Losses of Superconducting Niobium in Low Frequency Fields", Cryogenics, April 1967.
12. Pech, T., and Fournet, G., "50 c/s Losses in Coils Made with Superconducting Wire", Cryogenics, Feb. 1967.
13. Timoshenko, S., Vibration Problems in Engineering, D. Van Nostrand Co., Inc., (1955).
14. Concordia, C., Synchronous Machines, John Wiley & Sons, Inc., New York, (1951).
15. Timoshenko, S. and Woinousky-Krieger, S., Theory of Plates and Shells, McGraw-Hill Book Co., New York (1959).
16. Den Hartog, J. P., Advanced Strength of Materials, McGraw-Hill Book Co., New York (1952).
17. Thullen, P., "Analysis of the Application of Superconductivity to Commerical Electric Power Generation", M.I.T. Thesis, Sc.D., Dept. of Mechanical Engineering, 1969.
18. Smythe, W. R., Static and Dynamic Electricity, 3rd Ed., McGraw-Hill Book Co., New York (1968).
19. Watson, G. N., A Treatise on the Theory of Bessel Functions, Cambridge University Press, Cambridge, England (1966).
20. Holley, C. H., and Winchester, R. L., "Proposal for Revision of ANSI C 50.13, Section 6.3" (General Electric Co.).
21. Kirtley, J. L., M.I.T. Sc.D. Thesis (in preparation).
22. King, E. I., and Batchelor, J. W., "Effects of Unbalanced Currents on Turbine Generators", IEEE Trans. on Power Apparatus and Systems, PAS- 84 , February 1965.

BIBLIOGRAPHICAL NOTE

The author was born November 17, 1942, in Hillsboro, Ohio. After graduation from high school in 1960, he attended Ohio University in Athens, Ohio, graduating summa cum laude and receiving the B.S. degree in August, 1963. He was commissioned in the U.S. Navy after attending O.C.S. and was assigned to the Naval Radiological Defense Laboratory, where he served as a scientific investigator on the cyclotron project. In June, 1966, he entered the Naval Construction and Engineering course at M.I.T.; in June, 1969, he received the degrees of S.M.E.E. and Nav. E., and was presented the Brand Award. He is a member of Phi Beta Kappa, Tau Beta Pi, and Sigma Xi, as well as the American Society of Naval Engineers and the Institute of Electrical and Electronic Engineers.

1 MAR 75

127243

Thesis
L8915

Luck

Electromechanical
and thermal effects of
faults upon supercon-
ducting generators.

127243

127243
1 MAR 75

DISPLAY
127243

Thesis
L8915

Luck

Electromechanical
and thermal effects of
faults upon supercon-
ducting generators.

127243

thesL8915

Electromechanical and thermal effects of



3 2768 001 03270 9

DUDLEY KNOX LIBRARY